

Porous metal implants for enhanced bone ingrowth and stability

William van Grunsven¹, Russell Goodall¹, and Gwendolen C. Reilly¹

¹ *Department of Materials Science and Engineering, University of Sheffield, UK.*

INTRODUCTION:

Total joint replacement using cemented metal implants has been in clinical use for more than fifty years¹. A more recent development in orthopaedic surgery has been the use of non-cemented implants where fixation of the implant is the result of the formation of a direct bone-implant interface². In order to obtain the necessary fixation, implants with porous metal surfaces are being used that permit bone ingrowth into the pores after implantation. Furthermore, these structures could be seeded with osteoprogenitor cells to further stimulate the formation of bone matrix. Recently, Electron Beam Melting (EBM) has been proposed as a fabrication technique to gain greater control over the size and shape of the pores³. This project aims to investigate the possibility of using EBM to create new porous architectures for applications as bone implants.

METHODS:

To demonstrate this concept, one prototype of a porous metal structure was designed using Magics (Materialise NV, Leuven, Belgium). The thickness of the porous layer of the prototype is 4 mm and consists of diamond unit cells measuring 2 mm cubed (figure 1).

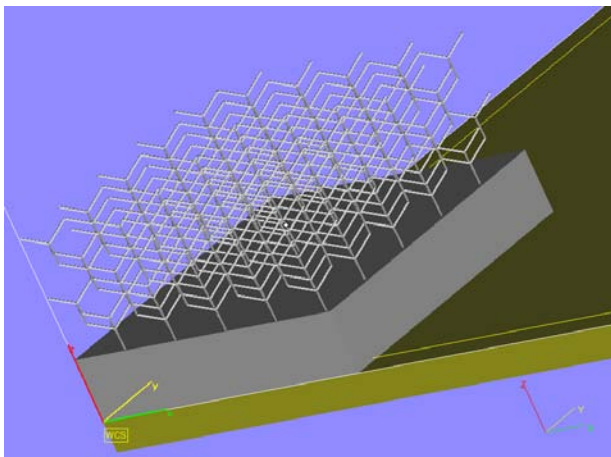


Fig. 1: Screenshot of Magics showing a 3d model of a porous structure.

RESULTS:

The prototype was created on an EBM-S12 (Arcam AB, Mölndal, Sweden) using powdered Ti6Al4V. The prototype was then cleaned and examined by light microscopy and SEM (figure 2). The SEM images show a regular pattern of pores with pore sizes of around 750 μm and strut sizes of around 600 μm .

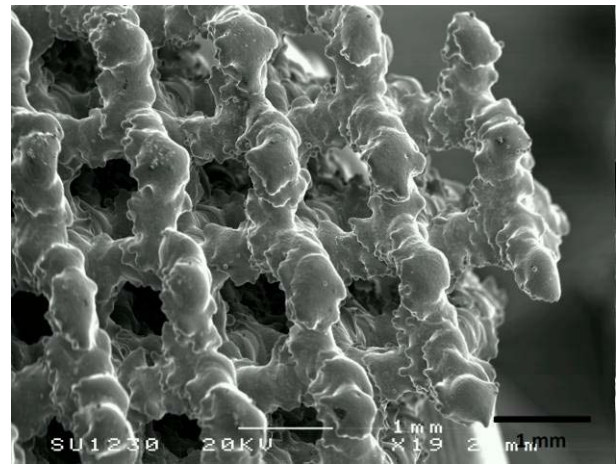


Fig. 2: SEM image showing the structure that was created by building the model in figure 1 using EBM of Ti6Al4V.

DISCUSSION & CONCLUSIONS:

These results show that porous metal structures with properties suitable for bone implants can be made using EBM. The next step in the project will be to use these structures and structures of different shapes and architectures for biological evaluation. Osteogenic cell lines will be used to assess biocompatibility as well as the formation and localisation of extracellular matrix. In later stages of the project the ingrowth of bone into the pores will be investigated in vitro.

REFERENCES:

1. Learmonth, I.D., Young, C., and Rorabeck, C., 2007. The operation of the century: Total hip replacement. *The Lancet*, 370, 1508-1519.
2. Bobyn, J.D., Stackpool, G.J., Hacking, S.A., Tanzer, M., and Krygier, J.J., 1999. Characteristics of bone ingrowth and interface mechanics of a new porous tantalum biomaterial. *Journal of Bone and Joint Surgery – Series B*, 81, 907-914.
3. Heintl, P., Rottmair, A., Körner, C., and Singer, R.F., 2007. Cellular titanium by selective electron beam melting. *Advanced Engineering Materials*, 9, 360-364.

ACKNOWLEDGEMENTS:

The authors would like to thank Dr Michael Blackmore and Mr Everth Hernandez for their help in using the EBM-S12 and the design software, and the Furlong Research Charitable Foundation for financially supporting this project.

Autologous keratinocytes and fibroblasts delivered on microcarriers in combination with Integra™ significantly reduce wound contraction *in vivo* in the porcine model of wound repair

Y Martin¹, M Eldardiri¹ & JR Sharpe¹

¹ [Blond McIndoe Research Foundation](#), Queen Victoria Hospital, East Grinstead, West Sussex.

INTRODUCTION: Large full-thickness injuries to the skin, caused by burns or other forms of trauma, can lead to the formation of scars and contractures. These cause pain to the patient and can significantly reduce mobility. Wound contraction can be reduced when wounds are treated with skin grafts or dermal substitutes, particularly in combination with autologous keratinocytes (AK) or fibroblasts (AF)^{1,2}. Biodegradable gelatin Cultisphere™-G microcarriers (PerCell Biolytica) can be used to expand and deliver cells directly to the wound bed.

Our *in vivo* study investigated the effect on wound healing and contraction after treatment with the dermal substitute Integra™ in combination with ultra-thin skin graft (uSTSG), sprayed autologous keratinocytes (SAK), and lastly, either autologous keratinocytes alone (MCAK) or a mixture of autologous keratinocytes and autologous fibroblast (MCAK/AF), both of these treatments being delivered to the wounds on Cultisphere™-G microcarriers. The quality of epithelial repair was assessed by histology and the extent of wound contraction measured over a 21 day treatment period.

METHODS: Twenty-four 4 x 4 cm square full thickness wounds in large white pigs were treated with Integra™, followed by uSTSG, SAK, MCAK or MCAK/AF. Contraction was measured using Visitrak™ (Smith&Nephew). Wounds were excised and snap frozen for histological analysis.

RESULTS: Histological analysis showed a comparable quality of epithelial repair in all treatment groups, as evidenced by H&E staining and markers for basal keratinocytes (cytokeratin 14) and the basement membrane (collagen VII and laminin) (Fig 1). We identified that contraction was significantly reduced upon treatment with SAK, MCAK and MCAK/AF compared to uSTSG. In addition, MCAK/AF-treated wounds contracted significantly less than all other groups.

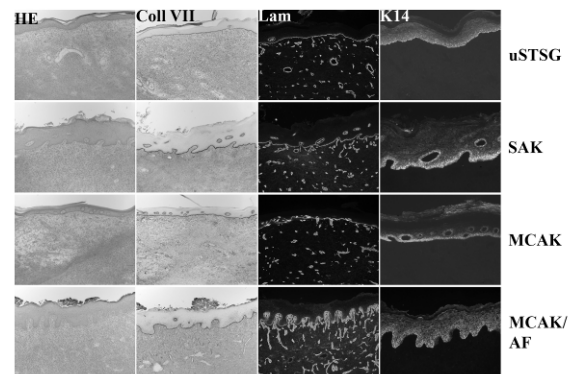


Fig. 1: Histology showed epithelial cover in all wounds (H+E staining, 5x), the presence of a basement membrane (Coll VII and Lam, 5x) and proliferating basal keratinocytes (K14, 10x).

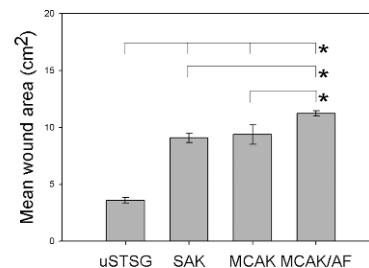


Fig. 2: Mean wound area at day 21 showed significant differences between treatment groups ($p = 0.05$), error bars show standard deviation.

DISCUSSION & CONCLUSIONS: The reduction in wound contraction observed in this *in vivo* study shows great potential for clinical benefit in the treatment of full thickness wounds in patients.

REFERENCES:

- ¹Reid, MJ, et al. Wound Repair Regen **15**, 889, 2007
- ²Lamme, EN, et at. J Pathol **190**, 595, 2000

ACKNOWLEDGEMENTS: This work was supported by Sparks and The Charles Wolfson Charitable Trust.

Investigation of seven candidate scaffolds for the production of an autologous tissue engineered connective tissue for use in stress urinary incontinence and pelvic organ prolapse

A Mangera^{1,2}, AJ Bullock¹, CR Chapple², S MacNeil¹

¹Kroto research institute, Department of tissue engineering, University of Sheffield, UK. ²Royal Hallamshire hospital, Sheffield, UK

INTRODUCTION: Currently no ideal material has been identified for use in the surgical management of stress urinary incontinence (SUI) and pelvic organ prolapse (POP). Our aim was to assess seven different scaffolds; Alloderm (AL), cadaveric dermis (CD), polypropylene (PPL), sheep forestomach (SF), porcine dermis (PD), porcine small intestinal submucosa (SIS) and thermoannealed poly(L)-lactic acid (Th PLA) for potential use as a scaffold for the attachment of fibroblasts to create a tissue engineered connective tissue suitable for use in SUI and POP.

METHODS: We expanded oral mucosal fibroblasts obtained with full patient consent and ethical approval. Fibroblasts (800 000) were seeded onto 4cm² pieces of the seven different matrix materials and were cultured for a period of two weeks in 10% DMEM medium. The tissue engineered matrices were assessed for: cell attachment using AlamarBlue (a vital stain) and DAPI (a nuclear stain), total collagen production by Sirius red staining, collagen types I,III, IV and elastin by immunostaining, and extracellular matrix (ECM) production by scanning electron microscopy (SEM).

RESULTS:

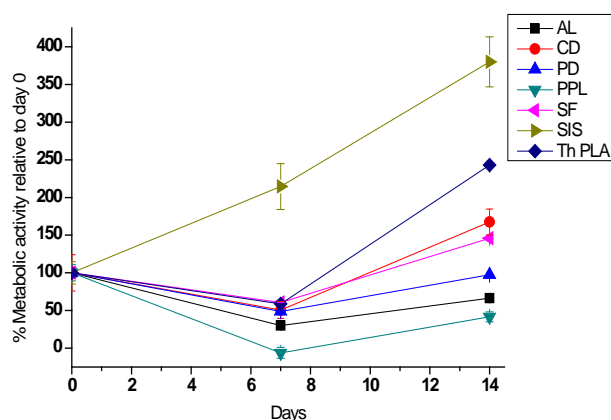


Fig. 1: Metabolic activity of cells on the different scaffolds over 14 days relative to day 0, $n=9 \pm SEM$

Fig 1. Shows that the metabolic activity of cells on the scaffolds was greatest on SIS followed by Th PLA. DAPI (images not shown) and Sirius red staining (Fig 2) revealed this was due to cell

proliferation and collagen/ elastin production. Fibroblasts produced collagen I, III and elastin (Table 1). SEM revealed abundant new ECM on Th PLA and a good matrix on SIS.

Table 1. Production of collagens I, III, IV and elastin assessed by immunofluorescence and ECM production by SEM. (Qualitative scale of: - absent, +/- equivocal, + some, ++ good, +++ abundant)

Material	Col I	Col III	Col IV	Elastin	ECM
AL	+	+	-	+	+
CD	+	-	-	-	+
PD	-	-	-	-	+/-
PPL	-	-	-	-	-
SF	+	-	-	+	+/-
SIS	++	+	-	++	+
Th PLA	++	+	-	+++	+++

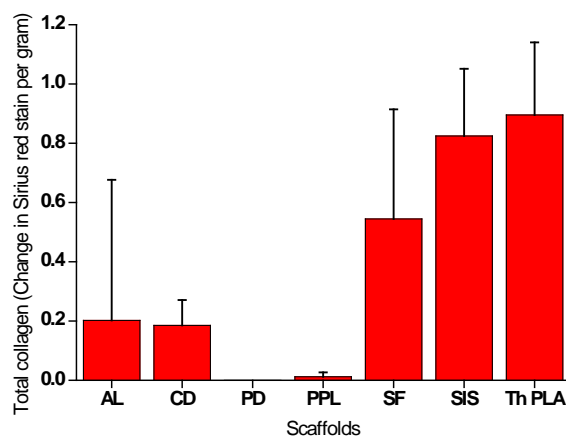


Fig 2. Production of collagen by cells on scaffolds over 14 days culture, $n=9 \pm SEM$

DISCUSSION & CONCLUSIONS: Both Th PLA and SIS are good scaffolds which support fibroblasts and allow the production of a new connective tissue matrix containing collagen I, III and elastin *in vitro*. We conclude that both should now be assessed in animal studies to assess tissue integration and vascularisation.

ACKNOWLEDGEMENTS: The Urology Foundation and Robert Luff foundation

INFLUENCE OF SURFACE PATTERN AND STERILISATION OF SOLVENT-CAST FILMS FOR PERIPHERAL NERVE GUIDANCE

A Gibb, SA Mobasseri, LA Bosworth & S Downes

Materials Science Centre, Faculty of Engineering and Physical Sciences, University of Manchester, UK

INTRODUCTION: Damage to peripheral nerves can result in considerable morbidity and loss of function. Poly-(ϵ -caprolactone) (PCL) and PCL/poly-(D,L-lactic acid) (PLA) blend nerve guidance conduits are a promising alternative to autologous nerve grafts in the treatment of peripheral nerve injury¹. The surface morphology of scaffolds is known to influence their physical properties and cell behaviour. Yet, as scaffolds progress further towards clinical trials, it is imperative that they are subjected to/and capable of withstanding approved sterilisation methods, such as gamma irradiation, without causing detrimental effects to the material physical properties and/or cell response. This study investigates how surface patterns affect PCL films and aims to assess whether PCL/PLA blend scaffolds are able to withstand gamma irradiation sufficient for medical sterilisation.

METHODS: PCL and PCL/PLA (4:1 w/w) blend solutions were prepared using dichloromethane (3% w/v). Smooth, pitted and micro-grooved PCL films were cast and imaged using scanning electron microscopy (SEM), while tensile testing was used to quantify their mechanical properties (Instron 1122, load cell 0.010 kN). NG108-15 cells were cultured up to 14 days on the various PCL film surfaces before fluorescence and SEM imaging were performed both to confirm biocompatibility and observe cell behaviour. PCL/PLA blend films will be sterilised at 7 incremental doses of gamma radiation (15-45 kGy) (Isotron). Mechanical testing, differential scanning calorimetry, Fourier transform infrared spectroscopy and gel permeation chromatography will be utilised to evaluate any changes in material properties or structure in comparison to unirradiated control samples.

RESULTS: The mean thickness of all types of solvent-cast film was less than 100 μm . The average porosity of the pitted PCL films was 53% with $2.1 \pm 0.5 \mu\text{m}$ diameter pits. Smooth films were significantly stronger, with greater modulus and strain (Table 1, * $p < 0.01$). NG108-15 cells attached and proliferated on the PCL films *in vitro* up to 14

days. However, only on the grooved samples did cells display organisation, demonstrating alignment in the same orientation as the grooves (Fig. 1).

Table 1. Mechanical properties of PCL films.

	Smooth	Pitted	Grooved
Max. Stress (MPa)	11.9 \pm 1.8*	5.9 \pm 1.5	4.4 \pm 1.3
Modulus (MPa)	106 \pm 25.5*	61.2 \pm 22.4	50.2 \pm 16.6
Max. Strain (mm/mm)	6.2 \pm 1.7*	3.8 \pm 1.1	3.6 \pm 1.2

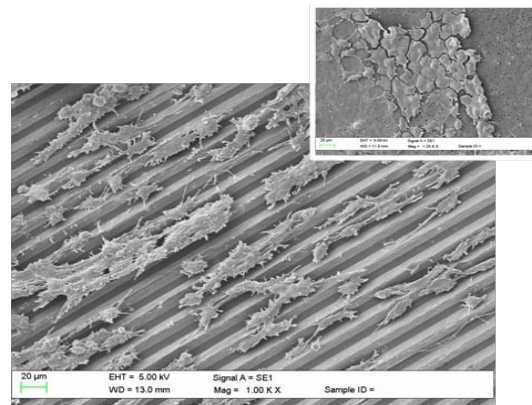


Fig. 1: Scanning electron micrograph of aligned NG108-15 cells on grooved PCL film, day 14. (Inset: unaligned cells on pitted film, day 10).

DISCUSSION & CONCLUSIONS: These findings support the use of solvent cast PCL films for fabricating nerve guides. Pits in the surface of the inner lumen are beneficial in cell growth and grooved surfaces enable the alignment of neurons. In this work all patterned surfaces had sufficient tensile strength to function as nerve conduits. PCL/PLA blended films were tested to see whether they would withstand medical-grade sterilisation. It is hypothesised that the polymer films will not be significantly affected by gamma irradiation.

REFERENCES: ¹ Sun, M., et al., *In vitro and in vivo testing of novel ultrathin PCL and PCL/PLA blend films as peripheral nerve conduit*. J Biomed Mater Res A, 2010. **93**(4): p. 1470-81.

Acellular Allogeneic Cardiac Valves

T Vafae¹, D Thomas¹, P Rooney², J Kearney², H Berry³, S Korossis¹, J Fisher¹ and E Ingham¹

¹*Institute of Medical and Biological Engineering, Faculties of Engineering & Biological Sciences, University of Leeds, Leeds, LS2 9JT, UK*

²*NHS Blood and Transplant Tissue Services, Speke, Liverpool, L24 8RB, UK*

³*Tissue Regenix Group plc, The Biocentre, York, YO10 5NY, UK*

INTRODUCTION: Over 5,000 patients benefit from heart valve replacement in the UK annually. Cryopreserved allografts are the “gold standard” but they are subject to immunological responses leading to calcification and stenosis resulting in multiple reoperations. We have previously developed methods to remove the immunogenic cells from porcine cardiac valves whilst maintaining the biochemical and biomechanical properties of tissues, creating immunocompatible replacements^{1,2}. These have been shown to regenerate in the pulmonary position of juvenile sheep. Acellular human pulmonary valves treated using our technology has been implanted into patients by our collaborators in Brazil³. This project aims to translate acellular human cardiac valve technology and produce biomechanically and immunologically compatible scaffolds for heart valve replacement in patients in the UK.

METHODS: Human aortic and pulmonary valves were obtained from NHS BT TS with full ethical approval. An established decellularisation process was applied to 5 aortic and 3 pulmonary conduits. Cryopreserved cardiac valve conduits were treated consecutively with hypotonic buffer, sodium dodecyl sulfate (0.1%) in hypotonic buffer plus protease inhibitors, and nuclease solution¹. Half of each of the decellularised conduits analysed by H&E and Dapi staining of two sections of each valve (200µm interval). Non-treated cryopreserved conduits were analysed for comparative purposes. The DNA content of the acellular tissues was compared to non-treated cryopreserved conduit tissues to assess the extent of decellularisation. DNA was extracted from 140-250 mg of the acellular and 25 mg of the non-treated leaflet, wall, ventricular muscle and junction (joining of the leaflet to the wall) from replicate tissues using the DNeasy kit. The levels of DNA were measured using a NanoDrop spectrophotometer and DNA content expressed as µg/mg of tissue. **RESULTS:** The histological analysis (H&E staining) of the control cryopreserved and acellular cardiac valve conduits revealed no evidence of cell nuclei or cell remnants in the leaflet, wall or ventricular muscle of the decellularised tissues.

The tissues retained histioarchitecture following the decellularisation process. The absence of cell nuclei was confirmed by Dapi staining. Quantification of the DNA remaining in the tissues compared to the control tissues confirmed that 94-99.6 % of the DNA had been removed from the aortic and pulmonary valve conduits (Fig1, Table1).

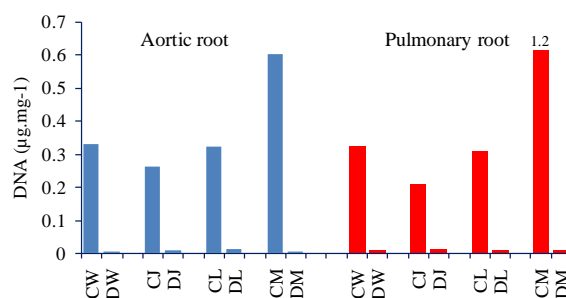


Fig. 1: Comparison of total DNA in cryopreserved and decellularised cardiac valve tissues.

Data is expressed as the means (n=3) ± 95% CL
C: cryopreserved, D: decellularised, W: wall, J: junction, L: leaflet, M: ventricular muscle.

Table 1. The percentage reduction in DNA content following decellularisation.

Cardiac valves	wall	junction	leaflet	muscle
Aortic	98.2 %	97.1%	97.3%	99.5%
Pulmonary	97.6%	94%	96.5%	98.3%

DISCUSSION & CONCLUSIONS: Allogeneic cardiac valves were successfully decellularised whilst maintaining their gross histioarchitecture. Future work will investigate the effect of the treatment on the biochemical properties and biomechanical behaviour of the allogeneic valvular scaffolds. In addition the process will be translated to NHSBT Tissue Services who will develop GMP manufacturing routes.

REFERENCES:

- Booth et al., J HVD (2002); 11(4): 457-62
- Korossis et al., J HVD (2002); 11(4): 463-7
- Da Costa et al., J HVD (2009); 18(1):84-941

ACKNOWLEDGEMENT: We would like to thank regeNer8 for funding this project.

Using a Tissue Engineering Approach for the treatment of Cleft Palate.

F. Bye¹, S. Puwanun, G. Reilly & S. MacNeil

¹ Department of Materials Science and Engineering, Kroto Institute, University of Sheffield.

INTRODUCTION: Cleft palate affects 1 in 700 live births in the UK and 1 in 1000 worldwide¹, requiring repeated surgery throughout childhood. Current implants used to replace the hard palate are inflexible and cannot grow with a child. The aim of this study was to develop an electrospun scaffold, which can be used for the closure of cleft palate defects and potentially, adapt to the rapid growth of a young patient's palate.

METHODS: The approach we are adopting is to produce a bi-layer electrospun membrane of poly hydroxybutyrate-co-valerate (PHBV) and poly L-lactide (PLA) resulting in a biocompatible, distensible and biodegradable graft material. This is being designed to allow growth of bone on one side, and oral mucosa on the other, preventing soft tissue invasion through the scaffold into the regions where the bone regeneration is required. A key requirement is to produce a scaffold which can respond to the rapid rate of growth of the young child. The mechanical properties were tested by spinning onto latex balloons (Fig.1) and observing the effects of inflation.

RESULTS: Scaffolds were designed to ensure a plastic deformation occurred, rather than elastic, to prevent upper jaw collapse (Fig 1). A bi-layer membrane was then synthesised (Fig 2) and dermal fibroblasts (used here as model cells) were labeled with fluorescent dyes and showed no exchange between cells initially seeded onto the separate layers after 24 hours (Fig. 3).

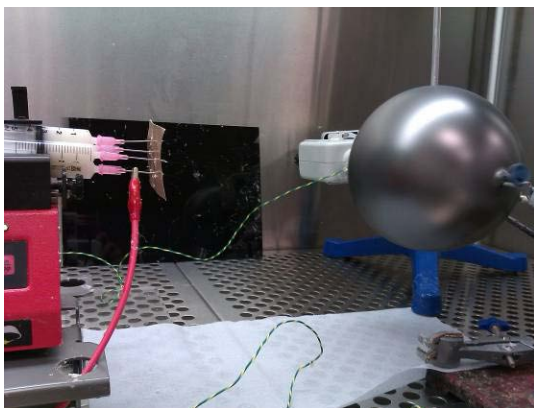


Fig. 1: Electrospinning onto a balloon.

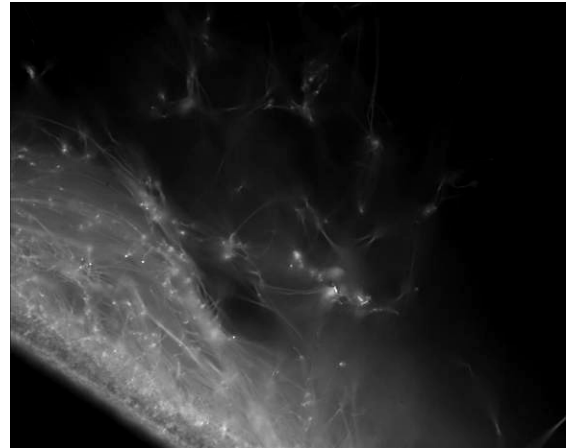


Fig.2: Electrospun PLA-PHBV bi-layer .

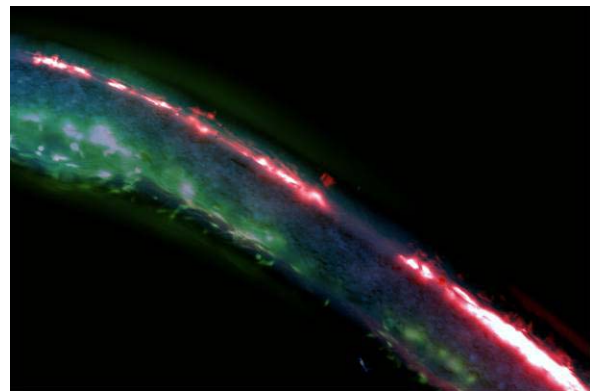


Fig. 3: Scaffold (blue) with red and green stained fibroblasts after 24 hours.

DISCUSSION & CONCLUSIONS: It is possible to create a bi-layer membrane that segregates labeled cells for at least 24 hours. This provides the basis for now seeding this scaffold with bone forming cells on one surface and oral mucosa forming cells on the other surface. The mechanical properties of the scaffold are being investigated and we are developing a system to examine growth of cells on a scaffold under varying degrees of distension .

REFERENCES: ¹ C. Chah, D.Wong (1980) Management of children with cleft lip and palate, *Canadian Medical Journal*. **122**:19-22.

ACKNOWLEDGEMENTS: BBSRC, Tony Ryan, Keyvan Moharamzadeh, Anthony Bullock.

Basement Membrane Protein Orchestrates Network Formation By Endothelial Cells in 3D: Laminin the Conductor

K Stamati¹, J V Priestley^{1,2}, V Mudera¹ & U Cheema¹

¹ Tissue Repair and Engineering Centre, Institute of Orthopaedics and Musculoskeletal Sciences, UCL Division of Surgery and Interventional Science, University College London, Stanmore Campus HA7 4LP ² Centre for Neuroscience & Trauma, Blizard Institute of Cell and Molecular Science Barts and The London School of Medicine and Dentistry, 4 Newark Street Whitechapel London E1 2AT

INTRODUCTION: Engineering vascular networks within 3D tissue models is paramount for the survival of cells in large 3D constructs. This is critical for both *in vitro* and *in vivo* survival. Our work has focused on network formation by endothelial cells in co-cultures with Human bone marrow stromal cells (HBMSCs) in 3D. We have examined the effect of matrix composition on endothelial cell morphology and our results emphasize the importance of basement membrane proteins for inducing network formation by endothelial cells.

METHODS: Human umbilical vein endothelial cells (HUVECs) and HBMSCs were cultured in 3D collagen type I constructs with and without the addition of the basement membrane protein laminin, to test the effect of matrix composition on endothelial cell morphology, assessed by CD31 immunostaining.

RESULTS: Differences in cell behaviour were significant, with cells showing distinct morphologies, dependent on the matrix composition they were seeded in. Cells in collagen type I only constructs aggregated in a cobblestone-like morphology, whereas endothelial cells in collagen with added laminin formed networks (figure 1). The networks showed variable characteristics, with smaller (~60µm) structures, to more multinucleate, longer (~170µm) structures.

DISCUSSION & CONCLUSIONS: Our results suggest that the interaction of endothelial cells to a basal membrane component such as laminin, is critical for network formation. Cell to matrix attachments, mediated by integrins are thought to be important regulators of cell behavior and angiogenesis in 3D [1]. Integrin expression has been manipulated extensively in experimental designs, with the addition of elements such as PMA (phorbol myristate acetate), known to increase specific expression of integrins as well as inducing collagen invasion, thereby affecting vessel-like tube formation [2,3]. Furthermore, cell-

cell interactions, such as adherens junctions and tight junctions differ dependent on the extracellular matrix components surrounding the cells [1]. Notably however, endothelial cells from different sources also show variable responses to each matrix component [1].

By identifying the parameters which lead to specific types of endothelial cell aggregation, we can develop strategies to predictably control cell morphologies in 3D.

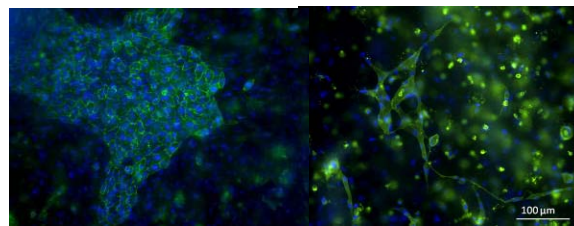


Fig 1. Cobblestone morphology in co-cultures of HUVECs and HBMSCs in 3D collagen type I (left) and network formation in 3D collagen type I with laminin (right) (CD31 staining in green, DAPI in blue).

REFERENCES: ¹Dye J.F., Lawrence L., Leach L., Firth J.A., Clark P. (2004) Distinct Patterns of Microvascular Endothelial Cell Morphology Are Determined by Extracellular Matrix Composition *Endothelium* **11**: 151-167. ²Montesano R. and Orci L. (1987) Phorbol Esters Induce Angiogenesis in vitro from large-vessel endothelial cells *Journal of Cellular Physiology* **130**:284-291. ³Defilippi P., van Hinsbergh V., Bertolotto A., Rossino P., Silengo L., Tarone G. (1991) Differential distribution and modulation of expression of Alpha1/Beta1 Integrin on Human Endothelial Cells *The Journal of Cell Biology* **114**:855-863

ACKNOWLEDGEMENTS: UC is a BBSRC fellow and KS is funded by the UCL Impact Studentship and Oxford Optronics.

Chemical treatment of PCL films affects biocompatibility for nerve regeneration

A C de Luca^{1,2}, G Terenghi¹ & S Downes²

¹ *Blond McIndoe Laboratories, School of Medicine, University of Manchester, UK*

² *Materials Science Centre, Department of Engineering and Physical Sciences, University of Manchester, UK*

INTRODUCTION: Synthetic materials, like polycaprolactone (PCL) have been used in tissue engineering to realise artificial conduits for nerve regeneration¹. The most important factors affecting material biocompatibility are wettability and surface charge^{2,3}. As PCL is classified as a hydrophobic material, in this study hydrolysis and aminolysis were carried out on the surface of the scaffold in order to create different functional groups characterised also by different contact angles. The NG108-15 cell response was finally investigated to compare the biocompatibility of all the scaffolds.

METHODS: PCL pellets were dissolved in dichloromethane (DCM) in a concentration of 3% wt/v and the solution was spread on glass coverslips, allowing the solvent to evaporate. Three different solutions were prepared: sodium hydroxide (NaOH) 10M, potassium hydroxide (KOH) 10M and hexamethyldiamine (HMD) in isopropanol (IPA) 10% wt/v. PCL films were soaked in one of the solutions for 1 hour at room temperature and rinsed with distilled water afterwards. The sessile drop contact angle was measured for each sample to evaluate surface hydrophilicity (n=5). Scaffold biocompatibility was finally assessed with NG108-15 cells through proliferation assay (Alamar Blue) (n=3) for 5 days and neurofilament staining.

RESULTS: Surface treatments with NaOH and KOH reduced remarkably the contact angle ($p < 0.05$), hence increasing the surface hydrophilicity compared to untreated and HMD treated films (Table 1). After treatment, the biocompatibility of PCL films increased remarkably, as shown in Fig. 1.

Table 1. Contact angle of the different scaffolds with and without surface treatments.

Material	Contact angle(°)
U-PCL	76.58±1.25
NaOH Treat.	54.13±2.73***
KOH Treat.	56.83±2.88***
HMD Treat.	70.33±0.87

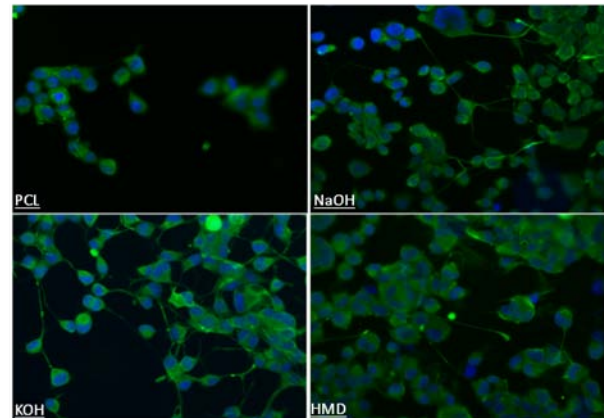


Fig. 1: Neurofilament staining of NG108-15 cells on untreated and treated PCL films.

DISCUSSION & CONCLUSIONS: Alkali treatment caused hydrolysis and increased film hydrophilicity by cleaving the ester bond of the polymer and introducing hydroxyl groups on the scaffold surface. No difference in cell interactions was observed when using the different hydroxide solutions (NaOH and KOH). It should be asserted that both alkali treatments enhanced PCL film biocompatibility. HMD treatment of PCL films did not decrease hydrophilicity, and yet cell proliferation was higher, as shown by Alamar Blue. This could be due to the formation of amino groups on the material surface. Importantly, the NG108-15 cell morphology was different from the other surfaces. The cells were more rounded with more cell to cell contact. This could not be attributed to differences in surface topography. Aminolysis may be used as a surface treatment for the inner lumen of PCL nerve conduits.

REFERENCES: ¹ M. Sun, P.J. Kingham, A.J. Reid, et al. (2010) *J Biomed Mat Res Part A* **93A**:1470-81. ² Y. Ikada (1994) *Biomaterials* **15**:725-36. ³ M.H. Lee, et al. (2005) *Biomaterials* **26**:1721-30.

ACKNOWLEDGEMENTS: The authors would like to thank Newby Trust Ltd. for providing financial support to this project.

IMMUNOGENICITY OF ALLOGENEIC MESENCHYMAL STEM CELLS

B Mukonoweshuro, C Brown & E Ingham

¹Institute of Medical and Biological Engineering, Faculty of Biological Sciences, University of Leeds, UK.

INTRODUCTION: Adult mesenchymal stem cells (MSC) have utility in tissue engineering, regenerative medicine and cell-based therapies¹. However, use of allogeneic MSC in clinical settings is hampered by histocompatibility barriers as the immunological properties of MSC remain controversial. Recent studies' investigating their immunogenicity suggests that allogeneic MSC are immunoprivileged and possess immunosuppressive properties which may be of therapeutic value in allogeneic transplantation in various clinical and medical applications². In this project, we seek to systematically investigate the immunological properties of allogeneic MSC using a mouse model system which employs 2 genetically distinct strains; Balb/c (*H2 d*) and C3H (*H2 k*) which are used as responder (recipient) and stimulator (donor) respectively.

METHODS: MSC were isolated from Balb/c and C3H mice by flushing femurs with culture medium. Plastic adherent cells were selected through continuous culture and passage until homogeneous cultures were obtained. The cells were characterised by flow cytometry for the expression of cell surface markers. Tri-lineage differentiation into adipogenic, chondrogenic and osteogenic lineages was confirmed by histological staining. Expression of lineage specific genes was determined by RT-PCR. One way mixed lymphocyte reactions (MLR) were used to test MSC immunosuppression and lymphocyte proliferation assays (LTA) to test for immunogenicity at various cell ratios and incubation periods up to 15 days. Mononuclear cells (MNC) used in the MLRs and LTAs were isolated from spleens and lymph nodes of mice by means of Lymphoprep gradients.

RESULTS: MSC from Balb/c and C3H mice expressed Sca-1, CD 29, CD 90.2, MHC 1, CD 44 and CD 105 but were negative for co-stimulatory molecules CD 80 and CD 86, MHC II, hematopoietic markers CD 34 and CD 45 and the macrophage marker CD 11b. MSC from Balb/c and C3H mice were differentiated into adipocytes, chondrocytes and osteocytes and expressed lineage specific markers (Figure 1). In one-way MLRs, both allogeneic and syngeneic MSC significantly suppressed Balb/c lymphocyte proliferation. However, allogeneic MSC, but not syngeneic MSC stimulated Balb/c lymphocyte proliferation (Figure 2).

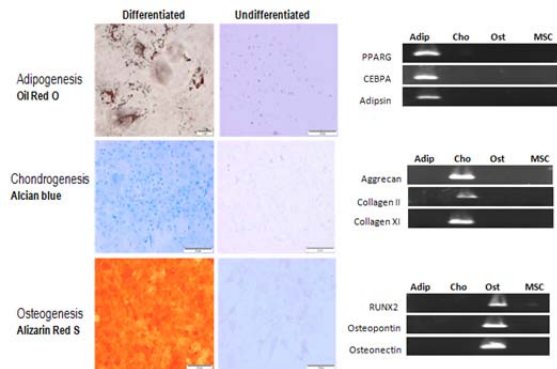


Figure 1: C3H MSC tri-lineage differentiation and gene expression

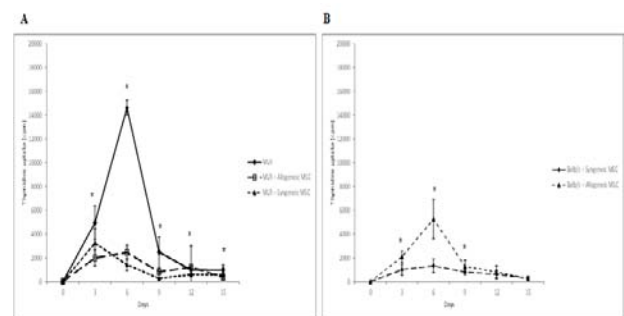


Figure 2 : MSC immunological properties (A) MSC mediated suppression of one –way MLR and (B) allogeneic C3H MSC stimulation of Balb/c MNC. (data shows mean \pm 95%CL)* $p < 0.05$ ANOVA

DISCUSSION & CONCLUSIONS: Despite their ability to inhibit immune responses, allogeneic MSC were shown to be immunogenic suggesting that MSC may not be immunoprivileged. Further investigations of the mechanisms underlying the immunological properties of the MSC are being carried out.

REFERENCES: ¹ Barry, F. P. & J. M. Murphy (2004). *International Journal of Biochemistry and Cell Biology* **36**(4): 568-584.

² Bartholomew, A., C. Sturgeon, M. et al (2002). *Experimental Hematology* **30**(1): 42-48.

ACKNOWLEDGEMENTS: This work is funded by the Faculty of Biological Sciences, The Beit Trust and also through WELMEC, a Centre of Excellence in Medical Engineering funded by the Wellcome Trust and EPSRC, under grant number WT 088908/Z/09/Z.

ASSESSMENT OF THE ANTIMICROBIAL ACTIVITY OF ACELLULAR VASCULAR GRAFTS.

K Owen, S-P Wilshaw¹, S Homer-Vanniasinkam², R Bojar, H Berry & E Ingham¹

¹*Institute of Medical and Biological Engineering, Faculty of Biological Sciences, University of Leeds, UK.*

²*Vascular Institute, Leeds General Infirmary, Leeds*

INTRODUCTION: Vascular graft infections are a devastating complication of bypass surgery. To address this problem antimicrobial impregnated synthetic vascular grafts are now available; however these grafts still exhibit the disadvantages of synthetic graft materials, namely thrombogenicity and poor patency rates. Several studies have reported biological vascular grafts to be more resistant to bacterial infection than synthetic counterparts *in vivo*¹, indeed small intestinal Submucosa (SIS) materials have previously been reported to be antimicrobial². The aim of this study was to assess the inherent antimicrobial activity of a novel acellular vascular graft and compare it to commercially available vascular materials.

METHODS: Acellular vascular grafts were prepared from porcine femoral arteries using a proprietary method³ which involved washing in hypotonic buffer with low concentration sodium dodecyl sulphate in conjunction with nuclease treatment⁴. Decellularisation was validated using histological methods and quantification of DNA. Biocompatibility of the acellular vessels was assessed using contact cytotoxicity and extract cytotoxicity tests. Antimicrobial activity was determined using the disk diffusion assay and minimum inhibitory concentration (MIC) assays using MRSA, MSSA, *S. epidermidis*, *E. faecalis*, *E. coli*, *P. aeruginosa*, *K. pneumoniae* and *C. albicans*. Positive control agents included: vancomycin, tobramycin, gentamycin, ciprofloxacin, levofloxacin, rifampin and fluconazole. Graft materials used were; fresh tissue, acellular tissue, SIS, ePTFE and Dacron. Two methods were used to extract materials into solution; the first was to extract into Dulbecco's modified Eagles medium (DMEM), the second was based on a published method³. Resistance to biofilm formation was assessed by growth of bacterial species on the surface of the vascular materials compared to a nitrocellulose disk control. The inoculated materials were incubated for 24 hours at 37°C. The colony forming units were released and enumerated.

RESULTS: Histological analysis confirmed porcine femoral artery decellularisation; DNA quantification indicated a 95-97 % reduction in total DNA. Biocompatibility analysis demonstrated that the acellular arteries did not affect the growth of the cell lines used, either as whole tissue or extracts. Disk diffusion assays did not identify antimicrobial activity for any of the materials tested (*Figure 1*). MIC results were similar for both extraction methods. None of the graft materials inhibited visible bacterial growth when cultured with microbes for 24 hours. Biological materials resisted biofilm initiation to a greater extent than synthetic materials when inoculated with MRSA and *S. epidermidis*.

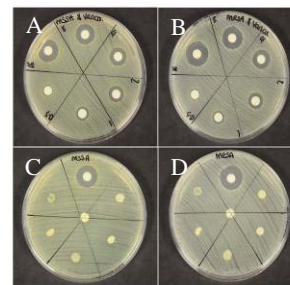


Fig. 1: Disk diffusion assay with MSSA and MRSA. A&B standard plates: disks loaded with various concentrations of vancomycin. C&D Positive controls produced a zone of inhibition, all materials failed to inhibit bacterial growth. Results are representative of all organisms tested.

DISCUSSION & CONCLUSIONS: Acellular grafts produced in this study were not antimicrobial but resisted the initiation of biofilm formation to a greater extent than the disk controls. SIS was not found to have antimicrobial activity as previously reported in the literature.

REFERENCES: ¹ P Klinkert, A Schepers, D Burger et al (2003) *J Vas Surg* 37: 149-155. ² A Sarikaya, R Record, C Wu et al (2002) *Tissue Eng* 8(1): 63-71 ³ Fisher J, Booth C, Ingham E, inventors, *Decellularisation of matrices. United States patent 7354749. 2008.*

ACKNOWLEDGEMENTS: *I would like to thank the BBSRC and Tissue Regenix Group PLC for funding this work.*

Tissue Engineering of the Anterior Cruciate Ligament; Current Clinical Opinions

S Rathbone¹, N Maffulli² & S Cartmell¹

¹ *Materials Science Centre, University of Manchester*

² *Institute of Health Sciences Education, Centre for Sports and Exercise Medicine,
Queen Mary University of London*

INTRODUCTION: There are an increasing number of injuries every year to ligaments, the majority of which occur through sporting activities such as skiing, football and basketball which involve running and jumping [1]. As a result over 800,000 people world wide need to obtain medical treatment annually [2]. The resulting rupture or tear causes great pain and results in loss of function of the associated joint which can lead to early development of osteoarthritis [3-4].

Donor site morbidity, poor graft site integration (causing slippage) and incorrect mechanical performance are all common problems with grafts currently used for repairing the anterior cruciate ligament (ACL) [5-7]. A tissue engineered (TE) ligament has potential to overcome these problems. We have obtained input from clinicians who currently treat these injuries to deal with any potential design short-comings associated with TE ACLs before they arise.

METHODS: An online questionnaire was created relating to ACL tissue engineering. The aim was to gain the opinions of orthopaedic surgeons towards using a tissue engineered ligament if it were an option, if it could be an improvement upon the existing methods. The questionnaire was peer reviewed and approved by local research ethics committee (project number 09/H1204/64, approved 15/10/09). Between July and October 2010, three hundred orthopaedic surgeons specialising in ligament and tendon repair in the UK were contacted by email and invited to participate. From this e-mailed input request, seventy nine surgeons responded.

RESULTS: 86% (61/71) of surgeons would consider using a TE ACL if it were an option (provided it showed biological & mechanical success), if it significantly improved the patient satisfaction (63% - 45/71) and shortened surgical time (62% - 44/71), where they would be prepared to wait 4-30 weeks for it to be created. 42% (30/71) were either concerned or very concerned (25% - 18/71) about its successful integration into

the bone. The majority of surgeons (76% - 53/70) felt that using a TE ACL would be more appropriate than a patellar tendon, hamstring or quadriceps autograft if it could be engineered to be an exact match to the native tissue. 62% (44/71) thought using a TE ligament would take less surgical time and felt surgical time needs to be reduced by 10-30 minutes to be considered to be a significant improvement.

DISCUSSION & CONCLUSIONS: Overall it appears that most surgeons would be prepared to use a TE ligament. Future research needs to concentrate on integration of the TE ACL into the patients' bone. This information confirms a demand for tissue engineered ACL's and highlights important areas for improvement.

REFERENCES: ¹ J. Cooper, H. Lu, F. Ko, et al (2005) *Biomaterials* **26**: 1523-1532. ² J. Cooper, L. Bailey, J. Carter, et al (2006) *Biomaterials* **27**: 2747-2754. ³ E. Gentleman, G. Livesay, K. Dee et al (2006) *Annals of Biomedical Engineering* **34**: 726-736. ⁴ D. Doroski, D. Brink, J. Temenoff, et al (2007) *Biomaterials* **28**: 187-202. ⁵ M. Hairfield-Stein, C. England, H. Paek, et al (2007) *Tissue Engineering*: **13**: 703-710. ⁶ H. Lu, J. Cooper, S. Manuel, et al (2005) *Biomaterials* **26**: 4805-4816. ⁷ A. Vergis and J. Gillquist (1995) *Arthroscopy: The Journal of Arthroscopic and Related Surgery* **11**: 312-321.

ACKNOWLEDGEMENTS: We acknowledge a BBSRC and Giltech Ltd. CASE studentship for funding. We also acknowledge the assistance of Mark Smith (Keele University) for website space.

Rapid Fabrication of Density Gradient 3D Collagen Constructs

N Tan¹, R Drake² & RA Brown¹

¹ *Institute of Orthopaedics and Musculoskeletal Science, University College London, London, UK*

² *TAP Biosystems, Royston, UK*

INTRODUCTION: The directional migration of cells is an important factor of wound healing, tumour metastasis and development. Therefore, understanding cell guidance would be instrumental in the understanding of tissue-cell physiology and the advancement of tissue engineering. Cell migration is a complex process which involves guidance cues such as soluble chemo-attractants/repellents, and the insoluble extracellular matrix (ECM). Substrate stiffness in the ECM is one of the signals that guides cell movement. Thus, a density gradient in 3D constructs would be useful as a tool for studies on cell guidance in a more physiological condition, which may shed light on the mechanisms of tissue repair and improve the field of tissue engineering.

Previous work from this group identified a simple method to make a 3D construct from cells and collagen with a linear density gradient¹. The advent of rapid tissue fabrication technology by collagen compression² (now a commercial device, RAFTTM, TAP Biosystems, Royston, UK) suggests that gradient constructs might also be made in the same way. We have also identified a simple means of measuring the density gradient formed.

METHODS: Each collagen gel was made up of a mixture of 1.6ml acid soluble rat tail collagen type I (2.20 mg/ml; First Link, UK), 0.2ml 10X Dulbecco's modified Eagle's medium (DMEM) (Gibco, UK) and 0.2ml 10X Eagle's minimum essential medium (MEM) (Gibco, UK) which was neutralised by drop-wise with 5M NaOH. Collagen gels with a density gradient were prepared by casting 2ml of collagen mixture each into 22mm diameter wells of a 12-well plate (Orange Scientific, Belgium) which had one end raised by 6cm, and allowed the collagen to set/stabilise in a 37°C CO₂ incubator for 30 minutes to give resultant gels with a 32° angle. After setting, the resulting gels were compressed vertically by paper rolls which absorbed the excess fluid in the gels as well as provided the force for compression, resulting in a dramatic decrease in construct height from 14mm (maximum thickness) to 25µm across its full diameter^{1,2}.

Staining and image analysis: Compressed constructs were immediately fixed with 4%

paraformaldehyde for routine wax embedding, sectioning and Picro-Sirius Red staining. The constructs were examined and imaged along their entire lengths using an Olympus BH-2 photomicroscope. The images were then converted to grayscale and inverted for the analysis using ImageJ. Regions of interest were selected along the length of the construct and the average staining intensity of each region determined by using the "Measure" function. A graph of staining intensity against distance along construct was then plotted (Fig. 1).

RESULTS: Discs of dense collagen (in multi-well plates) with a density gradient were made reproducibly following just 5min of compression using the RAFTTM system. The resulting constructs showed a stain gradient (\equiv density gradient) across in the predicted direction. Analysis of the staining intensity showed a linear increase from the predicted low density to high density side of the construct.

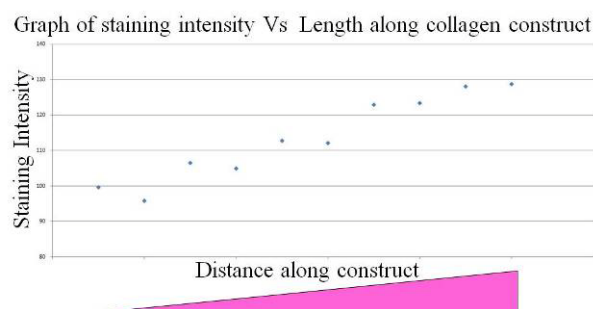


Fig. 1: Gradient of staining intensity \equiv density along the length of a collagen construct.

DISCUSSION & CONCLUSIONS: Rapid production of reproducible density gradients of collagen is now possible in a multi-well format using the RAFTTM technology. In addition, Picro-Sirius Red staining with image analysis is a good, rapid technique to confirm the gradient structure once made.

REFERENCES: ¹ E Hadjipanayi, V Mudera and RA Brown (2009). *Cell Motil. Cytoskeleton* 66:121-128. ² Alekseeva T., Jawad H., Purser M., Brown RA. 2011. *IFMBE Proceedings* 30:5-8.

ACKNOWLEDGEMENTS: BB-EPSRC funding.

Decellularisation of Super Flexor Tendon

G L Jones¹, A Llewellyn¹, H Berry², J Fisher¹ & E Ingham¹

¹ [Institute for Medical and biological Engineering](#), University of Leeds, Leeds LS2 9JT

² Tissue Regenix Group, The Biocentre York Science Park, Innovation Way, Heslington, York, YO10 5NY,

INTRODUCTION: Injuries to tendons and ligaments are becoming increasingly frequent, injury to the anterior cruciate ligament (ACL) being the most common. The current standard procedures for the reconstruction of the ACL are bone-patellar tendon-bone and hamstring autografts, however a major disadvantage is donor site morbidity. Allograft tissue is being used more widely, however the potential for disease transmission and immunogenic issues are a limitation. The ideal solution would be an “off the shelf” replacement. The aim of this project is to develop an acellular porcine super flexor tendon (SFT) graft which retains the essential biological and biomechanical properties of the native tissue, with a view to future clinical translation for ACL repair.

METHODS: Super flexor tendons were harvested from porcine hind legs obtained from an abattoir. The SFT runs from the ankle to the toes and is approximately 20 cm long. Whole tendons (n=8) were subjected to a decellularisation process adapted from a previously developed protocol for porcine meniscus¹. Following decellularisation, the tendon was sectioned into 4 cm length samples from each area of the tendon: toe attachment, middle and ankle attachment, for analysis. Removal of cells was determined by histological methods: haematoxylin and eosin, and DAPI stains. Non-treated tendons were analysed for comparative purposes. The DNA content of the acellular tissues was compared to non-treated tissues to assess the extent of decellularisation. DNA was extracted from 250 mg of the acellular and 25 mg of the non-treated tissues using the DNeasy kit. The levels of DNA were measured using a NanoDrop spectrophotometer and DNA content expressed as ng/mg of tissue. Biomechanical testing was by uniaxial tensile testing performed using a 5kN Instron 3365. Tendon was sectioned into 4 cm long samples from each area of the tendon, thinned and cut into a dumbbell shape. Tissues were preconditioned, before testing to failure at a strain rate of 150 % /minute.

RESULTS: The acellular tissue was shown to free of cells and cellular remnants in all regions as determined by H&E and DAPI staining (Figure 1). The DNA assay showed that the untreated tissue had 312 - 376 ng/mg of DNA and after decellularisation this was reduced to 2.8 - 6.5 ng/mg DNA showing 95 - 98 %

removal. Uniaxial tensile testing of different regions of the treated tissue showed that the failure strength was not significantly different to that of the fresh untreated tissue (Table 1).

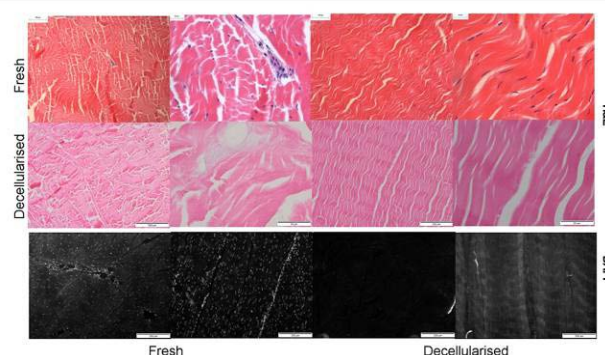


Figure 1, Haematoxylin and eosin, and DAPI staining of fresh (untreated) and decellularised tissue in cross section (through tissue and longitudinal (along crimp) sections).

	Failure Strength (MPa)		
	Toe	Middle	Ankle
Untreated	30.5±5.6	26.7±7.9	39.6±10
Decellularised	26.2±7.3	27.8±5.8	31.9±6.1

Table 1 Failure strength of fresh (untreated) and decellularised tissue. Data is presented as the mean (n=5 and ± standard deviation).

DISCUSSION & CONCLUSIONS: The porcine super flexor tendon was successfully decellularised with no major change in the tensile strength. Future studies will be carried out to determine the effects of the decellularisation process on the extracellular matrix composition of the treated tissue and biocompatibility of the acellular graft in small and large animal models.

REFERENCES: ¹ Stapleton *et al* 2008 Tissue Engineering Part A. 14(4):505-18.

ACKNOWLEDGEMENTS: This work was funded through WELMEC, a Centre of Excellence in Medical Engineering funded by the Wellcome Trust and EPSRC, under grant number WT 088908/Z/09/Z

Development of a microfabricated outer ring for corneal repair

I Ortega¹, P Deshpande¹, F Claeysens¹ & S MacNeil¹

¹ *Kroto Research Institute, Materials Science & Engineering Department, University of Sheffield, UK*

INTRODUCTION: Because of their unique features such as self-renewing and great capacity for specialization, stem cells are an interesting approach for the development of tissue regeneration techniques. Stem cells have specific locations in the body that are anatomical sites or microenvironments which regulate their behavior. Specifically, corneal epithelial stem cells are located at the limbus, in the structures known as Palisades of Vogt¹. Corneal epithelial regeneration and healing occurs by migration of cells from the limbus to the cornea. When the limbus is destroyed, the lack of limbal stem cells results in the migration of adjacent cells from the conjunctiva. These give a scar tissue with reduced vision or even blindness². For this reason, there is a necessity to develop new approaches for stem cell delivery onto damaged corneas. In this work we are designing a microfabricated outer ring for the cornea with micropockets that will simulate stem cell microenvironments.

METHODS: PEG diacrylate rings were fabricated using layer by layer photopolymerisation microstereolithography.

The polymer (purchased from Aldrich) was mixed with the photoinitiator (Camphorquinone, Aldrich) in a percentage 1% w:w. After stirring, the mixture was irradiated with a blue laser (MBL-III 473 nm; 150 mW) at times ranging from 30 to 120s. The uncured polymer was washed out with methanol and then dried for subsequent sterilization.

Preliminary cell work was performed using rabbit limbal fibroblasts. Cells were seeded at a concentration of 175,000 cells/ml and incubated for 7 days. The samples were observed using fluorescence microscopy and scanning electron microscopy.

RESULTS: The microstereolithography device allowed the preparation of big structures, rings around 1.2-1.3 cm in diameter, suitable for the size of the limbus area in the human eye. The microstructured holes were around 300µm in diameter (figure 1a). Using different microscopy techniques it was demonstrated that the cells used in these initial tests were able to move into the microfabricated holes or niches as shown in figures 1b and 2.

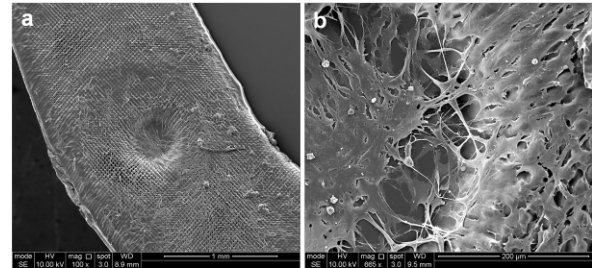


Fig. 1: SEM images of microfabricated niche (a) and rabbit limbal fibroblasts inside the niche (b).

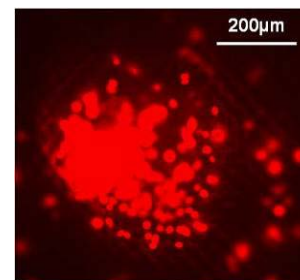


Fig. 2: Fluorescence image of limbal cells inside a microfabricated niche using Cell-Tracker Red.

DISCUSSION & CONCLUSIONS: PEG-diacrylate is widely used in the microfabrication of stem cell niches^{3,4}. In this study we have shown how cells can be located inside the microfabricated niches and successfully imaged using different techniques. As PEG-diacrylate is a not good cell-adhesive polymer we are now exploring different methods for functionalizing the basic structure and anchoring different proteins that will enhance limbal stem cell attachment. In conclusion, in this study we have fabricated an outer ring with 300 µm holes that will be used as possible stem cell niches. This provides the foundation for future research with limbal stem cells examining their behavior in these microfabricated structures.

REFERENCES: ¹ H S Dua, VA Shanmuganathan, et al. (2005) *Br J Ophthalmol* **89**:529-32. ² AJ Huang, SC Tseng (1991) *Invest Ophthalmol Vis Sci* **32**:96-105. ³ JM Karp, J Yeh, G Eng, et al. (2007) *Lab Chip* **7**:786-94. ⁴ YY Choi, BG Chung, DH Lee, A. Khademhosseini, et al. (2010) *Biomaterials* **31**:4296-303.

ACKNOWLEDGEMENTS: This work is supported by the Wellcome Trust Foundation.

Microstructuring of Photocurable Biomaterials with Applications in Neuronal Repair

A Gill¹, K Pawar¹, I Ortega¹, J Haycock¹ & F Claeysens¹

¹ *Biomaterials and Tissue Engineering Group, Kroto Research Institute, Department of Materials Science and Engineering, University of Sheffield*

INTRODUCTION: Photocurable low molecular weight oligomers of the well described biomaterials polylactic acid and polycaprolactone have been developed for microstructuring via projection microstereolithography, two-photon laser direct write or soft-lithography (PDMS stamping)

Initial structuring results with these materials have been promising and the suitability of these materials for the fabrication of nerve guidance conduits (NGC's) and cell encapsulation devices is being explored. Initial cell culture results indicate that the materials are biocompatible, cell adhesive and capable of supporting Schwann cell growth.

METHODS: *Polymer Synthesis:* Polymers were prepared in a two step process. Initially multi-armed oligomers of the selected biomaterial are synthesised using stannous octoate catalyst. The terminal hydroxyl groups are then methacrylated in a second step before precipitation in isopropanol or ethanol at -20°C, according to a published protocol.¹

Two Photon Microstereolithography: Structures are created in a laser direct write fashion, where the sensitised sample is moved by a xyz-translation stage and laser radiation (810nm, 150mW, 76MHz, 200fs) focussed to a point within the resin by a high NA objective lens. Uncured resin is then removed by developing in 4-methyl-2-pentanone. Patterns were designed using the program 'nView'.

PDMS Stamping: Photosensitised PLA photocurable oligomer was placed in PDMS molds created by laser direct write (Courtesy of Laser Zentrum Hannover, Germany) and cured under UV light on a silane methacrylated glass surface.

RESULTS: Rapid microstructuring of photocurable biomaterials via laser direct write was achieved (Figure 1). Schwann cells were culture on flat films of the PCL and PLA-based polymer for 7 days and immunocytostained with S100. Proliferation was compared to glass treated with laminin (Figure 2). Schwann cells were also cultured for ten days on PLA microstructures fabricated by PDMS stamping before fixing with HMDS and imaging via SEM.

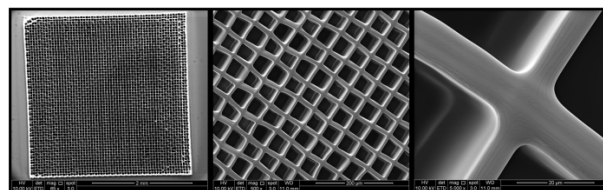


Figure 1: PLA microstructures microfabricated by laser direct write.

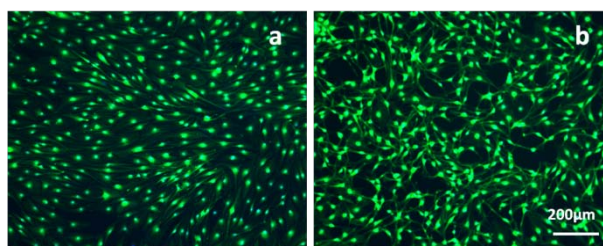


Figure 2: Schwann cells cultured on glass control treated with laminin (a) and thin film of photocured PLA (b).

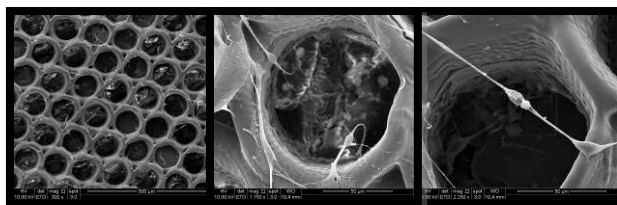


Figure 3: Schwann Cells cultured on PLA microstructures for 10 days.

DISCUSSION & CONCLUSIONS: Photocurable analogues of PLA and PCL have been developed, facilitating rapid microstructuring of these materials for three-dimensional cell culture.

Two photon laser direct write is a high resolution microstructuring technique ideal for creating highly aligned microstructures capable of guiding cell migration and alignment, an important factor in creating devices such as conduits for peripheral nerve repair.

ACKNOWLEDGEMENTS: Thanks to EPSRC, NIHR and the laser loan pool for funding.

1. Gill, A. A.; Claeysens, F., 3D Structuring of Biocompatible and Biodegradable Polymers Via Stereolithography. In *3D Cell Culture*, 2011; Vol. 695, pp 309-321.

ADIPOSE-DERIVED STEM CELLS FOR PERIPHERAL NERVE REPAIR

¹Rossukon Kaewkhaw, ²Andrew M Scutt & ¹John W Haycock

¹Departments of Materials Science & Engineering & ²Medicine, University of Sheffield, UK.

INTRODUCTION: The use of primary Schwann cells in conjunction with nerve guidance conduits has been shown to improve regeneration and remyelination of injured peripheral nerve [1]. However, clinical application of primary Schwann cells for nerve repair is limited due to the requirement of nerve biopsies, and slow growth of Schwann cells *in vitro*. Adipose-derived stem cells (ASCs) may be an optional cell source for derivation towards Schwann-like cells. In this study adipose-derived stem cells from three anatomically different sites were explored for differentiation towards a Schwann phenotype which included protein expression, morphology and function.

METHODS: Stem cells were isolated from: i) subcutaneous; ii) perinephric adipose and iii) epididymis adipose tissue of adult male Wistar rats according to the method of Bjornorp et al [2]. Plastic-adherent multipotent cells were then cultured according to an experimental differentiation protocol using β -mercaptoethanol, retinoic and growth factors. The protein markers S100 β , GFAP and p75NGFR were studied by Western blotting, together with phenotypic changes. A Transwell co-culture system containing NG108-15 neuronal cells and ASCs was employed to study the promotion of neurite growth. Neurite extension was determined after co-culture. Soluble neurotrophins contributing to neurite growth in co-culture medium was analyzed by ELISA and blocking antibodies used to determine specificity of action.

RESULTS AND DISCUSSION: Western blotting demonstrated an up-regulation of the Schwann cell marker S100 β , GFAP and p75 NGFR in perinephrium-ASCs. However, only S100 β expression was up-regulated in subcutaneous-ASCs while GFAP and p75NGFR were up-regulated in epididymis-ASCs. In addition, differentiated cells from all ASC sources formed an elongated shape, whereas undifferentiated cells displayed a polygonal and flattened morphology. A functional assay demonstrated that differentiated ASCs could stimulate neurite extension of NG108-15 neuronal cells by $36.44\mu\text{m} \pm 1.55\mu\text{m}$ (subcutaneous), $40.93\mu\text{m} \pm 2.02\mu\text{m}$ (perinephrium) and $27.29\mu\text{m} \pm 2.63\mu\text{m}$ (epididymis). This was in comparison with undifferentiated ASCs which stimulated neurite growth by $13\mu\text{m} \pm 0.98\mu\text{m}$, $18\mu\text{m} \pm 0.96\mu\text{m}$ and $13\mu\text{m} \pm 1.07\mu\text{m}$. In addition, the neurotrophins NGF and BDNF (but not NT-3) were detected in the co-culture medium. Subcutaneous-, perinephrium- and epididymis-ASCs produced NGF at 26.5-fold, 23.7-fold and 10.2-fold higher and BDNF 6.9-fold, 5-fold and 5-fold higher than undifferentiated-ASCs, respectively.

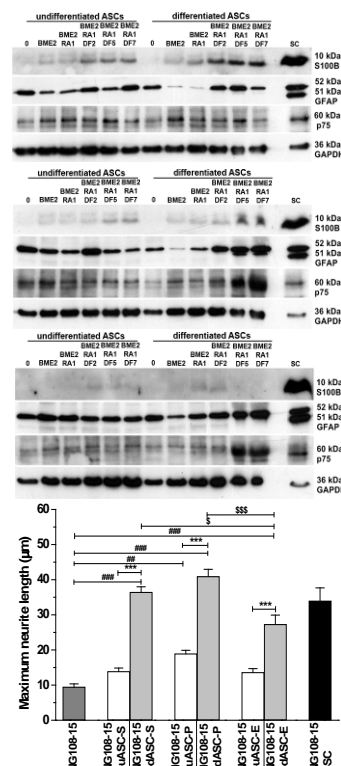


Figure 1. Differentiation of adipose-derived stem cells (ASCs) into Schwann-like cells. A-C. Western blotting for S100 β , GFAP and p75 proteins of A) subcutaneous-, B) perinephrium- and C) epididymis-ASCs. D. The promotion of neurite elongation from NG108-15 neuronal cells by ASCs or primary Schwann cells (SC). ### or *** or \$\$\$ $p <$

CONCLUSIONS: The use of ASCs as an alternative to Schwann cells for peripheral nerve repair shows good potential. Differentiated ASCs from three different anatomical fat sources showed an up-regulation of Schwann markers to varying extents. However, all differentiated ASCs were able to support neurite elongation in co-culture, mediated by neurotrophin secretion. This work forms the basis for extending work towards the use of injury models *in vivo* [3].

REFERENCES:

1. T Hadlock et al., *Tissue Eng*, 6, 119–127 (2000).
2. P Bjornorp et al., *J Lipid Res*, 19, 316-324 (1978).
3. R Kaewkhaw et al., *Glia*, (2011) In press.

ACKNOWLEDGEMENTS SFR Scholarship programme (Thailand) for financial support.

Directing Neuronal Cell Outgrowth and Schwann cell organisation with Aligned Polycaprolactone Microfibre Scaffolds

¹Muhammad FB Daud, ²Anthony J Ryan & ¹John W Haycock

¹Materials Science & Engineering and ²Chemistry, Sheffield University, UK

INTRODUCTION

The ability of the peripheral nervous system to regenerate following injury is limited. Autografting is the gold standard treatment but there are a number of drawbacks to this procedure including donor site morbidity and lack of donor material. High cell death and a lack of accurate axonal orientation following injury has led to an increased interest in the use of nerve guidance conduits (NGC). NGCs can be surgically implanted to bridge the gap left by injury to provide mechanical strength and physical guidance cues but these devices do not encourage re-innervation beyond a few millimeters. NGCs can incorporate a number of features to improve the basic design. The aim of the present study was to systematically investigate the optimal diameter of electrospun degradable polycaprolactone microfibrils to support neuronal and Schwann cell guidance and differentiation.

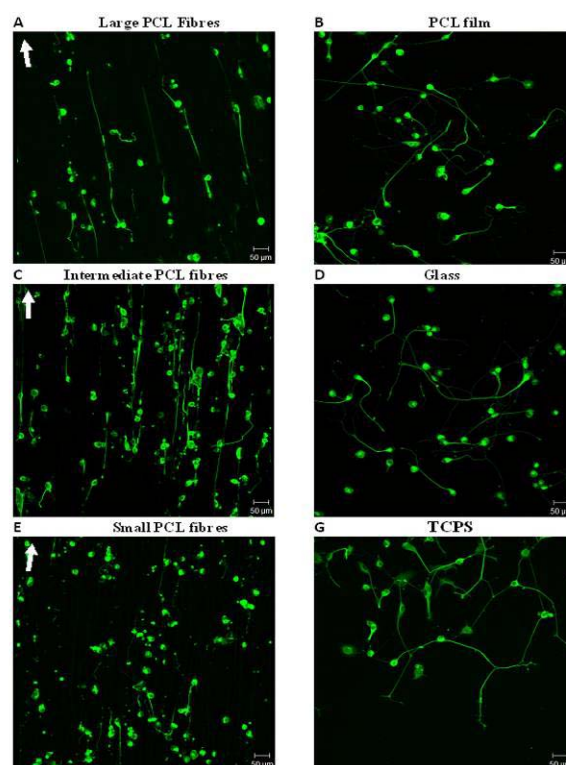
EXPERIMENTAL METHODS

Electrospinning parameters were devised for systematically producing aligned polycaprolactone (PCL) fibres with specific diameters of 1, 5, and 8 μm . SEM was used to characterize fibre diameters and the orientation of fibres as a population when fabricated as mats. Neuronal and primary Schwann cell attachment and growth was investigated in vitro on aligned fibres and cell number and differentiation examined using 3D confocal microscopy and immunolabelling. Cell behaviour was also investigated in 2D on a range of materials for the purposes of control.

RESULTS AND DISCUSSION

Three features were analysed to characterize the three fibre groups: i) fibre alignment; ii) fibre density and iii) fibre diameter. All three fibre groups exhibited sharp peak distribution confirming that a high number of fibres were parallel to each other. More than eighty percent of fibres measured varied within $\pm 6^\circ$ for all three groups. Mean fibre diameter was $8.06 \pm 0.22 \mu\text{m}$ for large fibres, $5.08 \pm 0.05 \mu\text{m}$ for intermediate fibres, and $1.02 \pm 0.07 \mu\text{m}$ for small fibres. NG108-15 neuronal cells were stained for β -tubulin-III. The figure shows data for large fibres (1A), intermediate fibres (1C) and small fibres (1E). Figure 1B, 1D and 1G show neuronal cells on control substrates which are PCL film, glass and tissue culture polystyrene (TCPS), respectively. Figure 1A, 1C and 1E show that the direction of neurite growth corresponded to the direction of fibre alignment. In order to investigate the effect of differing fibre diameter on neurite outgrowth, maximum neurite length, number of neurites per neuron and

percentage of neurite bearing neurons were measured. The longest neurite was measured on 8 μm fibre (large) with a mean length of $121.11 \pm 10.53 \mu\text{m}$. On 5 μm fibres (intermediate), the mean length was $95.42 \pm 5.63 \mu\text{m}$, while the mean neurite length on 1 μm fibres (small) was $71.88 \pm 4.40 \mu\text{m}$, which was almost half the length on $\sim 8 \mu\text{m}$ fibres. Assessment of the number of neurite per neurons on PCL fibres revealed that there was no significant difference between the three fibre diameters.



CONCLUSIONS

In summary, the study shows that fibre size influences neurite outgrowth and that larger micro-size fibres support better directed neurite elongation than smaller sized fibres. This work will go forward to the better design of nerve guidance conduit internal structures for peripheral nerve repair.

REFERENCES

1. Murray-Dunning (2011) *Methods. Mol. Biol.* 695, 155-166.

ACKNOWLEDGMENTS The authors are grateful to the EPSRC for funding this work.

Elucidating Cellular Reaction to Biomaterial Substrates Using a Metabolomics Approach

E. V. Alakpa¹, K. Burgess¹, V. Jayawarna², R.V. Ulijn², and M.J. Dalby¹

¹University of Glasgow and ²University of Strathclyde, Glasgow, United Kingdom.

INTRODUCTION: Mimicry of the elastic properties of the biomaterial substrate on which mesenchymal stem cells (MSCs) are cultured to match that of native tissue types is known to have influence on cell lineage commitment as they differentiate. The cells' metabolomic profile is predicted to be highly indicative of phenotype. This is potentially of particular importance in stem cell research as the cells are metabolically inactive in their self-renewing states in the natural niches and the metabolome is thought to become up-regulated during active differentiation. Using peptide based hydrogel scaffolds of tunable stiffness and MSC culture coupled with Fourier transform Orbitrap mass spectroscopy to investigate MSC metabolites during directed differentiation has enabled scrutiny of the cell phenotype and has potential to influence the way biomaterials are designed for cell culture.

METHODS: Short chain peptide hydrogels were made with approximate Young's modulus of 1, 6 and 36kPa, similar to that of adipose, muscle and bone tissue. Mesenchymal cells were seeded onto these hydrogels and cultured over a period of 7 days. Cells were also differentiated conventionally over 7 days using inductive culture media (adipo, myo and osteoinductive). After this time, cells were denatured and metabolites extracted by incubating with chloroform:methanol:water (1:3:1, v/v) at 4°C for an hour. The 'liquid' was then removed from the hydrogel and centrifuged at 13000rpm for 5 minutes to remove debris. The resulting supernatant was then injected onto an LC-MS system and metabolites identified using accurate mass cross referenced with an in-house database of named metabolites.

RESULTS: Peak areas determined from liquid chromatographs were normalised to control samples, mapped to metabolic pathways and interpreted graphically. Unpaired t-tests were performed for control samples and against media induced differentiated cells which is the conventional method used for instigating cell differentiation *in-vitro*.

DISCUSSION & CONCLUSIONS: Cell growth and differentiation on the hydrogel biomaterials show a prominent effect on cellular metabolic activity increasing turnover to up to 30 times compared to cells that are cultured in differentiating media alone. Furthermore, immunofluorescence shows large differences in MSC fate on the different materials and subsets of metabolites will be presented that reflect these materials effects. Effects are generally evident for 'work-horse' compounds such as amino acids and pyruvate. Our results support the hypothesis that metabolic profile is indicative of stem cell phenotype and could thus be exploited to follow stem cell fate.

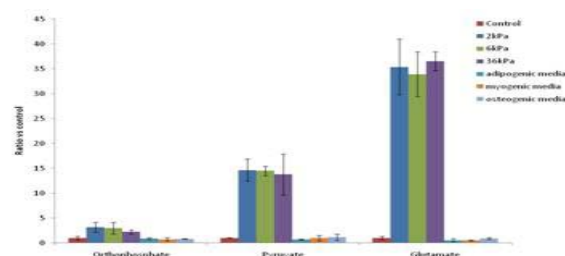


Fig. 1: Effect of biomaterials on phosphate and amino acid production in MSCs. In this metabolite subset, the materials produce a pronounced effect compared to using defined media.

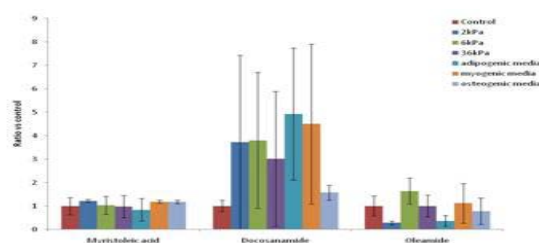


Fig. 2: Effect of biomaterials on fatty acid and fatty acid amine production in MSCs. In this metabolite subset, the materials produce a negligible effect compared to using defined media.

REFERENCES: ¹A. Engler *et al* (2006) *Cell* 126:677-689. ²V. Jayawarna *et al.* (2009) *Acta Biomaterialia* 5(3):934-943

ACKNOWLEDGEMENTS: E. Alakpa is supported by the EPSRC DTC in Proteomic and Cell Technologies.

INVESTIGATING VARIOUS MRI CONTRAST AGENTS AT DIFFERENT CONCENTRATIONS FOR THE PURPOSE OF TAGGING AND IMAGING MESENCHYMAL STEM CELLS AND CHONDROCYTES FOR ACI

H. Markides , A. J. El Haj

Institute for Science and Technology in Medicine, Keele University

INTRODUCTION:

Autologous Chondrocyte Implantation (ACI) is a realistic alternative to current osteoarthritic therapies, a disease that affects some six million people in the UK¹. ACI involves the isolation of chondrocytes from the patients' knee, expansion *in vitro* and their re-implantation into the defected area². However, further optimisation of this technique is required. Having a practical means of visualising and monitoring the implanted cells *in vivo* can provide us with the ability to quantify and track cells thus aiding the enhancement of the therapy.

METHODS:

Human Bone marrow derived Mesenchymal stem cells (MSC) and primary chondrocytes were cultured and passively loaded with Magnetic Nanoparticles (MNP) at passage 4. Magnetic nanoparticles used were superparamagnetic nanoparticles (SPIOs) ranging in size between 50-1000 nm in diameter. MNP concentration and cell dosages were also investigated. MNP-loaded-cell populations were then implanted into cadaveric porcine knees and visualised by MRI (Magnetic Resonance Imaging).

RESULTS:

Both MSCs and chondrocytes were found to uptake MNP at variable efficiencies depending on particle size and dosage in culture. A relationship was established between MNP size and loading for the optimal *in vivo* visualisation using MRI.

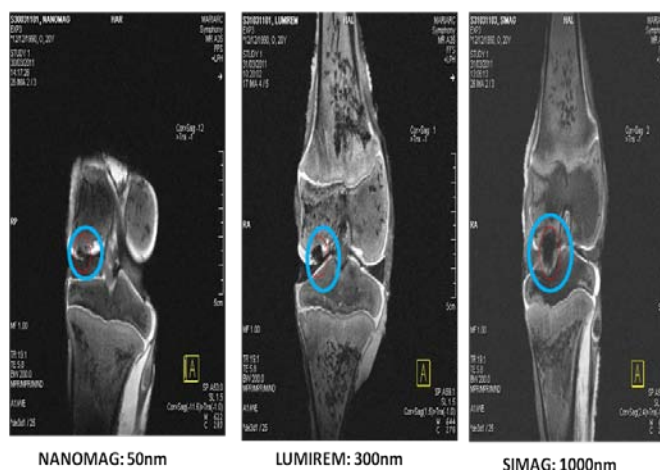


Fig 1. Three Million chondrocytes were loaded with MNP of varying sizes (50nm, 300nm and 1000nm in diameter) in excess and implanted into cadaveric porcine knees. The knees were then scanned and imaged by Siemens 1.5T MRI scanner. MRI scans showed areas of signal disturbance highlighting the position of MNP-loaded-Chondrocytes.

DISCUSSION & CONCLUSIONS:

MNP size and dosage have been found to impact the loading of both MSCs and chondrocytes. Imaging of these loaded populations implanted in porcine knee joints shows good contrast although differences are observed dependent upon particle size, concentration and cell number.

REFERENCES:

1. Arthritis Research UK (2008)
2. M.Brittberg, A.Lindhal et al (1994) The New England Journal Of Medicine, **331**: 889-895

ACKNOWLEDGEMENTS: I would like to acknowledge my supervisor, Prof. Alicia J. and the EPSRC Doctoral Training Center for funding this research.

ALIGNED CELLULAR AND ACELLULAR COLLAGEN GUIDANCE SUBSTRATES FOR PERIPHERAL NERVE REPAIR

M. Georgiou, J. Loughlin, J. P. Golding & J. B. Phillips

The Open University, Department of Life Sciences, Milton Keynes, MK7 6AA.

INTRODUCTION: There is a clinical demand to shorten the delay of reinnervation and improve functional recovery after peripheral nerve injury. A peripheral nerve repair device with the ability to direct and promote axon growth across a lesion would be a promising alternative to nerve autograft repair, the current gold standard treatment. The growth of axons across a lesion is most effective when supported by columns of aligned Schwann cells, as found in an autograft. Here we report the development of a robust aligned cellular collagen biomaterial that supports and directs neuronal growth. We also investigate the potential of these aligned cells to precondition the collagen biomaterial, before they are freeze-killed, leaving an acellular guidance matrix.

METHODS: The rat Schwann cell line SCL 4.1/F7 was used throughout. Cells were mixed with neutralised type I rat tail collagen (2 mg/ml). As gels formed they were tethered to permit cellular alignment¹. 24 hours later, gels were plastic compressed (PC) by the rapid removal of the interstitial fluid from fully hydrated gels. The preconditioned acellular matrix was prepared in the same way but the compressed gels were then submerged in liquid nitrogen to kill the cells². To investigate neuronal growth on these aligned cellular and preconditioned acellular biomaterials, adult rat dissociated dorsal root ganglia (DRG) cells were cultured on their surfaces for 3 days. Plastic compressed collagen matrix in which no cells had been seeded was used as a control. In all cases, neurite growth was quantified using immunostaining, with anti-S100 and anti- β III tubulin, and confocal microscopy.

RESULTS: Around 70% of DRG neurons growing on the aligned cellular biomaterial did not deviate from the angle of Schwann cell alignment by more than 20 degrees (Fig 1A). Less neuronal growth was observed on the preconditioned acellular matrix (Fig 2B), compared to the aligned cellular biomaterial (Fig 1A & B). Pilot data suggest growth of regenerating neurites on the acellular matrix was guided by the direction of the previous cellular alignment (Fig 2B) compared to control.

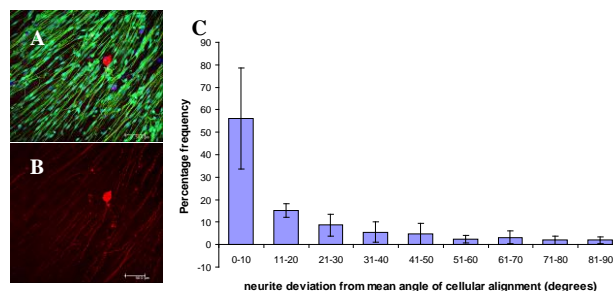


Fig. 1: Aligned Schwann cell biomaterial guides neurite growth. **A** Confocal micrograph projection showing neuronal growth on the surface of the aligned Schwann cell biomaterial. **B** Red channel only (neurite growth). **C** Deviation between angle of neurite growth and Schwann cell alignment (means \pm SEM)

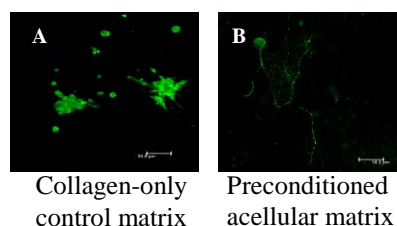


Fig. 2: Confocal micrograph projections showing neuronal growth on collagen-only control (A) & preconditioned acellular (B) matrices.

DISCUSSION & CONCLUSIONS: Aligned Schwann cells within a PC 3D collagen matrix promote and support neuronal growth in a directed manner. This occurs whether the Schwann cells are alive or dead, although neurite growth is more robust on a live Schwann cell substrate.

We are currently integrating the aligned cellular biomaterial into a repair device. The matrix is rolled into columns¹ which are then packed together within a silicone tube. Testing this 'engineered endoneurium', using *in vitro* and *in vivo* models, will demonstrate the potential of the device as an implantable conduit for peripheral nerve repair.

REFERENCES: ¹ E. East et al (2010) *Tiss Eng Part A* **16**: 3173-3183. ² E. Hadjipanayi et al. (2010) *British Journal of Surgery* (pp. S37-S37).

ACKNOWLEDGEMENTS: This research was funded by an Open University Studentship. We are grateful to Dr Emma East for providing expertise & advice.

Evaluation of mesenchymal stem cells (MSCs) from whole umbilical cord for bone repair applications

Dimitrios Kouroupis, Sarah Churchman, Dennis McGonagle and Elena Jones

Leeds Institute of Molecular Medicine, University of Leeds, Leeds UK

INTRODUCTION: Human umbilical cord (UC) represents an attractive MSC source for bone regeneration¹. Furthermore, UC tissue contains easily-obtainable endothelial cells (ECs). Co-implantation of UC MSC+EC mixtures may be beneficial for restoring long lasting appropriately vascularized bone following complex fractures.

METHODS: The aim of this study was to isolate UC MSCs and ECs and to explore their phenotypic and gene expression profiles in comparison to bone marrow (BM) MSCs. The phenotypes of UC and BM MSCs were similar and stable (**CD90⁺CD73⁺CD105⁺CD146⁺CD31⁻CD34⁻CD45⁻**) even though UC MSCs had faster growth rates and better telomere stability. UC ECs expanded in EBM2 media were characteristically **CD31⁺CD90⁻CD34⁻CD45⁻**, but also **CD73⁺CD105⁺CD146⁺** suggesting that CD73, CD105 and CD146 could be used for the simultaneous isolation of UC MSC+EC mixtures.

RESULTS: Gene array cards revealed distinct clustering of UC MSCs with BM MSCs but not with UC ECs. UC MSCs however, expressed considerably lower levels (<5-200 fold) of transcripts encoding BMP2, osteomodulin, insulin growth factor 2, and secreted frizzled-related proteins 1 and 4. The expression of Wnt pathway genes in MSCs being driven down an osteogenic pathway in vitro increased equally in UC and BM MSCs but remained markedly lower in UC MSCs due to poorer baseline levels. In concordance, UC MSCs displayed lower rates of mineralization during standard in vitro osteogenesis assay. Osteogenically-driven UC MSCs up-regulated KDR/VEGFR2 (>100-fold), which is known, in its soluble form, to stimulate blood vessel stabilization². UC MSCs produced larger vessel-like structures in Matrigel.

DISCUSSION & CONCLUSIONS: These data demonstrate that UC MSCs are less osteogenically-committed than BM MSCs. For bone repair applications involving intramembranous ossification/direct MSC conversion to osteoblasts,

UC MSCs may be inferior to BM MSCs. However, UC MSCs may be advantageous for repairing long bone fractures via endochondral ossification, due to their potential ability to support vascularization. Supplementation UC MSCs with ECs may further accelerate bone formation and maturation. The immunoregulatory capacity of UC MSC+EC mixtures merits therefore further investigation.

REFERENCES: ¹ Wang et al. (2011) Musculoskeletal tissue engineering with human umbilical cord mesenchymal stromal cells. *Regen Med.* 6:95-109. ² Lorquet S et al. (2010) Soluble forms of VEGF receptor-1 and -2 promote vascular maturation via mural cell recruitment. *FASEB J.* 24:3782-95.

The Influence of Electrical Stimulation on Primary Human Mesenchymal Stem Cell Activity

R Balint¹, NJ Cassidy² & S Cartmell¹

¹ School of Materials, Faculty of Engineering and Physical Sciences, University of Manchester, UK.

² School of Physical and Geographical Sciences, Keele University, UK.

INTRODUCTION: Physical and chemical stimuli, mimicking the endogenous signals, are widely applied in Tissue Engineering to improve the quality of the engineered product. As it is known that endogenous electrical fields are able to influence proliferation and differentiation and play a crucial role in the genesis, repair and regeneration of human tissue, while medical therapies exploiting the beneficial effects of electricity, are in existence since several decades, we felt that there is strong basis to examine, what this modality could give to Tissue Engineering.

METHODS: Various regimes of voltage pulses were delivered to primary human Mesenchymal Stem Cells through stainless steel electrode wires. In the first part of this study the effects of each parameter (amplitude, frequency and pulse width) of the stimulating signals were assayed upon the proliferation of the cells, while the second part was designed to compare the proliferative and differentiating effects of combinations of high and low amplitude and short and long pulse width settings. To further assess the influence of electrical signals on the differentiation of these cells the “short pulse high amplitude” combination was also applied synergistically with an osteogenic chemical stimulus. Cell numbers were measured using Alamar Blue staining, viability and morphology were examined through Live/Dead staining visualised with confocal microscopy, and quantitative real-time RT-PCR was performed to assay the expression of 11 markers of differentiation.

RESULTS: While some settings of all three parameters had a positive, some others had a negative effect on cell numbers. The difference between the results was greatest in the case of the different pulse widths. The 10 μ s pulses enhanced proliferation by 68 % compared to sham-treated control groups ($p < 0.005$), while cell numbers were greatly reduced by the 1 μ s signals ($p < 0.005$). The stimulation regimes in most cases when applied in growth medium, could not alter the expression of the 11 assayed genes, with the exception of a non significant up-regulation of ACAN with the 250 μ s

($p = 0.06$) and a significant decrease of CNN1 levels with the 1 μ s pulses ($p < 0.05$). On the other hand when the short pulse high amplitude regime was combined with osteogenic medium, the stimulation was able to interfere with ACAN, CNN1 and GFAP expression, and significantly elevated ($p < 0.05$) ALPL levels (Figure 1).

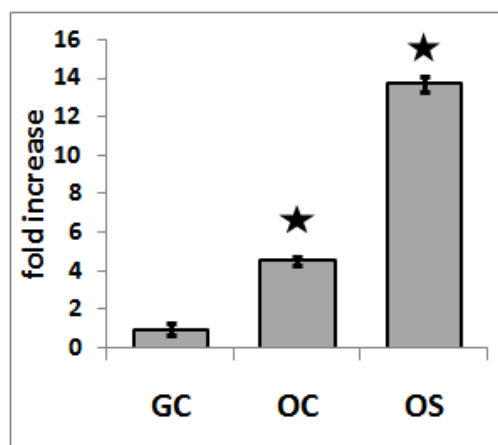


Fig. 1: mRNA expression of Alkaline Phosphatase. OS – Stimulated in osteogenic medium. OC – Osteogenic control group. GC – Growth medium control group.

DISCUSSION & CONCLUSIONS: This study demonstrated that directly coupled electrical stimulation can influence both the proliferation and differentiation of human Mesenchymal Stem Cells. The effect on the cell numbers depends heavily on the exact parameter combination, as both positive and negative outcomes were seen. Any positive effect also seems to be reduced by the harmful processes (e.g. pH changes) associated with direct coupling. Though injected stimuli were able to enhance gene expression significantly in growth medium, this was observed only in one instance. As when applied in osteogenic medium the effects on differentiation were much stronger, it is suggested that the synergistic application of a chemical stimulus is necessary for this modality to be truly effective.

ACKNOWLEDGEMENTS: We would like to thank the EPSRC 3ME “Bridging the gaps” award, the BBSRC and Lorenpick Biotechnology for their support.

THE USE OF PLASMA POLYMERISED ACRYLIC ACID AND MALEIC ANHYDRIDE FOR NEURONAL CELL ENGINEERING

JHA Bell & JW Haycock

Department of Materials Science and Engineering, University of Sheffield, UK

INTRODUCTION: Materials used for peripheral nerve guide conduits should degrade at an appropriate rate. However, the maximum distance for re-innervation is limited at approximately 10mm. Improvements to this could be made in terms of materials which better support cell attachment and proliferation. Coating existing FDA approved materials may be a way of increasing nerve regeneration across conduits. The aim of the present work involved plasma polymerisation of acrylic acid[1] and maleic anhydride[2] to investigate if these surface coatings improved neural attachment, growth and differentiation.

METHODS: XPS was used to confirm the presence of acid and anhydride groups after deposition. Contact angle was also used to analyse hydrophobicity differences between coated and uncoated slides.

NG108-15 neuronal cells were then cultured under serum free conditions on the surfaces for 4 days, after which they were fixed and stained with β -tubulin III and DAPI. Epifluorescence microscopy in conjunction with ImageXpress analysis software quantitatively analysed the neurite lengths of NG108-15 neuronal cells on the different surfaces.

RESULTS:

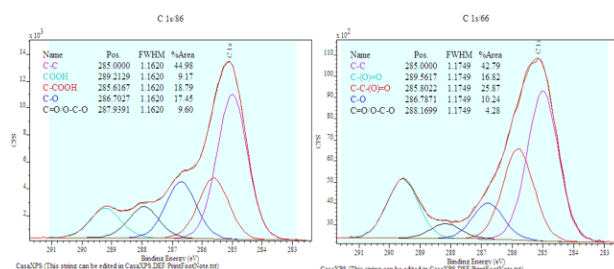


Fig. 1: XPS C1s high resolution narrow scans. Left graph shows fresh acrylic acid, right graph shows fresh maleic anhydride.

Contact angle measurements were 55° for acrylic acid and 49.5° for maleic anhydride. Maleic anhydride coated surfaces stimulated the longest neurite length compared to all other surfaces.

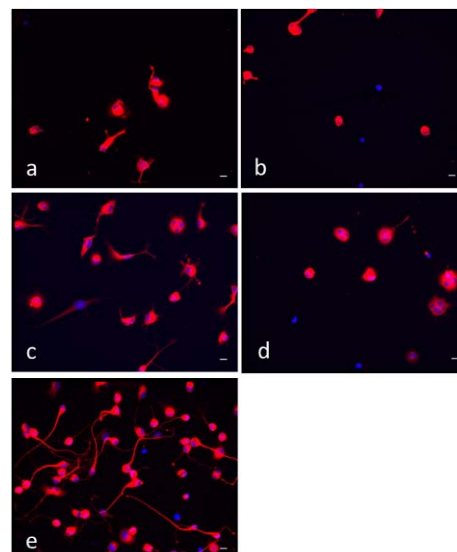


Fig. 2: Micrographs of β -tubulin III and DAPI stained NG108-15 neuronal cells. 1×10^4 NG108-15 neuronal cells were cultured for 4 days. Photos show a) TCPS b) Glass c) Laminin d) Acrylic acid and e) Maleic anhydride. Scale bar shows $20 \mu\text{m}$.

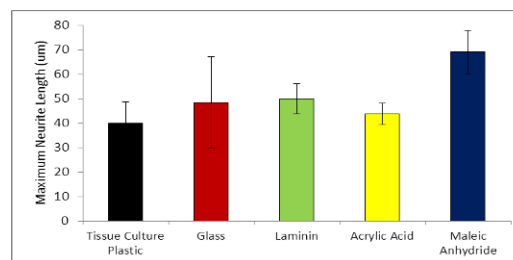


Fig. 3: Comparison of different surfaces on maximum neurite length. NG108-15 neuronal cells were fixed and stained with β -tubulin III then analysed using ImageXpress analysis software. Data points show mean \pm SD ($n=3$).

DISCUSSION & CONCLUSIONS: Present work shows that surface chemistry influences neurite formation of neuronal cells. This work is being developed to improve the regeneration distance of nerve guide conduits.

REFERENCES: ¹P.C Eves, A.J Beck, A.G. Shard, S MacNeil (2005) *Biomaterials* **34**: 7068-708. ²G Mishra, S.L. McArthur (2010) *Langmuir* **12**:9645-9658.

ACKNOWLEDGEMENTS: Thanks to Dr Claire Hurley. This work was sponsored by the EPSRC.

PLGA-based Microparticles for the sustained release of BMP-2

G. T. S. Kirby¹, L. J. White¹, C. V. Rahman¹, H. C. Cox¹, F. R. A. J. Rose¹, D. W. Hutmacher², K. M. Shakesheff¹ & M. A. Woodruff³

¹ School of Pharmacy, University of Nottingham, University Park, Nottingham, UK

² Regenerative Medicine Group, Institute of Health and Biomedical Innovation, Queensland University of Technology, Kelvin Grove, Queensland, Australia

³ Biomaterials and Tissue Morphology Group, Institute of Health and Biomedical Innovation, Queensland University of Technology, Kelvin Grove, Queensland, Australia

INTRODUCTION: Bone repair is not always spontaneous. In some pathological cases intervention is required. Biomaterials are currently being explored as an alternative to grafting. These exogenous 'scaffolds' offer advantageous structural properties but are often more effective when combined with cells or bioactive molecules such as growth factors. Growth factors generally have a short *in vivo* half-life so in order to maintain active therapeutic doses a controlled release system is required.

This study demonstrated the effective encapsulation of Bone Morphogenetic Protein-2 (BMP-2) within a tailored polymeric microparticle matrix that is able to achieve sustained release. Furthermore this released BMP-2 remained active and able to induce differentiation of a murine calvarial osteoblast cell line leading to bone-like mineral deposition.

METHODS: Polymer microparticles were formed using a double emulsion solvent evaporation technique. The BMP-2 was combined with human serum albumin as a bulk carrier. A formulation consisting of poly(lactic-co-glycolic acid) (PLGA) 85:15 (lactide:glycolide) and a more hydrophilic plasticiser was selected because of favourable release kinetics. Particles were sized using laser diffraction. Protein release was measured by suspending particles in phosphate buffered saline, incubating at 37 Centigrade on a rocker shaker and regularly sampling the release media. This release media was assayed for protein content and activity. BMP-2-containing microparticles and appropriate controls were cultured with the MC3T3-E1 cell line and assayed at three time points (10, 17 and 24 days). At these time points, bone-like calcium deposition was qualitatively determined using alizarin red and the early osteogenic differentiation marker alkaline phosphatase was quantitatively measured.

RESULTS: Particle size was tightly controlled within defined limits by optimizing the emulsion process. Mean particle diameters of 110-120µm

were obtained. The release profile demonstrated sustained zero order release kinetics with minimal burst release. These particles induced MC3T3-E1 bone-like mineral deposition in a dose dependent manner. The expression of alkaline phosphatase was also detected at significantly higher concentrations in the BMP-2 group showing that differentiation was taking place.

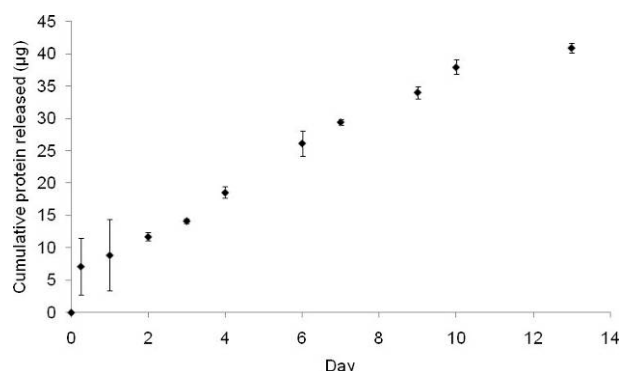


Fig. 1: Cumulative protein release from microparticles over a 13 day period.

DISCUSSION & CONCLUSIONS: This study has addressed key areas of difficulty experienced when trying to achieve controlled release of proteins from a polymeric matrix. The burst release was mitigated by using a custom plasticiser. Biocompatibility of the PLGA-based microparticles was demonstrated with MC3T3 cells. BMP-2 was shown to have maintained bioactivity when released from the microparticles.

ACKNOWLEDGEMENTS: This work was a collaboration between the University of Nottingham (UK) and the Queensland University of Technology (Australia) with funding from the Engineering and Physical Sciences Research Council (EPSRC) Doctoral Training Centre in Regenerative Medicine and The Australian Research Council Discovery Grant (DP089000).

Bone Tissue Engineering: Using surfaces to direct function

AJ Taylor¹, MR Alexander² & LDK BATTERY¹

¹Division of Drug Delivery & Tissue Engineering, School of Pharmacy, University of Nottingham.

²Laboratory of Biophysics & Surface Analysis, School of Pharmacy, University of Nottingham

INTRODUCTION: By manipulating the mechanical and chemical properties of culture surfaces, it is possible to direct cellular fate and behaviour. Engler et al. [1] showed that MSCs commit to phenotypes with extreme sensitivity to the tissue-level elasticity of collagen coated polyacrylamide gels, with comparatively rigid matrices (25–40 kPa) that mimic collagenous bone proving osteogenic. Benoit et al. [2] showed that MSCs can be induced to differentiate down specific pathways through the integration of tethered small molecules. Here we control both gross surface chemistry and surface elasticity and examine the response of primary bone cells to these surfaces, and compare them to decellularised ECM produced by primary bone cells. We aim to use to use these controllable surfaces as tools to probe the development, mineralisation, and regeneration of murine bone.

METHODS: Surfaces of controllable stiffness are produced by adjusting the level of bis-acrylamide cross-linking in thin polyacrylamide gels cast between glass coverslips. A uniform gross surface chemistry is produced by plasma polymer deposition of monomers containing straight chain, amino acid or phosphite functional chemistries. Surfaces characteristics are analysed using a range of techniques including AFM force measurement, TOF-SIMS, XPS and WCA. Primary bone cells are extracted from the calvariae of neonatal CD1 mice, and mineralisation induced by osteogenic supplementation with BGP and ascorbate for 21 days of culture.

RESULTS: Preliminary results have shown that we can produce substrates of defined and controllable stiffness and surface chemistry.

ToF-SIMS analysis 24 hours after deposition of plasma polymerised trimethylphosphite (ppTMP) show uniform release of relevant secondary ions (PO₂⁻, PO₃⁻) and a corresponding decrease of secondary ions found in the substrate and oxygen etched samples. Further analysis of the ppTMP coat will be undertaken using XPS and other techniques.

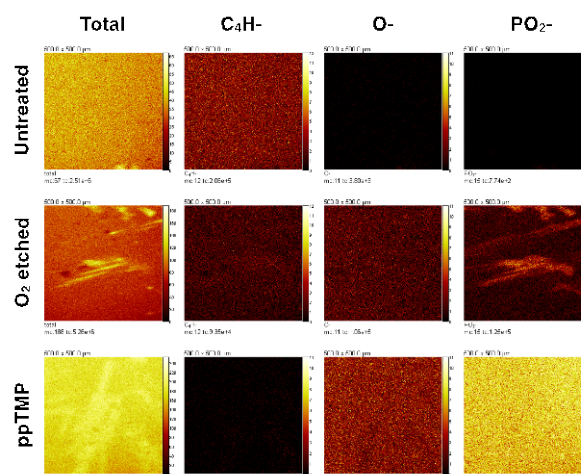


Fig 1: ToF-SIMS results from untreated, oxygen etched, & plasma polymerised trimethylphosphite (ppTMP) coated polystyrene samples (1 kA @ 300 mTorr, 20W, <1W reflected) showing 500x500 μm representative intensity images for C₄H⁻, O⁻, and PO₂⁻ secondary ions.

DISCUSSION & CONCLUSIONS: In a future clinical in vivo environment the media environment is difficult to control. It is therefore key to understand how the surface features of both potential scaffolds and ECM, rather than media supplements, can be used to direct cellular fate and function.

Future work will examine the response of a range of cell types, including primary bone and mouse embryonic stem cells, to the synthetic plasma polymerised polyacrylamide gel substrates as well as decellularised primary bone cell ECM.

REFERENCES:

1. Engler, A.J., Sen, S., Sweeney, H.L. & Discher, D.E. Matrix elasticity directs stem cell lineage specification. *Cell* 126, 677–689 (2006).
2. Benoit, D.S.W., Schwartz, M.P., Durney, A.R. & Anseth, K.S. Small functional groups for controlled differentiation of hydrogel-encapsulated human mesenchymal stem cells. *Nat Mater* 7, 816–823 (2008).

ACKNOWLEDGEMENTS: Thanks go to the EPSRC Doctoral Training Centre for Regenerative Medicine.

Primary calvarial cells and mouse embryonic stem cells as potential cell sources for development of an *in vitro* inflammatory model for testing anti-inflammatory osteochondral tissue engineering strategies

L. E. Sidney & L. D. K. Buttery²

Drug Delivery and Tissue Engineering, Department of Pharmacy, University of Nottingham, UK.

INTRODUCTION: Non-union fractures and inflammatory diseases are significant targets for osteochondral tissue engineering strategies. In these cases, the tissue engineering approach may have the capacity to modulate the inflammatory environment. If such strategies are developed, the current validation method would be an expensive *in vivo* animal model. Development of an *in vitro* model of basic inflammation would allow initial screening of anti-inflammatory tissue engineering strategies at a lower cost and easier set-up.

The development of such a model also allows the investigation of how an inflammatory environment affects different cell types, in this case embryonic stem cells. This basic model is created from the addition of proinflammatory cytokines such as interleukin-1 β (IL-1 β), tumour necrosis factor- α (TNF- α) and interferon- γ (IFN- γ), that are associated with the innate inflammatory response during tissue healing and are also critical for control of bone tissue remodelling¹.

METHODS: Primary calvarial cells were extracted from neonatal CD1 mice by sequential trypsin and collagenase digestion. Mouse embryonic stem cells (mESCs) were cultured on a feeder layer of mitotically inactivated mouse fibroblasts in basal media containing leukaemia inhibitory factor (LIF). Differentiation was induced by spontaneous formation of embryoid bodies (EBs) by mass suspension.

Calvarial cells and dissociated EB cells were seeded separately in osteogenic media containing 50 μ g/mL ascorbate-2-phosphate and 50 mM β -glycerophosphate.

Different concentrations of IL-1 β , TNF- α , IFN- γ were added to induce inflammation and cell viability was monitored. Culture supernatants were also collected after 72 hours for use in nitrite and prostaglandin E₂ (PGE₂) assays.

Validation of the model using anti-inflammatory treatment will be performed before further validation with anti-inflammatory tissue engineering strategies.

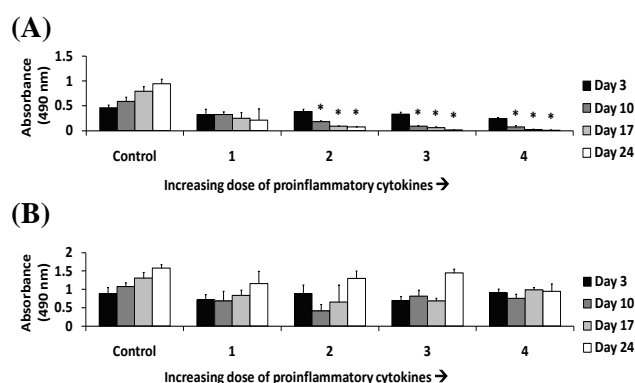


Fig. 1: Viability (MTS assay) of (A) primary calvarial cells and (B) mESCs in response to increasing concentrations of IL-1 β , TNF- α and IFN- γ .

Table 1. Corresponding doses and concentrations of the proinflammatory cytokines.

Dose	IL-1 β (ng/mL)	TNF- α (ng/mL)	IFN- γ (ng/mL)
1	0.03125	0.3125	3.125
2	0.125	1.25	12.5
3	0.5	5	50
4	1	10	100

RESULTS: Increasing the dose of IL-1 β , TNF- α and IFN- γ , caused a decrease in primary calvarial cell viability across all time points (fig.1A). At the lowest dose, decreased calvarial cell viability was still apparent. This decrease in viability was not seen in the mESCs at any dose of cytokines (fig.1B).

DISCUSSION & CONCLUSIONS: The differing response of the two cell types to stimulus suggests a difference in the mechanism of response to proinflammatory cytokines. For a model inflammatory environment the primary cells have more promise but for potential cell therapies the embryonic stem cells may be more suitable due to a subdued response. Nitrite and PGE₂ responses will allow an enhanced comparison of the effects of inflammation on the two cell types.

REFERENCES: ¹T.Skerry, (1994) *Eur. J. Clin. Nutr.* **48**, S190-S198.

ACKNOWLEDGEMENTS: EPSRC Doctoral Training Course in Regenerative Medicine, EMDA and University of Nottingham for funding.

Multi-layered collagen scaffolds with engineered microchannels for skin tissue engineering applications.

T. Alekseeva¹, N. S. Tan¹, M. H. Purser², R. A. Brown¹

¹ UCL, Institute of Orthopaedics-TREC, Stanmore Campus, London UK, ² TAP Biosciences Ltd, Royston, Hertfordshire, UK

INTRODUCTION: One of the challenges of engineering thick constructs is control (normally enhancement) of blood vessels and nerve elements ingrowth after implantation. Several strategies have been developed to overcome this obstacle, e.g. particulate leaching (salt, ice) and inclusion of directional microfibers. A version of this has been used to microchannel plastic compressed (PC) collagen constructs using soluble glass fibres so that microchannels of known geometry and direction are left when the glass fibres dissolve (1, 3). Such microchannels in the PC collagen constructs dramatically increase core oxygenation of constructs (2). However use of soluble fibers is limited by the added complexities of glass dissolution. We report an alternative route to engineering microchannels in the dense, multilayered collagen constructs for use in skin tissue engineering.

METHODS: Neutralised collagen solution (rat tail type I collagen, First Link) was set at 37°C for 30 minutes in the 12-well plate (Orange Scientific). Each gel (height of 10.6 mm, surface area 380 mm²) was compressed using modified upward flow PC technique with the rolls of absorbent paper (4.4 g) under load. Ladder-shaped templates, with the rungs widths of 25, 50 and 100 µm and depth of 75 µm were used to micro-mould the surface of the constructs by placing the template on the set gel prior to compression. After first layer was compressed, a 2nd gel was set on its surface and process repeated. Double- and triple-layered constructs were made; the depth and width of the channels were assessed.

RESULTS: In the double-layered constructs the open channels were formed with the widths closely resembling those of the moulding templates (25 and 50 to 100 µm) and average depth of 30 µm deep (Fig 1). When triple-layered constructs were fabricated,

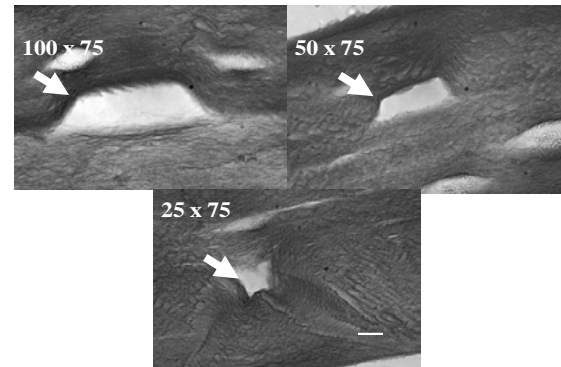


Fig.1 Representative histological images of the channels between layers in the double-layered PC collagen constructs. Dimensions of the channels in µm. Scale bar – 20 µm. Arrows point at the channels opening.

dimensions of the channels in the second (middle) layer did not differ from those in the double-layered constructs. Dimensions of the channels made in the base layer, with 25 and 50 µm templates also did not differ from those in the double-layered construct. However, with 100 µm template, resulting channels did not have an open cross-section, suggesting channel collapse during the construct assembly.

DISCUSSION & CONCLUSIONS: Method reported here allows for simple and rapid fabrication of multi-layered collagen construct with controlled micro-architecture. The dimensions of the channels suggest close dependence of the process on the template shape and collagen density. Collapse of the wider channels suggests different mechanical stability of the channels, depending on the shape of the template. In conclusion, roofing of microchannels in dense collagen scaffolds is a valuable tool for advancing skin tissue engineering.

REFERENCES: Alekseeva et al. (2011) *Biomaterial Applications - in press*, Cheema et al., (2010) *Eur Cell Mater.* 6 (20):274-80, Nazhat et al., (2007) *Biomacromolecules* 8 (2): 543-51.

ACKNOWLEDGEMENTS: TSB-EPSRC for funding.

Development and Optimisation of a Functional Vertebral Endplate Construct

N Gosling^{1,2&3}, R Hall², D Wood³ & P Genever¹

¹*Biomedical Tissue Research Group, Department of Biology, University of York.* ²*Institute of Medical and Biological Engineering, The University of Leeds.* ³*Oral biology, Department of Dentistry, The University of Leeds.*

INTRODUCTION: Intervertebral disc (IVD) degeneration is a substantial contributor to lower back pain which is believed in some instances to be initiated by calcification in the region of the vertebral endplates. Calcification is believed to restrict the nutrient diffusion into the IVD leading to reduced cell viability and extracellular matrix degradation.

Here, a novel porous glass-ceramic, apatite-mullite (A-M), has been reproducibly manufactured and characterised with regard to providing a functional endplate construct. This material has also been investigated for bio-compatibility with specific focus on mesenchymal stem cell (MSC) culture under both basal and osteogenic conditions.

METHODS: A-M parent glass was produced in the 45-90 μ m particle size range via a sequential melting, quenching, grinding and sieving process. The novel porous A-M glass-ceramic scaffolds were then developed through controlled sintering of the glass particles in carbon molds.

The reproducibility of A-M production was investigated in six separately manufactured batches, scanning electron microscopy (SEM), differential thermal analysis (DTA) and powder x-ray diffraction (XRD) techniques were employed to assess scaffold micro-structural composition and architecture. Flexural strength testing was also carried out in accordance with the British standard for the mechanical testing of dental ceramics (BS EN ISO 6872:2008).

SEM was used to determine an appropriate cell seeding density, while live/dead staining was used to determine cell viability over a 21 day period. Cell proliferative capacity was also examined through both a Click-IT EdU nucleic acid incorporation assay and a kit-8 quantitative dehydrogenase activity assay. MSC osteogenic capacity was investigated through real-time quantitative PCR for both early and late stage differentiation markers at 0, 7, 14 and 21 day time points. Alkaline phosphatase (ALP) staining was

also carried out on the scaffolds at these time points to determine osteogenic status and mineralisation.

RESULTS: The DTA showed a good comparison between 6 A-M batches with standard deviations of 4.7°C and 18.7°C for apatite and mullite peak crystallisation temperatures respectively, with near identical trace patterns seen from the XRD analysis. Flexural strength tests found that there was a significant difference ($P < 0.05$) between batch strength at all but two instances, however, batch 1 was markedly stronger than all other batches. SEM imaging showed there to be good formation of crystalline fluorapatite and/or mullite with possible residual glass phases present, samples also showed good sintered morphology with a porous microstructure present.

SEM identified an MSC seeding density of 5×10^5 cells over a 10mm diameter scaffold surface was suitable, giving a confluent cell layer at 24 hours in culture. Cells maintained viability over the scaffold surface for up to 21 days in both basal and osteogenic media. MSCs proliferated at a rate of 8.5 cells.hr⁻¹ over the A-M substrate, which was illustrated through the EdU incorporation assay. Real-time qPCR found there to be an up regulation of all osteogenic markers with reference to day 0 expressions levels on the scaffolds. ALP staining also showed clear up regulation on the scaffold surface over the 21 day culture period.

DISCUSSION & CONCLUSIONS: A-M provides a stable non-resorbable and bio-compatible glass-ceramic, able to maintain MSC viability in culture and support cell proliferation and osteogenic differentiation. This material can be manufactured repeatedly and has the potential to function as a suitable substrate for the further *in vitro* development of a functional vertebral endplate construct.

Utilising Stem Cells and Poly (3-hydroxybutyrate-co-3-hydroxyhexanoate)/collagen hybrid scaffolds for Tendon Tissue Engineering.

AJ Lomas, J Han, GQ Chen, AJ El Haj, NR Forsyth.

Guy Hilton Research Centre, Keele University, Stoke on Trent, ST4 7QB, UK.

INTRODUCTION: Tendon injury is an increasing problem in medicine, with over 300,000 tendon procedures performed annually in the United States [1]. Tendon is characterized by poor repair following injury or disease primarily due to being relatively acellular and having a poor blood supply [2]. Treatment can involve many different types of surgical intervention, however potential problems with these methods (such as foreign body reaction) can occur [3]. This investigation looks into the possibility of using human Embryonic Stem Cells (hESCs), Spontaneously Differentiated hESCs (SDhESCs) and Mesenchymal Stem Cells (hMSCs) in conjunction with novel polymers (PHBHHx) and collagen to create an artificial replacement for damaged tendon, with the aim of improving its healing rate.

METHODS: Collagen gel (1.5mg/ml, 3 mg/ml) contraction was monitored by seeding hESCs, SDhESCs, and hMSCs at set densities (0, 10^3 , 10^4 , 10^5 cells/mL) and measuring length and diameter at regular time intervals when cultured in complete media. Cell viability was measured by trypan blue exclusion at the experimental end point. Porous tube scaffolds were prepared with a dipping method followed by particle leaching. Reverse Transcription (RT) PCR was used to determine cell fate, with tendon-, bone-, cartilage-, fat-, hESC-, and hMSC-linked transcript expression being explored at days 0, 5, 10 and 20 with cells in a scaffold of collagen and PHBHHx.

RESULTS: Contraction of 1.5 mg/ml collagen gel tubes required $\geq 10^5$ hMSCs or SDhESCs (Figure 1). Collagen gel tubes with a concentration of 3 mg/ml underwent no significant contraction when seeded with 10^5 hMSCs or SDhESCs. Cell viability was found to be approximately 50% for SDhESC and 90% for hMSCs at all cell densities in a porous PHBHHx tube/3mg/ml collagen hybrid scaffold. Undifferentiated hESCs did not contract collagen gel tubes and were trypan blue negative after 20 days culture, indicating massive cell death.

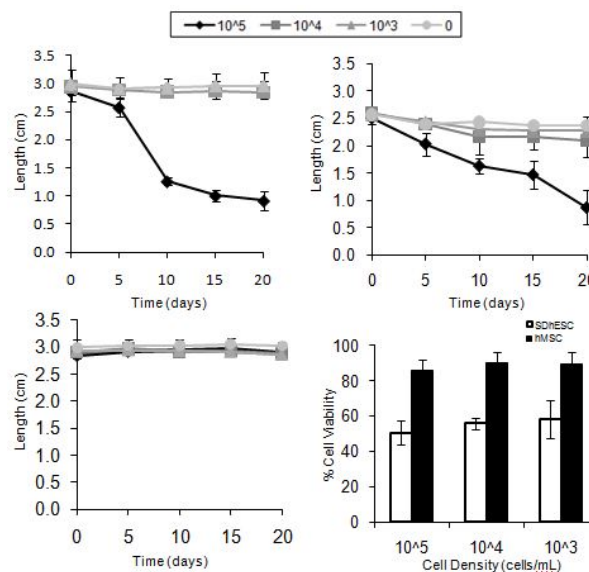


Figure 1. Collagen gels seeded with hMSCs (top left), SDhESCs (top right) and hESCs (bottom left) contraction over time. Graph shows mean length \pm one standard deviation. $n=3$. Bar chart shows mean cell viability of all cell densities in PHBHHx/collagen scaffold at day 20 of culture \pm one standard deviation. $n=3$.

DISCUSSION & CONCLUSIONS: Collagen gel tubes were suitable for maintenance of viability of both hMSCs and SDhESCs. Undifferentiated hESC were non-viable after 20 days of collagen gel tube culture. PHBHHx/collagen scaffolds have been successfully used to culture both adult and embryonic stem cells and under the correct conditions over prolonged cell culture times, indicating that this scaffold combination could be used for tendon tissue engineering applications.

REFERENCES: [1] Pennisi E. Tending Tender Tendons. *Science* 2002;295:1011-1011. [2] Doral MN, et al. Functional anatomy of the Achilles tendon. *Knee Surg Sport Tr A* 2010;18:638-643. [3] Longo UG et al. Tendon augmentation grafts: a systematic review. *Brit Med Bull* 2010;94:165-188.

ACKNOWLEDGEMENTS: Funding for this research was kindly provided by the EPSRC DTC in Regenerative Medicine and the European Commission Framework 7 program.

CONTROLLING ENVIRONMENTAL CONDITIONS TO GENERATE HOMOGENEOUS BIODEGRADABLE POLYMERIC FILMS FOR NERVE GUIDE CONDUITS

S A Mobasseri¹, O Onel², G Terenghi³, S Downes¹

¹Materials Science Centre, School of Engineering and Physical Sciences, The University of Manchester

²Sackville Street Building, School of Electrical & Electronic Engineering, The University of Manchester

³Blond McIndoe Laboratories, Stopford Building, School of Medicine, The University of Manchester

INTRODUCTION: Biodegradable polymeric conduits can be applied in peripheral nerve regeneration following trauma and nerve damage. We have developed a method to make biodegradable conduits using polycaprolactone (PCL) films by solvent casting. An environmental chamber has been modified and utilised in the experiments. The aim of the present study was to evaluate the effect of the environmental factors on the surface structure of the PCL films in order to optimise cell attachment, proliferation and nerve regeneration.

METHODS: Films were made in environmental chamber with glove ports and controlled conditions. The 3% wt/v PCL ($M_n \sim 70,000-90,000$ g/mol) in dichloromethane (99% purity) was cast on the glass cover slip (18 X 18mm). Films were imaged by scanning electron microscopy and interferometer and analysed by imaging processing and analysis software. The statistical analysis was performed by GraphPad Prism5.03. One way ANOVA with $P < 0.05$ was used to determine the statistical difference.

RESULTS: Preliminary study on PCL/PLA (80/20%) films was comparing the surface structure of the nine batches in uncontrolled and controlled T-RH (temperature-relative humidity) conditions. Only four batches in uncontrolled condition produced pitted films. However all samples in controlled conditions (23°C -50%) were pitted with average depth and width of 2.32 μ m, 4.33 μ m, respectively. Further study was performed in the environmental chamber with the constant temperature (23°C) and variable humidity (20-80%). Analysis of SEM images was carried out to measure the pit size and the area fraction of the surface covered by pits. The pit size was in a range of 1-700 μ m² and divided in to two groups; pits larger than 80 μ m² and smaller than 80 μ m². Humidity affects the surface morphology by changing the pit size and porosity. The large pits formed randomly, however the size of the small pits and its porosity, increased by increasing the humidity up to 50%.

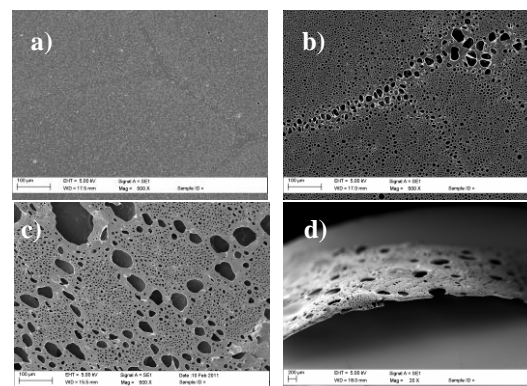


Fig. 1: Effect of humidity on the surface structure of films were made in different T-RH conditions, a) 23C-20% b) 23C-40% c) 23C-60% d) 23C-80%.

DISCUSSION & CONCLUSIONS: This study has demonstrated that environmental temperature and humidity affect the surface structure and morphology of the solvent cast films. By altering the environmental conditions, the pit size, porosity and pit distribution could be controlled. It is most likely that the changes in the environmental conditions affect the rate of the solvent evaporation directly. This has enabled us to produce pitted or non-pitted polymer surface. By controlling the rate of evaporation, it is possible to tailor the final structure with the desired surface morphology. The ability to control the surface features of biopolymers used in regenerative medicine is essential, for appropriate cell differentiation and tissue repair. Further work will analyze the combined effects of all the variables on the final morphology of the film with structured experiments and multivariate data models.

REFERENCES: Jiang, X., et al (2010), *Experimental Neurology*. 223(1): p. 86-101.

ACKNOWLEDGEMENTS: This abstract presents independent research commissioned by the National Institute for Health Research (NIHR) under the invention for Innovation (i4i) programme (11-AR-0209-10050). The views expressed in this abstract are those of the author(s) and not necessarily those of the NHS, the NIHR or the Department of Health.'

Integrin Expression and Reliance are Oxygen Concentration Dependant in Human Embryonic Stem Cells

D Kumar, S Gupta, Y Yang & N R Forsyth

Institute of Science and Technology in Medicine, University of Keele, Stoke-on-Trent, UK

INTRODUCTION: Integrins are transmembrane signalling glycoproteins which function as surface receptors to facilitate cell-cell interaction and cell adhesion to extracellular matrix (ECM) receptors¹. Microarray analysis of human Embryonic Stem Cells (hESCs) has revealed significant upregulation of specific integrin sub-units when cultured in physiological normoxia (2% O₂) relative to hyperoxia (21% O₂). This study identifies the key adhesion molecules (integrins) in hESCs that are expressed significantly higher in 2% O₂ relative to 21% O₂ and the effects of blocking these integrins on cell attachment.

METHODS: hESCs (SHEF1) were cultured and expanded on Matrigel™ with conditioned media from mouse embryonic fibroblasts in both oxygen concentrations; 2% O₂ and 21% O₂. Integrin blocking experiments were performed where hESCs were pre-incubated with anti-integrin antibodies; alpha V, beta 5, alpha V beta 5 and alpha 6 at pre-determined concentrations and conditions. Post-incubation 4 X 10⁵ cells were seeded per well of a Matrigel™ coated six-well plate. 3ml of hESC media was added to each well and cells were incubated in the relevant oxygen concentration. After 24 hours cells were trypsinised and counted in order to determine cell attachment rates. Statistical analysis was performed using Excel.

RESULTS: Microarray data analysis revealed that integrins; alpha V, beta 5, alpha E, and alpha 6 expression was significantly higher in 2% O₂ relative to 21% O₂ (Figure 1). Quantification of hESC attachment after 24 hours post-antibody pre-treatment revealed that blocking of alphaVbeta5 and alpha 6 significantly reduced hESC attachment to Matrigel™ in 2% O₂ conditions but not 21% O₂, as shown in Figure 2. When alpha V and beta 5 anti-antibodies were used independently, no significant cell inhibition was experienced in either oxygen concentrations although qualitatively there was a reduction in cell attachment in 2% O₂.

DISCUSSION & CONCLUSIONS: Oxygen concentration has an effect on integrin profiling in hESCs. Integrin binding subsequently activates

focal adhesion kinase, which spreads integrin signals to allow binding with signalling proteins which aid in various cell functions and thus identification of key integrins will help define the exact molecular signalling and cell-matrix interaction pathways involved in hESC attachment and proliferation.

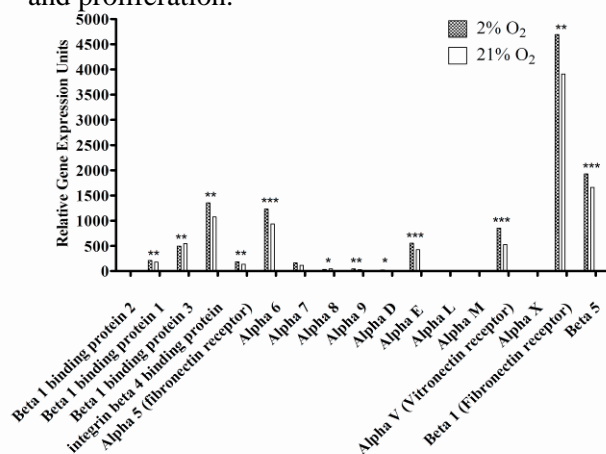


Fig. 1: Microarray analysis of integrin expression in hESCs; in both 2% and 21% O₂ concentrations. **p* < 0.05, ***p* < 0.01, ****p* < 0.001.

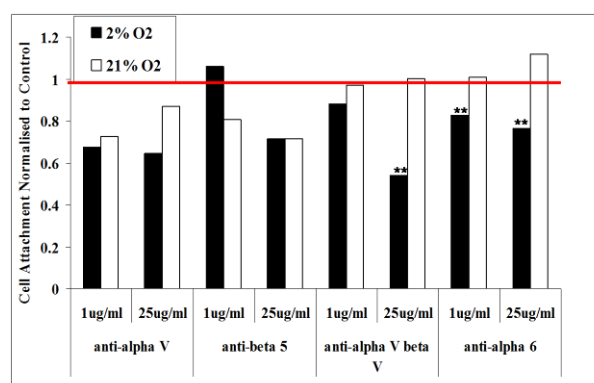


Fig. 2: Cell attachment after 24 hrs post-antibody treatment in relevant Anti-antibody solution in both 2% and 21% O₂. Values normalised to control. (n=3) Red line indicates control values. **p* < 0.05, ***p* < 0.01, ****p* < 0.001.

REFERENCES: 1. S.R. Braam et al, 2008. Recombinant Vitronectin Is a Functionally Defined Substrate That Supports Human Embryonic Stem Cell Self-Renewal via α V β 5 Integrin. Stem cells: 26(9): 2257-2265.

ACKNOWLEDGEMENTS: Keele University Acorn funding.

Investigation of Mesenchymal Stem Cells (MSC) Attachment to Cartilage in the Presence of Synovial Fluid – Towards Novel Cartilage Regeneration Strategies Based on Endogenous MSC

T Baboolal¹, E Jones¹, S Calder², R Foster¹, A Radjenovic¹, D McGonagle¹.

¹Section of Musculoskeletal Disease, Leeds Institute of Molecular Medicine, University of Leeds, UK;

²Department of Trauma and Orthopaedics, Leeds Teaching Hospital Trust, Leeds, UK

INTRODUCTION: Mesenchymal stem cells (MSCs) are highly proliferative multipotential stromal cells with the ability to regenerate cartilage, bone and other joint tissues (1). Historically MSCs were thought to reside exclusively within the bone marrow. The success of the orthopaedic microfracture procedure to repair focal cartilage defects has thus been attributed to percolation of MSCs from the marrow cavity (2).

Our group discovered synovial fluid (SF) had a resident population of MSCs, which express typical MSC markers and have tripotentiality. We have identified SF MSCs in normal joints of humans and bovines and have shown that their numbers are elevated in chronic OA (3). Thus we have discovered an intrinsic population of MSCs that reside in the knee and have direct access to superficial cartilage and joint structures independent of a bone or circulatory route.

METHODS: To investigate MSC attachment to cartilage and plastic in the presence of different SF, novel model systems were employed with the use of confocal microscopy and magnetic resonance imaging (MRI). Using MSCs tagged with fluorescent micron-sized particles of iron oxide (F-MPIOs), the attachment of MSCs to cartilage was followed by confocal microscopy and MRI. Augmentation of the SF to increase attachment was followed using a modified XTT assay. Rheumatoid arthritic (RA), non-arthritic (NA) and osteoarthritic (OA) SF was treated with 5U/ml hyaluronidase prior to addition of 10⁴ cells per well of a 96 well plate. MSCs were allowed to attach overnight before SF was replaced with XTT reagents.

RESULTS: In cartilage attachment model, SF from RA patients was seen to be less anti-adhesive than synovial fluid from OA patients (Fig 1a) allowing more cells to adhere to the cartilage surface. The anti-adhesive nature of SF prevents MSC adhesion to tissue culture plastic. Enzymatic digestion of a principle component of SF (hyaluronic acid, HA) significantly enhances MSC adhesion in osteoarthritic SF (Fig 1b).

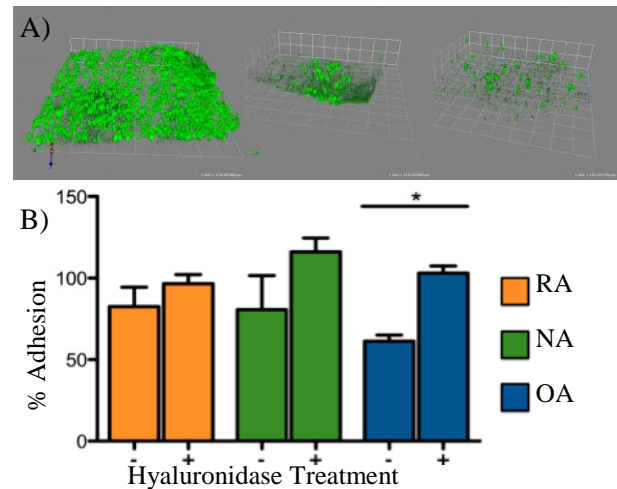


Fig. 1: A) Confocal images of F-MPIO tagged MSCs adhered to the surface of OA cartilage. B) Effect of hyaluronidase treatment on MSC adhesion to plastic in SF.

DISCUSSION & CONCLUSIONS: Data is presented showing SF is anti-adhesive, but this property can be overcome by enzymatic degradation of HA. Here we have found a possible barrier, which may functionally cripple MSCs by blocking their adhesion and integration to damaged cartilage

REFERENCES: ¹ M Pittenger, *et al.* (1999). Multilineage potential of adult human mesenchymal stem cells. *Science* **284**(5411): 143-147. ² J Steadman, *et al.* (1997). Microfracture technique for full-thickness chondral defects: Technique and clinical results. *Operative Techniques in Orthopaedics*: 300-304. ³ E Jones, *et al.* (2004). Enumeration and phenotypic characterization of synovial fluid multipotential mesenchymal progenitor cells in inflammatory and degenerative arthritis. *Arthritis and Rheumatism* **50**(3): 817-827.

ACKNOWLEDGEMENTS: This work was funded through WELMEC, a Centre of Excellence in Medical Engineering funded by the Wellcome Trust and EPSRC, under grant number WT 088908/Z/09/. E.J and D. M. are additionally part supported by NIHR-Leeds LMBRU and by PurStem – FP7 project No.223298.

Nanoscale properties of collagen in ageing

T. Abioye¹, V. Mudera² and L. Bozec¹

¹*Division of Biomaterials & Tissue Engineering, Eastman Dental Institute, University College London, WC1X 8LD*

²*Tissue Regeneration & Engineering Centre, Institute of Orthopaedics, University College London, London HA7 4LP, UK*

Introduction: Collagen is the most abundant structural protein in the human body. It is highly conserved across species and is found in our skeleton, tendons, cornea, and skin for example. Although collagen has been widely studied over the past 30 years, the relationship between its structural behaviour and its mechanical properties with ageing still remains poorly understood especially at the molecular level (nano-scale). This research looks at a novel approach to quantify the effects of collagen cross-linking due to ageing at the molecular scale by using both engineered / aged biomimetic collagen matrices. This is an inter-disciplinary approach integrating fields of nanotechnology, tissue engineering and systems biology.

Methodology and Results: There is evidence of the role of non-enzymatic glycation (NEG) cross-linking in collagen as part of the ageing process in tendons. A model system that mimics this behaviour is used enabling empirical assessment of this effect at molecular level. The model incorporates collagen matrices constructed using a standard protocol of collagen gel compression in accordance with that demonstrated by Brown et al. (2005), the gels are subsequently functionalised and aged photochemically.

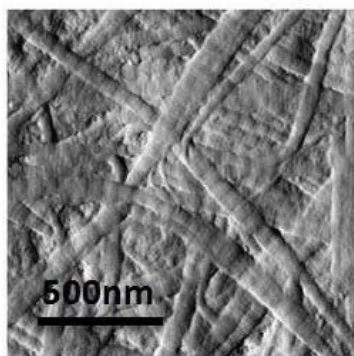


Fig 1. Plastically compressed Collagen Type I matrix with characteristic D-banding (67nm) periodicity
hydrogel resulting in improved mechanical

stability. This technique alone is however incomparable with the enhanced mechanical integrity generated through formation of NEG cross-linking. The mechanical behaviour of these collagen gels is determined quantitatively using single molecule stretching experiments performed on an Atomic Force Microscope, providing data for a supportive mathematical model. AFM, an established technique in nanotechnology, makes possible 3-dimensional imaging (Fig 1.) and quantitative mechanical response assessment (Fig 2.) of collagen at each hierarchical level that is from single molecule (nm) through to bulk tissue macro- scales.

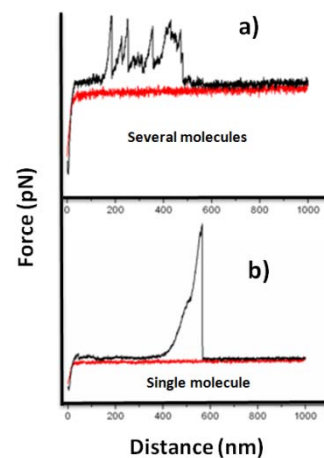


Fig 2. Single molecule force distance curve

vitro model
ies of AFM
e structural
and mechanical properties of isolated single collagen molecules in relation to other neighbouring collagen molecules within its host fibrils, specifically in the context of ageing.

References: U. Cheema, M. Wiseman, C.B. Chuo, R.A. Brown & S.N.Nazhat. (2005). *European Cells and Materials*, **10**, 39.

Acknowledgments: UCL Crucible, Evolving Health & Wellbeing, for funding on behalf of RCUK (BBSRC/EPSC/ERC/MRC).



Poly(3-hydroxybutyrate-co-3-hydroxyhexanoate) (PHBHHx) Scaffolds for Tendon Repair in the Rat Model.

William R. Webb¹, Alex J. Lomas¹, Guodong Zeng², Guo Qiang Chen², Alicia J. El Haj¹ & Nicholas R. Forsyth¹

¹ Guy Hilton Research Centre, Institute of Science and Technology in Medicine, Keele University, Stoke-on-Trent, ST4 7QB, UK.

² Department of Biological Sciences and Biotechnology, School of Life Sciences, Tsinghua University, Beijing, 100084, China

INTRODUCTION: PHBHHx is a polyhydroxyalkanoate molecule comprising random copolymers of 3-hydroxybutyrate and 3-hydroxyhexanoate produced by bacteria in response to stressed growth conditions [1]. Tendon connects bone to muscle and is characterised by impaired repair following injury or disease due to its relative acellular and poor vascularity. Tendon is comprised mainly of type I collagen fibrils arranged in a hierarchical structure, which confers its unique mechanical properties [2]. To date, a lack of successful strategies for the repair of tendons has led to the development of engineered alternatives designed to improve the healing rate or replace the tendon completely [3]. This investigation employs both *in-vitro* and *in-vivo* experiments to assess PHBHHx as a potential material for tendon tissue engineering.

METHODS: Scaffold constructs comprised of 3 fibres (produced by extrusion) and reinforced porous tubes (produced by particle leaching). Scaffold designs were mechanically tested and compared to native rat tendon using NTS tension/compression load cell tester (NTS, Canada) and elongated at a rate of 10mm/s until failure. Serum β -hydroxybutyrate was measured along with C-reactive protein to measure both polymer breakdown and immune response at multiple time points. Statistical significance was assumed if $p < 0.05$ using two tailed t-test.

RESULTS: Mechanical testing demonstrated the PHBHHx scaffold had comparable mechanical properties to native tendon ($23.73 \pm 1.06\text{N}$ vs. $17.35 \pm 1.76\text{N}$ for native tendon) (Figure 1). Restoration of movement was observed at day 10 for scaffold implanted animals and day 20 for control animals. *In vitro* mechanical testing of explanted scaffold+collagen implant was comparable to that of native rat tendon ($18.02 \pm 7.45\text{N}$ vs. $17.35 \pm 1.78\text{N}$). No significant secondary immune response to PHBHHx implant was observed over the 40 days (Figure 2). Serum measurement of β -Hydroxybutyrate (a degradation product of PHBHHx) demonstrated no correlation to immune response.

DISCUSSION & CONCLUSIONS: PHBHHx and PHBHHx+collagen hybrids have been successfully used as scaffolds for tendon tissue engineering *in vitro*, with improved mechanical properties and no long term immune response being observed.

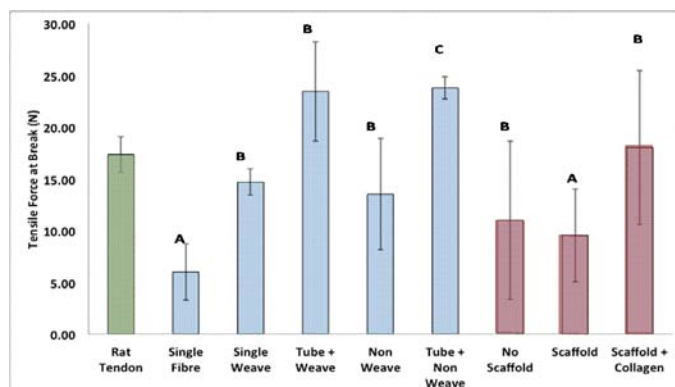


Figure 1 Mechanical testing. Green bar: shows undamaged rat Achilles tendon. Blue bars: show *in vitro* pre-implantation scaffold design. Red bars: explanted scaffold. A) Significantly lower breaking force when compared to native tendon, B) No significant difference when compared to native tendon & C) Significantly higher breaking force when compared to native tendon.

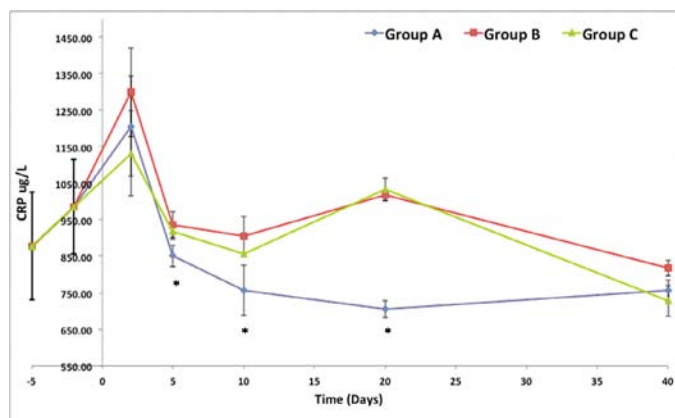


Figure 2 CRP blood serum concentrations over time for different experimental groups. Prior to implantation (Day 0) all animals were considered as one group $n=15$. Post implantation animals were split into 3 surgical groups $n=5$. * indicates results significantly lower than other experimental groups.

REFERENCES: 1) Qin YZ *et al.* Production of poly(3-hydroxybutyrate-co-3-hydroxyhexanoate) from gluconate and glucose by recombinant *Aeromonas hydrophila* and *Pseudomonas putida*. *Biotechnol. Lett* 2005; 25: 1381-1386. 2) Doral MN *et al.* Functional anatomy of the Achilles tendon. *Knee Surg. Sport Tr, A.* 2010; 18:638-643. 3) Liu Y *et al.* Tendon tissue engineering using scaffold enhanced strategies. *Trends in Biotech.* 2008; 26; 4: 201-209

ACKNOWLEDGEMENTS: European Commission Seventh Framework Programme.

Controlling Corneal Stromal Cell Phenotype via Chemical Cues

S.L. Wilson¹, M. Ahearne², S. Rauz³, A.J. El Haj¹ and Y. Yang¹

¹ Guy Hilton Research Centre, Institute for Science & Technology in Medicine, Keele University, Keele, UK.

² Trinity Centre for Bioengineering, Trinity College, Dublin, Republic of Ireland.

³ Academic Unit of Ophthalmology, School of Immunity & Infection, University of Birmingham, Birmingham, UK.

INTRODUCTION: Collagen hydrogels have been extensively used as scaffolds for corneal tissue engineering¹. However, corneal keratocytes are notoriously difficult to culture and often differentiate into fibroblasts in the scaffolds *in vitro*². This causes the construct to contract and become opaque. The aim of this study is to encourage contractile corneal fibroblasts to trans-differentiate into non-contractile keratocytes via chemical cues supplied by the media and explore the phenomena occurring both macro- and microscopically with regards to the contraction of the collagen.

METHODS: Hydrogels with collagen concentrations of 3.5 mg/ml and 5×10^5 cells per gel were manufactured. Accellular gels were also prepared to serve as a control. The hydrogels were cultured at 37°C, 5% CO₂ over a seven day period under fibroblast and keratocyte media respectively. Fibroblast media consisted of Dulbecco's modified eagle medium (DMEM; Biowest, France), supplemented with 10% foetal calf serum (Biowest, France), 1% antibiotic and antimyotic solutions (Sigma, UK) and 1% 200mM L-glutamine (Sigma, UK). Keratocyte media consisted of DMEM-F12 (Biowest, France), supplemented with 1% 100mM ascorbic acid (Sigma-Aldrich, UK), 1% antibiotic and antimyotic solution (Sigma-Aldrich, UK) and 0.1% 10mg/mL insulin (Sigma-Aldrich, UK).

Macroscopic contraction was monitored using digital imaging over a 7-day culture period and the percentage change in gel area calculated.

Microscopic contraction was monitored using FESEM imaging.

RESULTS: Hydrogels cultured under keratocyte media contracted less than hydrogels cultured in fibroblast media and maintained gel area and volume (Fig 1). As the hydrogels contract the ratio of cells to total volume increases; the collagen concentration increases as the water is forced out of the gel; and the collagen lattice density increases (Fig 2).

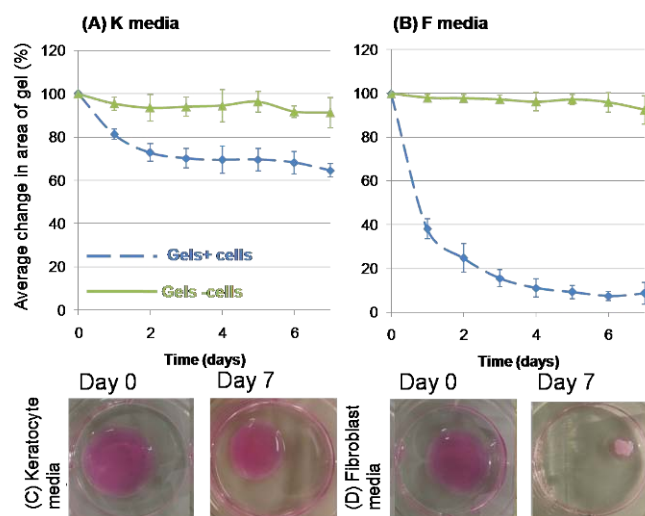


Fig 1: Average change in gel area of collagen hydrogels when cultured under (A) & (C) keratocyte media, (B) & (D) fibroblast media following 7 days culture

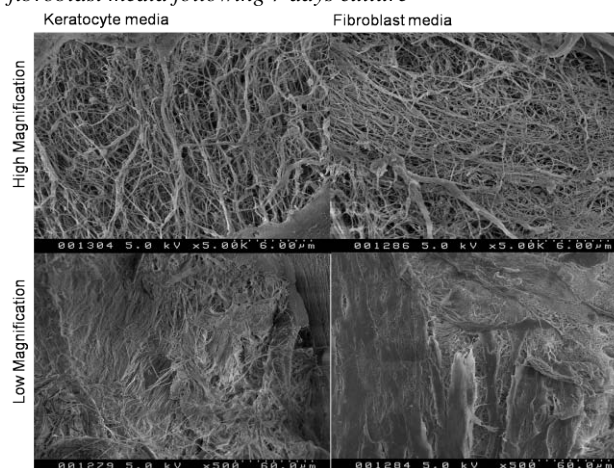


Fig 2: Images obtained by FESEM of collagen hydrogels cultured under fibroblast and keratocyte media for 7 days.

DISCUSSION & CONCLUSION: It has been demonstrated that when cultured in serum-free, media containing insulin contractile fibroblasts can be encouraged to partially trans-differentiate into a non-contractile keratocyte phenotype.

REFERENCES: ¹ Ahearne, M., Yang, Y., Then, K.Y. & Liu, K.K. (2007), *Annals of Biomedical Engineering*, **35**:1608-1616. ² Schneider, A.I., Maier-Reif, K. & Graeve, T. (1999), *In Vitro Cellular & Developmental Biology-Animal*, **35**: 515-526.

Directed differentiation of human Pluripotent cells to allow Patient-Matched Cardiac Tissue Engineering

James E. Dixon¹, Emily Dick², Isha Paik¹, Kevin M. Shakesheff¹ and Chris Denning²

School of Pharmacy¹ & School of Clinical Science², Wolfson Centre for Stem Cells, Tissue Engineering, and Modelling (STEM), Centre for Biomolecular Sciences, University of Nottingham, Nottingham, NG7 2RD, UK.

Kevin.Shakesheff@nottingham.ac.uk or Chris.Denning@nottingham.ac.uk

INTRODUCTION: The limited ability of the heart to regenerate has prompted development of new systems to produce contracting cardiomyocytes (CMs) for therapeutics. While differentiation of human embryonic stem (hESCs) and induced pluripotent stem cells (hiPSCs) into CMs has been well documented, the process remains inefficient and / or expensive, and progress would be facilitated by better understanding the early genetic events that result in cardiac specification. Also systems with simple molecular triggers over complex differentiation strategies are preferred. Previously we demonstrated that dual over-expression of *GATA4* and *TBX5* as the minimum requirement to activate the cardiac gene regulatory network (GRN) in hESCs, while a combination of *GATA4*, *TBX5*, *NKX2.5* and *BAF60c* (*GTNB*) is necessary to generate populations beating CMs positive for cardiac troponin I (cTnI) and α -actinin. Here we aimed to improve the efficiency of the system and to allow the use of characterized patient-matched pluripotent cell lines for tailored tissue engineering.

METHODS: We employed HUES7 hESCs, H9 hESCs, and iPSCs derived from hESC fibroblasts. For the initial work we used a HUES7 cell-line (MYH6-mRFP) which reports CM differentiation by expressing mRFP (monomeric red fluorescent protein). We used constitutive SIN and DOX inducible lentiviruses to over-express proteins to direct differentiation of human Pluripotent cells.

RESULTS: Here we show that inclusion of the chemotherapeutic agent, Ara-C, from day 10 of induced differentiation strategy inhibited proliferative cells thereby enriching for cTnI / α -actinin double positive CMs to 45%. Furthermore transient expression of *GTNB* using TET-on (DOX) lentiviruses for 5-7 days was necessary to activate the cardiogenesis through progenitor intermediates in a manner consistent with normal heart development. To achieve reproducible and facile production of cardiac progenitors and CMs from human pluripotent cells we have developed a

novel inducible gene-expression system and are creating pluripotent patient-matched cell lines which can be triggered to produce large quantities of cardiac tissue for engineering and therapeutics.

DISCUSSION & CONCLUSIONS: Here we demonstrate that defined factors can direct hESCs and iPSCs to functional CM through a cardiac progenitor cell intermediate. The generation of large numbers of patient-specific contractile heart cells is important for large-scale cardiac tissue engineering projects, and these cells will be employed to generate functional tissue constructs. Furthermore the creation of large quantities of therapeutic cells through a simple molecular trigger in a characterised cell line will have important implications for cardiac disease modelling, aid cell therapy approaches and validate drug screening in more physiological patient-specific contexts.

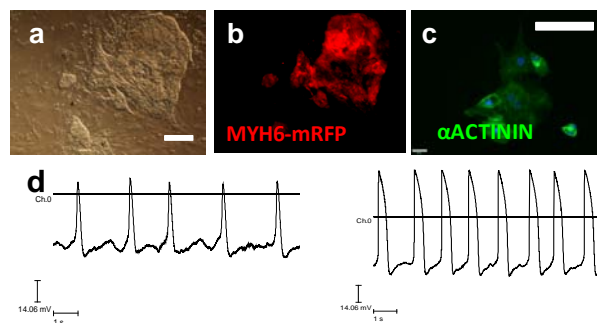


Figure 1. Directed Cardiogenesis of Human Pluripotent cells: a,b) MYH6-mRFP+ CMs. c) α -actinin immunolabelling of CMs. d) Single CM Patch-clamp traces. Bar=100 μ m

REFERENCES: ¹K. Takahashi, et al. (2006) *Cell*, **126**: 663-76. ²T. Vierbuchen, et al. (2010) *Nature*, **463**: 1035-1041. ³J. Yu, et al. (2007) *Science* **318**: 1917-1920.

ACKNOWLEDGEMENTS: We would also like to thank the BBSRC, MRC, BHF and Stem Cells for Safer Medicine for funding.

Numerical Simulations of Decellularised Aortic Valve Scaffolds

A Joda^{1,2}, S Korossis¹, Jon Summers¹, John Fisher¹ & Z Jin¹

¹ Institute of Medical and Biological Engineering, University of Leeds,

² School of Engineering, University of Liverpool

INTRODUCTION: Although prosthetic valves have been successfully used clinically over the last 50 years, conventional valve replacements are associated with significant disadvantages. Tissue-engineered heart valves offer an attractive alternative in valve replacement. A bioreactor is used with a view to acquiring appropriate biomechanical and biological functionality prior to implantation. However, the optimal culture conditions have yet to be established. Numerical simulations can provide an effective solution for quantifying the stress-strain distributions on bioreactor-conditioned valves in response to the simulated flow and pressure conditions (bottom-up approach), as well as for determining the flow and pressure conditions necessary for producing a required stress-strain distribution to the conditioned valve (top-down approach).

METHODS: The decellularised aortic scaffold was assumed to have the same geometry and dimensions as the natural aortic valve. The mechanical properties of the valve decellularised valve in the circumferential and radial directions were taken from (Korossis *et al.* 2002) and an anisotropic nonlinear model were used to fit the experimental data. The aortic model was modelled as isotropic nonlinear. The finite element software (LS-DYNA) was employed to model fluid-valve interaction.

The bioreactor was assumed to run at different operation conditions. The study assumed three cases: in the first study the bioreactor was assumed to run at different systolic transvalvular pressure. In the second study, the bioreactor was assumed to run at different diastolic transvalvular pressure and in the third study, the bioreactor was assumed to operate at different cycling rate.

RESULTS: The stress distribution in the three regions at peak systole revealed a linear increase of the mean maximum principal stress with systolic transvalvular pressure. The mean effective strain at the three regions at different diastolic transvalvular pressure showed nonlinear variation with the peak transvalvular pressure. This was due to the fact that the strain developed at these transvalvular pressures was in the post-transition region of the stress-strain curve. The strain at the belly of the decellularised valve at different transvalvular

pressures was compared with corresponding of the natural valve in Figure 1. The results indicated that in order for the decellularised scaffold to experience similar levels of strain to the natural valve, it needs to be conditioned at lower transvalvular pressures \approx (-30 mm Hg) in the bioreactor.

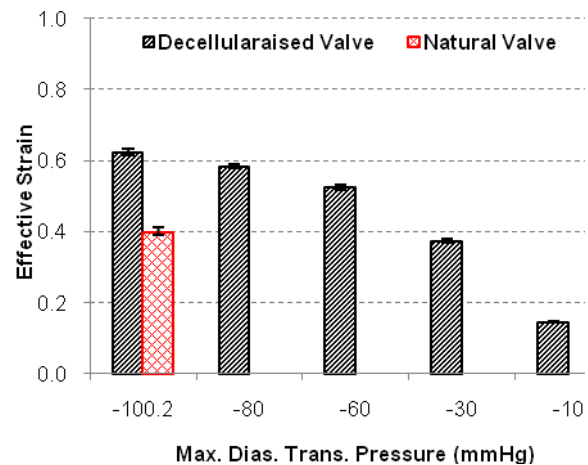


Fig. 1: Comparison of the strain in the decellularised aortic valve at different diastolic transvalvular pressures and the natural strain at the physiological condition.

DISCUSSION & CONCLUSIONS: In this study it was found that, the stress and strain distributions in the decellularised aortic valve scaffold were linearly related to the applied systolic transvalvular pressure. In addition, a bioreactor conditioning under a peak transvalvular pressure of \approx 30 mm Hg would be sufficient to obtain physiological strain levels in the decellularised scaffold.

REFERENCES: ¹ Korossis, S. A., Booth, C., Wilcox, H. E., Watterson, K. G., Kearney, J. N., Fisher, J. and Ingham, E. (2002). "Tissue engineering of cardiac valve prostheses II: Biomechanical characterization of decellularized porcine aortic heart valves." *Journal of Heart Valve Disease* **11**(4): 463-471.

ACKNOWLEDGEMENTS: This work was funded by a Marie Curie Early Stage Fellowship.

Mechanical stimulation of 3D Bio-Engineered Skeletal Muscle

D.J. Player¹, N.R.W. Martin¹, P.C. Castle¹, S. Passey¹, A.P. Sharples¹, V. Mudera²,
& M.P. Lewis^{1,3,4,5}

¹Muscle Cellular and Molecular Physiology Group, Institute of Sport and Physical Activity Research, University of Bedfordshire, Bedford, ²UCL Institute of Orthopaedics and Musculoskeletal Science, ³UCL School of Life and Medical Sciences and ⁴School of Sport, Exercise and Health Sciences, Loughborough University, ⁵Cranfield Health, Cranfield University.

INTRODUCTION: Skeletal muscle is a highly plastic tissue, responding to exercise and mechanical loading. *In vitro* culture systems have been used to replicate this mechanical stimulus in order to study cellular and molecular adaptations. Previous research using such models has often lacked bio-mimicry, with respect to the *in vitro* culture, the mechanical loading, or both. This has led to contradictory findings with regards to a variety of molecular outputs. Cell culture matrix and environment (2D or 3D), the type of mechanical loading (uni-axial or multi-axial) and the extent, speed and duration of stretching, are all likely to affect the adaptive responses of the cells and their maturation into functional muscle models. It is therefore necessary to develop a model which has greater physiological relevance if such models are to be used to further understand *in vivo* physiology.

METHODS: 3D collagen based constructs seeded with C2C12 cells (n= 6) were engineered as previously described (Mudera *et al.* 2010). Following 14 days of maturation, the constructs were transferred to an alternative chamber and tethered to the Tensioning Culture Force Monitor (t-CFM) (Fig. 1). The t-CFM is an apparatus whereby programmable regimes of mechanical strain can be applied to the construct by mounting the construct mould to a stepper motor. The mechanical stimulus used was as follows; 7.5% strain, continuous cyclic stretch for 60 minutes. N= 3 constructs were used as static controls. Conditioned media was sampled immediately post stretch for Lactate analysis. Gels were also sampled for RNA extraction. qRT-PCR was performed and gene expression was conducted using the $\Delta\Delta C_T$ method. Statistical analyses were performed using SPSS.

RESULTS: The t-CFM was successfully installed in the laboratory. Different stretch modalities have been programmed for further experimentation, including cyclic and ramp modalities.

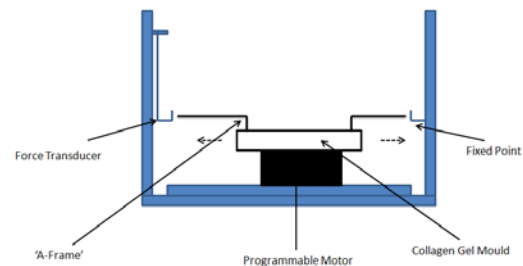


Fig. 1 Schematic diagram of the t-CFM

The stretch protocol used for the current investigation induced significantly higher concentrations of Lactate versus control immediately post stretch (3.17 ± 0.1 mmol.L and 9.8 ± 0.2 mmol.L, $p < 0.05$). Total RNA concentrations were also significantly higher (316.07 ± 249.21 ng/ μ L) in stretch versus control (121.27 ± 100.07 ng/ μ L, $p < 0.05$). Relative expression of Myogenin, a Myogenic Regulatory Factor (MRF) implicated in muscle adaptation increased immediately post stretch versus control (0.087 ± 0.48 and 2.15 ± 1.67 , $p = 0.13$).

DISCUSSION & CONCLUSIONS: Initial stretch experiments have shown acute responses similar with those seen in exercise *in vivo*. These include both classical biochemical markers of responses to exercise (Lactate) and molecular outputs (Myogenic gene expression). Further experimentation within our laboratory aims to specifically identify responses associated with different exercise modalities e.g. resistance and endurance training.

REFERENCES: Mudera V, Smith AS, Brady MA, Lewis MP, (2010), The effect of cell density on the maturation and contractile ability of muscle derived cells in a 3D tissue-engineered skeletal muscle model and determination of the cellular and mechanical stimuli required for the synthesis of a postural phenotype. *J Cell Physiol.* Vol. 225(3):646-53.

ACKNOWLEDGEMENTS: DP and NM are funded by UoB studentships.

Replicative ageing of myoblast in 3-D tissue engineered collagen constructs

AP Sharples¹ DJ. Player¹ NRW Martin¹ S Passey¹ CE Stewart³ & MP Lewis^{1,2}

¹Muscle Cellular and Molecular Physiology Group (MCMPRG), Institute for Sport and Physical Activity Research (ISPAR), University of Bedfordshire, Bedford, UK.

²UCL School of Life and Medical Sciences, London, UK.

³Institute for Biomedical Research into Human Movement and Health (IRM), Manchester Metropolitan University, Manchester, UK.

INTRODUCTION: Natural muscle wasting with age (sarcopenia) is a significant contributor to the loss of physiological and functional capacity and is strongly correlated with morbidity and mortality. After the age of 50, humans lose muscle mass at a rate of 1-2% per year with more than 50% of the population over 80 years suffering from sarcopenia. This impacts drastically on muscle strength, size and metabolic performance. Preventing muscle wasting with age is therefore of high clinical relevance. Adult skeletal muscle fibre numbers are set *in-utero* and are terminally differentiated or post-mitotic. Despite these phenomena, skeletal muscle displays astounding plasticity undergoing rapid growth (hypertrophy) during exercise, stretch and mechanical loading, yet severe loss (atrophy) with ageing, disuse and disease. This process is regulated by resident mono-nucleated satellite cells located underneath the basal lamina (termed myoblasts once activated) that do have mitotic potential essential to successful skeletal muscle plasticity and regeneration. Recently, myoblasts that have undergone replicative senescence *in-vitro* have been investigated as a model to investigate ageing in monolayer cultures (Bigot *et al.* 2008; Sharples *et al.* 2010). Although good models for the cellular mechanisms of ageing, they lack bio-mimicity. Also, as large cell numbers are needed i.e. for transplantation/grafting, it is necessary to understand the effects of multiple population doublings on the ability of myoblasts to differentiate into skeletal muscle when seeded into an *in-vivo* like 3-dimensional collagen construct.

METHODS: Serially passaged C₂C₁₂ skeletal myoblasts (58 doublings; passage 20) were compared with un-passaged cells. Cells were seeded at 4×10⁶ cells/ml in type-1 rat tail collagen (3ml) and plated in chamber slides. Floatation bars at either end provided attachment points (Fig 1), enabling the polymerised collagen/myoblast constructs to be suspended in growth medium (20% FBS) for 24hrs prior to transfer into low serum medium (2% HS) to enable differentiation.

The constructs were sampled at 3, 7 and 14 days (d).

RESULTS: Myoblasts that have undergone multiple population doublings result in reduced adhesion and ability to remodel the collagen matrix (Fig. 1). Underpinned by a reduced transcript levels of matrix remodelling metalloproteinases 2 and 9 (MMP2 9). This was followed by reduced myotube formation (multi-nucleated muscle fibres) confirmed by a reduction in IGF-I and myogenin mRNA.

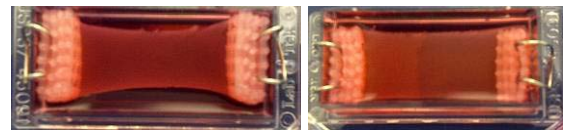


Fig. 1: An 'Un-aged/young' collagen/myoblast construct (Left) vs. collagen/myoblast construct that has undergone 58 population doublings (right). Aged cells show poor adhesion and remodelling capacity indicated by reduced 'bowing.'

DISCUSSION & CONCLUSIONS: Myoblasts that have undergone replicative ageing display reduced ability to form physiologically relevant skeletal muscle constructs and therefore may present difficulties if required for transplantation. However, constructs seems to mimic the degeneration observed during ageing *in-vivo*, and therefore presents a more biomimetic model to distinguish key mechanisms of ageing skeletal muscle..

REFERENCES: Sharples AP, Al-Shanti N, Stewart CE (2010). *J Cell Physiol.* **225**, 240-250. Bigot A, Jacquemin V, Debacq-Chainiaux F, Butler-Browne GS, Toussaint O, Furling D, Mouly V (2008). *Biol Cell.* **100**, 189-199.

Cellular interaction on a nanofibre-hydrogel composite for neural tissue engineering

Alan Weightman, Abigail Rutter, Ying Yang

Institute for Science and Technology in Medicine, Keele University, Stoke-on-Trent, UK

INTRODUCTION: Intensive research has demonstrated the clear biological potential of electrospun nanofibres for neural tissue regeneration and repair. Highly aligned nanofibre scaffolds can provide contact guidance to neural cell populations that require spatial targeting across damaged areas of the central nervous system upon injury. Radial glia are a subpopulation of astrocytes that have been shown to act as functional biological scaffolds, promoting neuronal cell guidance in the developing nervous system. This study aimed to identify whether astrocytes can differentiate into radial glia and promote the contact guidance of a co-cultured neuroblastoma in a 3D aligned nanofibre-hydrogel construct.

METHODS: Aligned, poly(L-lactic acid) (PLLA) nanofibres were produced by electrospinning 2 wt% PLLA solution onto a parallel electrode collector with a self build electrospinning machine using two oppositely charged, high voltage power supplies (Spellman HV, UK). The base of the hydrogel constructs were produced from rat tail collagen and allowed to set. The aligned PLLA nanofibres were subsequently placed on top. Primary rat astrocytes were seeded on the nanofibres with a seeding density of 100,000 cells/per scaffold. For the co-culture of astrocytes and SH-SY5Y neuroblastoma cells, the astrocytes were seeded over half of the construct area and SH-SY5Y were seeded in isolated inserts with retinoic acid (for neural differentiation) in culture media. The neuroblastoma cells were subsequently cultured for 2 days before insert removal, then co-cultured for a further 5 days.

RESULTS: Astrocytes displayed a strong response to the topography of the aligned nanofibre scaffold. Within two days of culture the majority of the cells displayed an elongated morphology, aligned in the same direction as the nanofibres. Nestin immunocytochemistry staining confirms these projections (*figure 1*). After the removal of the insert in co-culture specimens, the

differentiated neuroblastoma cells projected their extended their cellular projection toward the aligned astrocytes side (*figure 2*).

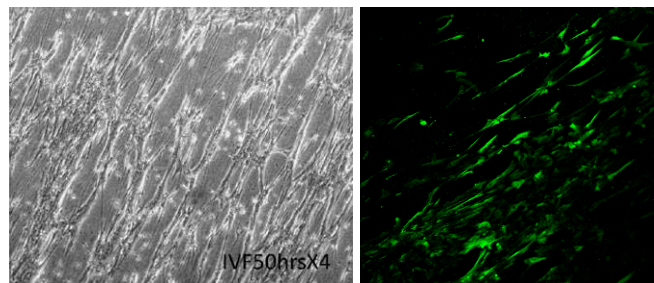


Fig. 1: (left) Alignment of astrocytes: light microscopic image. (right) Alignment of SH-SY5Y cells: Nestin staining. Both on 3D nanofibrous constructs

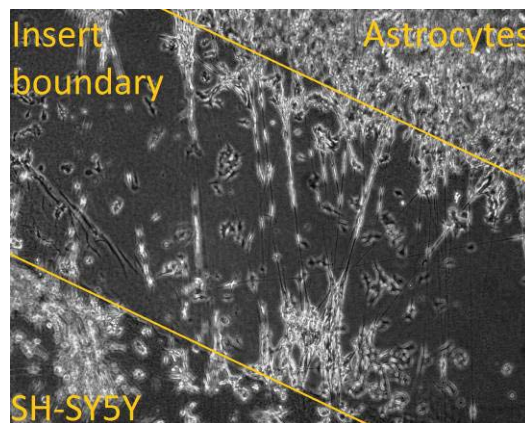


Fig. 2: Astrocytes and SH-SY5Y cells migrating across the gap left after insert removal on 3D constructs, three days after inducing SH-SY5Y cell differentiation

DISCUSSION & CONCLUSIONS: It is possible to align astrocytes in 3D scaffolds to potentially form functional biological scaffolds. Staining to identify radial glial cells will be undertaken soon. With the new insert culture system it is possible to co-culture astrocytes with neural cells and investigate effects of astrocytes on neural cell behaviour.

Engineering Skeletal Muscle Using Cellulose Nanowhiskers

J M Dugan¹ J E Gough¹ & S J Eichhorn^{1,2}

¹ School of Materials, The University of Manchester, Manchester, UK

² Northwest Composites Centre, Manchester, UK

INTRODUCTION: Cellulose nanowhiskers (CNWs) are nanofibrillar particles with extremely high aspect ratios and lateral dimensions on the order of a few nanometres. We have previously shown that CNWs are highly bioactive and may be used to impose structural order in tissue engineering applications¹. Here we have produced particularly high aspect ratio CNWs with thickness of only 6nm from cellulose extracted from the marine organism *Asciidiella aspersa*. We show that in spite of their extremely small lateral dimensions, oriented surfaces of the CNWs induce significant contact guidance in myoblasts, enabling us to engineer highly structured muscle-like tissue *in vitro*. Additionally we show that CNWs are non-cytotoxic and non-immunogenic even at relatively high concentrations.

METHODS: CNWs were prepared by partial hydrolysis of *Asciidiella aspersa* tunics. The CNWs were adsorbed onto polyallylamine coated glass using a spin-coating. The radial flow generated during the coating process was utilized to induce a high degree of orientation on the CNW surfaces. The degree of orientation was modulated by altering spin speed. C2C12 myoblasts were seeded to the surface and differentiation was induced. Myotube morphology, differentiation and matrix deposition were investigated using immunocytochemistry. The cytotoxicity and immunogenicity of both surface bound and feely dispersed CNWs was also assessed using proliferation and macrophage activation assays.

RESULTS: Proliferating myoblasts as well as terminally differentiated myotubes displayed significant contact guidance on the oriented CNW surfaces. Four days after the onset of differentiation, significant quantities of fibrillar fibronectin had been deposited by the cells. On the highly oriented surfaces the fibrils had been remodelled to reflect the orientation of the myotubes and the underlying CNWs. From proliferation data it was clear that the CNWs were highly biocompatible to the extent that no cytotoxicity was observed even at concentrations well in excess of those shown to be cytotoxic for other nanoparticle systems².

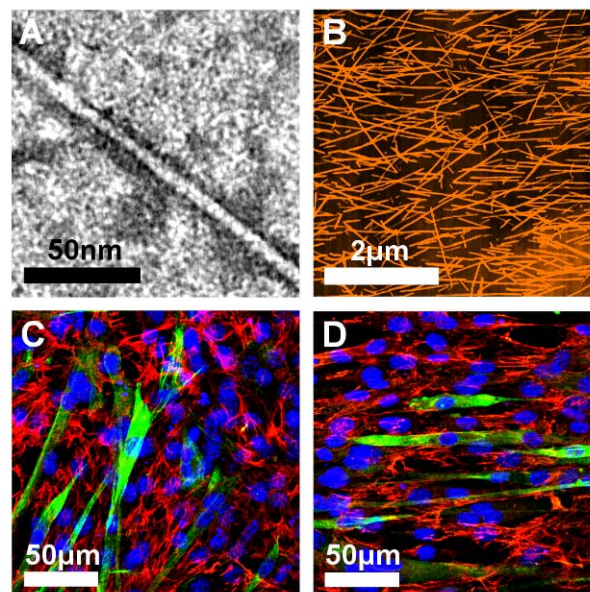


Fig. 1: (A) TEM micrograph of a short section of a single CNW. The twisted tape-like morphology of the particle can be observed. (B) AFM micrograph of a highly oriented surface of adsorbed CNWs. (C) Myotubes (green) surrounded by fibrillar fibronectin matrix (red) on an isotropic CNW surface and (D) on a highly oriented anisotropic surface.

DISCUSSION & CONCLUSIONS: We have shown that CNWs with a minimum dimension of only 6nm induce contact guidance on myoblasts and myotubes and that oriented surfaces of CNWs can be used to impart structural orientation in tissue engineering applications. The CNWs are not cytotoxic and do not induce activation of murine macrophages. We expect CNWs to become an important tool in tissue engineering and regenerative medicine.

REFERENCES: ¹ J Dugan, J Gough, S Eichhorn (2010), *Biomacromolecules*, 11, 9, 2498. ² N Lewinski, V Colvin, R Drezek (2008), *Small*, 4, 1, 26.

ACKNOWLEDGEMENTS: The project was funded by the EPSRC via a doctoral training account.

Formation of Extracellular Matrix in Bioactive Fmoc-peptide Hydrogels

M Zhou¹, RV Ulijn², JE Gough¹

¹ Materials Science Centre, School of Materials, The University of Manchester, Grosvenor Street, Manchester M1 7HS, UK. ² Department of Pure and Applied Chemistry/WestCHEM, University of Strathclyde, Cathedral Street, Glasgow G1 1XL, UK.

INTRODUCTION: We reported in 2009 the design of a biomimetic nanofibrous hydrogel through molecular self-assembly¹. The building blocks for the gel were a mixture of two aromatic short peptide derivatives: Fmoc-FF (fluorenyl-methoxycarbonyl-diphenylalanine) and Fmoc-RGD (arginine-glycine-aspartate) as the simplest self-assembling moieties reported so far for the construction of small-molecule-based bioactive hydrogels². The hydrogel promoted adhesion and proliferation of 3D-encapsulated cells through specific RGD-integrin binding. As a continuation of the previous work, we now report the extracellular matrix (ECM) depositions inside the cell-containing Fmoc-peptide hydrogel as an important measure for natural tissue regeneration. Alongside the gradual ECM formation and the previously-reported gel contraction, the cell-gel constructs were mechanically strengthened as measured by rheometry.

METHODS: The aqueous solution of 20 mM Fmoc-FF, the mixed solution of 14 mM Fmoc-FF and 6 mM Fmoc-RGD, and the mixed solution of 14 mM Fmoc-FF and 6 mM Fmoc-RGE were prepared as previously reported¹. The solutions were maintained at 4 °C for 24 hours and then mixed with either DMEM (Dulbecco's modified Eagle's medium) alone or HDFa (human dermal fibroblasts, adult) in DMEM to create either medium-induced hydrogels or cell-gel constructs with 5 million cells / ml of gel. These hydrogels with/without cells were maintained in fibroblast growth medium (DMEM supplemented with 10 % FBS (foetal bovine serum)) for 14 days.

At 1, 3, 7 and 14 days post culture, the cell-containing hydrogels were fixed in 4 % paraformaldehyde, permeabilized with 0.5 % Triton-X100, and blocked with 1 % BSA (bovine serum albumin). They were then stained with antibodies for fibronectin, collagen I, or collagen III and counter-stained with dapi.

An AR-G2 rheometer in the oscillation mode was used to measure the visco-elasticity of the hydrogels with/without cells at 1 hour, 1 day and 7 days. The elastic moduli were recorded with the increase of the oscillating frequency (1-100 Hz)

and the average value was used to indicate the stiffness of the gel.

RESULTS: ECM components of both fibronectin and collagen I were observed to deposit within the Fmoc-peptide hydrogel containing Fmoc-RGD and the distinct filamental proteins had formed mesh-like structures since day 7 (Fig 1). Depositions of these ECM proteins were also observed with the gels containing Fmoc-RGE, but the depositions were localized to around cells and no fibrous structures were detected. Collagen III was not secreted by cells in either of these gels.

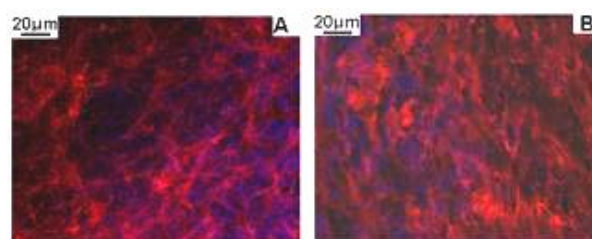


Fig. 1: Fluorescence micrographs of fibronectin (A) and collagen I deposition at day 7 within the gel containing Fmoc-RGD.

Along with the formation of ECM, the stiffness of the gel containing Fmoc-RGD was increased over the time from an average of 566 Pa to 7234 Pa. Gels of Fmoc-FF alone or containing Fmoc-RGE were not stiffened. Gels without cells degraded overtime in medium as observed.

DISCUSSION & CONCLUSIONS: The deposition of fibronectin and collagen I as fibrous networks within the gel containing Fmoc-RGD suggested the HDFa cells functioned to secrete ECM in order to reconstruct a native tissue. The involvement of RGD ligands into the self-assembled gel actively promoted cell secretion and their reorganization on ECM, which led to the strengthening of the cell-gel constructs. These evidences suggest the hydrogel may provide a bioactive scaffold for the reconstruction of a natural tissue *in vitro*, which may be useful for cell therapies and regenerative medicines.

REFERENCES: ¹ M. Zhou et al (2009) *Biomaterials* 30:2523-30. ² MO Guler et al (2006) *Biomacromolecules* 7: 1855-63.

The potential use of konjac glucomannan for wound healing and cell transportation

[Munira](#) Shahbuddin, Sheila MacNeil and Stephen Rimmer

*The Kroto Research Institute, Department of Materials Science & Engineering,
University of Sheffield, UK.*

INTRODUCTION: Konjac glucomannan (KGM) is a plant heteropolysaccharide that is comprised of D-mannose and D-glucose linked by β 1-4 glycosidic chains. KGM has long been used in food and as a medicine to treat wounds, to lower cholesterol level and to enhance insulin production in the treatment of diabetes. Due to its characteristics of low cost, high viscosity, excellent film forming ability, good biocompatibility and biodegradability, KGM and its derivatives have been used widely in the food, pharmaceutical, biomaterials and fine chemical industries. The low molecular weight KGM is becoming important in the development of biodegradable hydrogels. In this study, two methods were used to determine the low molecular weight components of KGM which are ethanol extraction and enzymatic hydrolyzation.

METHODS: 1. Determination of different molecular weight distribution of KGM

1.1 Extraction of high molecular weight from low molecular weight sugars in KGM by ethanol.

1.2 Enzymatic hydrolyzation.

(500 U/mg) β -mannanase from *C.japonicus*

C.

2. The study on the effect of different molecular weight distribution of KGM on skin cells.

Powders obtained from extraction and hydrolyzation were tested on skin cells at different concentrations for 1, 3, 5 and 7 days.

3. The effect of native KGM with skin cells in unchanged media cultured for up to 17 days.

RESULTS:

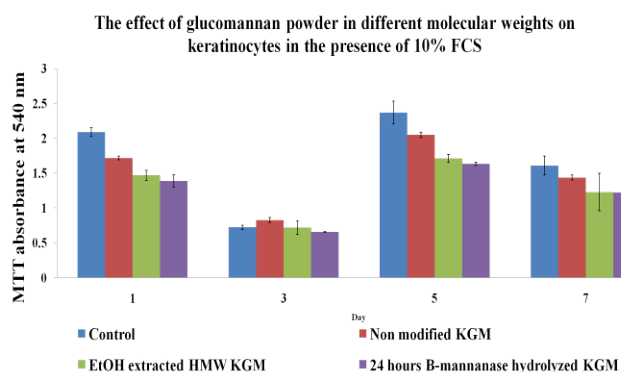


Fig. 2: The effect of 5 mg/ml glucomannan powder of different molecular weight on keratinocyte viability using MTT assay

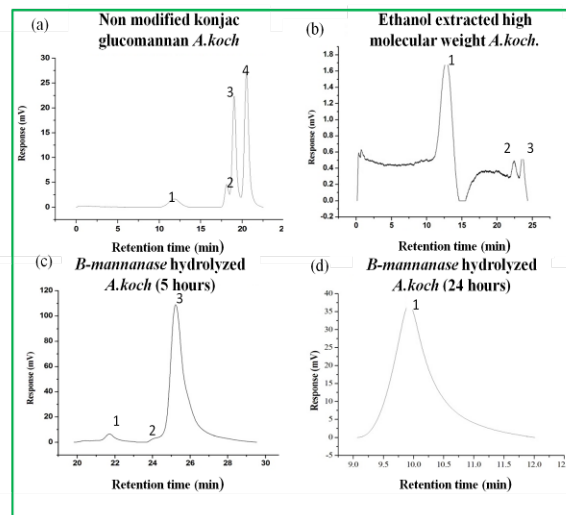


Fig. 1: Gas Permeation Chromatograms of native, extracted and hydrolyzed KGM.

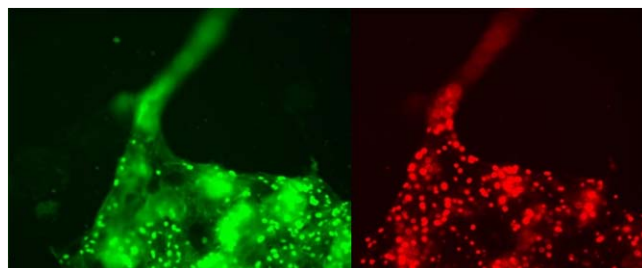


Fig. 3: Live (a) and Dead (b) stained keratinocytes showed inhibitory response to native KGM hydrogels on day 10

DISCUSSION & CONCLUSIONS:

Different molecular weight distribution of KGM can influence cellular viability which is very important for wound healing.

Native KGM showed the most significant effect on both cells, being inhibitory to keratinocytes and stimulatory to fibroblasts.

Native KGM hydrogels support cultivation of fibroblasts in unchanged media up to 17 days and is a good candidate for the development of hydrogels for cell transportation.

ACKNOWLEDGEMENTS: financial support from The Ministry of Higher Education (Malaysia).

Morphological Influence of Functionalised Nanodiamond Surfaces on Neuronal Cells

A P Hopper¹, F Claeysens¹

¹*Dept. of Materials Science & Engineering, The Kroto Research Institute, North Campus, University of Sheffield, Broad Lane, Sheffield S3 7HQ*

INTRODUCTION: Detonation nanodiamond (ND), first produced four decades ago [1], has recently found an intriguing niche in biological research. Normally, primary neuronal cultures require the prior deposition of an organic layer, composed of extracellular matrix proteins, in order to facilitate *in vitro* attachment and proliferation. Interestingly, the unique combination of material characteristics associated with ND particles (their nanometre dimensions, spherical topography, electrical properties, biocompatibility and functionalisation versatility) make it well suited for the formation of *in vivo* electrically conductive neuronal interfaces in applications such as nerve conduits. Such particles can be applied to surfaces by ultrasonication in a matter of minutes making the procedure quick and simple to undertake.

The aim of this study is to assess the suitability of amine functionalised nanodiamond particles for the coating of neural implants. Neuronal adhesion and cytocompatibility of nanodiamond substrates were assessed using NG108-15 neural cells.

METHODS: Glass cover slips (13mm) were coated with acrylic acid by plasma polymersiation (10 mins, 15W). Detonation nanodiamond was hydrogenated by microwave-assisted chemical vapour deposition (MWCVD) by exposure to 100% H₂ plasma. The particles were then photochemically functionalised with trifluoroacetic acid protected 10-amino-dec-1-ene (TFAAD) ($\lambda=254\text{nm}$, 4 hours) and subsequently deprotected over 24 hours. These particles were applied to plain and acrylic acid coated glass cover slips by ultrasonication for 10 mins. Neuronal NG108-15 cells were then cultured on these glass slides for up to 7 days in serum-free media. Cell morphology was analysed by fluorescence microscopy, labelling cells with Phalloidin-FITC and DAPI.

RESULTS: MTT assays of NG108-15 cell growth on functionalised ND indicates that ND is capable of sustaining neuronal cells, and that photochemical functionalisation with UV light greatly improves neural adhesion and proliferation on these surfaces. Cell aspect ratio measurements indicate that neurite outgrowth is more prevalent in cultures grown on functionalised ND/acrylic acid coated glass.

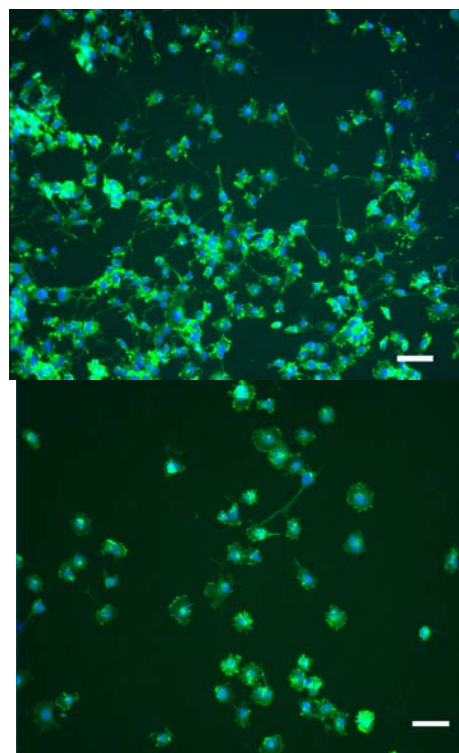


Fig. 1: Fluorescence staining of NG108-15 cells cultured on (Top) amine functionalised nanodiamond Layered upon Acrylic Acid Coated Glass and (Bottom) Acrylic Acid Coated Glass (green = phalloidin-FITC stain, blue = DAPI). Neuronal cells cultured in the presence of the functionalised ND demonstrated greater neurite outgrowth and proliferation. Scale bar: 100 μm

DISCUSSION & CONCLUSIONS: Our data highlights that ND is a modifiable substrate suitable for culturing neuronal cells. The amine functionalisation enhances the proliferative capacity of NG108-15 cells and increased neurite outgrowth significantly. The use of acrylic acid as an initial surface coating prior to nanodiamond deposition increases neuronal cell attachment. The most optimal results were observed in samples concomitantly cultured on acrylic acid coated glass layered with amine functionalised ND.

REFERENCES: ¹ A. Krueger et al. (2005) Unusually tight aggregation in detonation nanodiamond: identification and disintegration, Carbon 43(8):1722-30.

ACKNOWLEDGEMENTS: We are grateful to the EPSRC for funding this research.

Cytokines Modulated Myofibroblast Induction and Force Generation in Dupuytren's Fibroblasts; Lessons for Tissue Engineering?

J.S.N. Verhoekx^{1,2}, J.F.A. van der Werff, V². Mudera¹

¹ *Tissue Repair and Engineering Centre, Stanmore Campus, UCL*

² *Dept of Plastic, Reconstructive and Hand Surgery, Leiden University Medical Centre*

INTRODUCTION: Tissue engineering aims to get cells in vitro to lay down collagen and generate living functional 3D structures for implantation. The major challenge is getting fibroblasts to lay down functional collagen in vitro. We studied a natural condition where fibroblasts secrete excess collagen and shorten the matrix by remodelling it (Dupuytren's disease). Some of the collagen laid down is organised and has the structure of tendon (cord) but the active state is the nodule. The cells responsible for the fibrotic contractures seen in Dupuytren's disease are the myofibroblasts, expressing α -smooth muscle actin (α -SMA), correlating with increased deposition of extracellular matrix (ECM) components¹ and contractile force generation, contracting the ECM². Cytokines are potential targets for myofibroblast modulation, as they control expression of myofibroblast marker α -SMA³. We have examined the effect of cytokines, TGF- β 1 and PDGF-BB, on force generation and matrix remodeling.

METHODS:

Dupuytren's nodule and flexor retinaculum fibroblasts were cultured in 2D for myofibroblast induction and in 3D collagen type I constructs under isometric tension with and without the stimulation of cytokines, to test the effect of force generation in a culture force monitor (CFM)⁴.

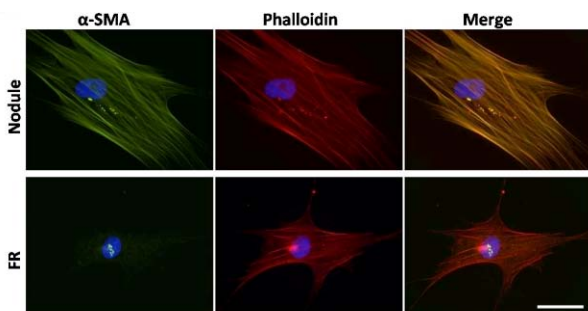


Fig. 1: α -SMA localisation to stress fibres in Dupuytren's nodule (myofibroblast) and flexor retinaculum cells

RESULTS:

Differences in force generation and myofibroblast induction were significant, and were modulated by cytokine stimulation. 12.5 ng/ml TGF- β 1 resulted in highest force generation and myofibroblast induction, however at higher concentrations there was a feedback inhibition. Stimulation with PDGF-BB resulted in lower force generation, correlation with decreased myofibroblast induction.

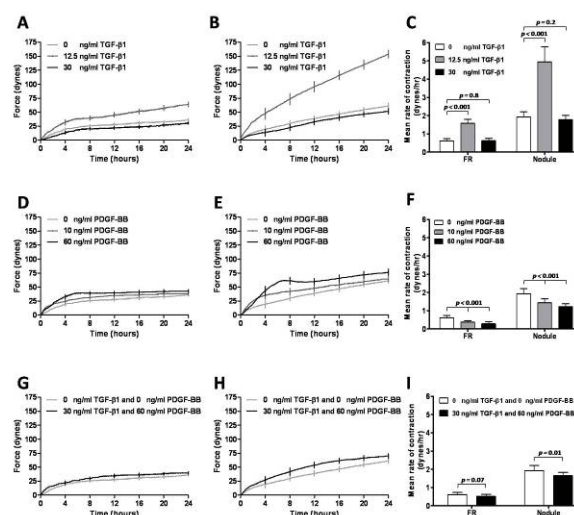


Fig. 2: Isometric contraction of collagen gels by Dupuytren nodule (B,E,H) and flexor retinaculum (A,D,G) cells after cytokine stimulation

DISCUSSION & CONCLUSIONS: Our findings suggest there is a correlation between cytokine concentration and matrix remodelling and force generation in 3D. This data can be used to modulate fibroblasts for tissue engineering applications.

REFERENCES: ¹ Marenzana et al., 2006 ² Rayan and Tomasek, 1994 ³ Hinz, 2007 ⁴ Eastwood, 1996

ACKNOWLEDGEMENTS: We would like to thank the Rijnland Hospital Leiderdorp in The Netherlands for their financial support for funding this project.

Lattice-Boltzmann Mathematical Model of cell attachment in a perfusion bioreactor: validation using microCT

[LA Hidalgo-Bastida](#)¹, [TJ Spencer](#)², [T Lowe](#)³, [P Withers](#)³, [I Halliday](#)², [C Care](#)² & [SH Cartmell](#)¹

¹*Materials Science Centre, University of Manchester, UK*

²*Materials and Engineering Research Institute, Sheffield Hallam University, UK*

³*Henry Moseley X-Ray Imaging Facility, University of Manchester, UK*

INTRODUCTION: The optimisation of tissue engineering bioreactors is a lengthy and expensive experimental process. Mathematical modelling can reduce cost and time by providing a very close approximation of the operational parameters. Although different models have been used in bioengineering, only the lattice-Boltzmann code allows the simulation of multi-scale systems such as these. Cell attachment and subsequent proliferation and differentiation are determined by the cell (particle) behaviour in a given perfusion environment (flow rate, cell concentration, nutrients availability and waste removal). By using this mathematical tool we aim to optimise a perfusion bioreactor by developing a code that can simulate all these conditions and then conducting experimental work to validate it.

METHODS: The lattice-Boltzmann model was developed to predict cell adhesion based on surface, perfusion rate (fluid velocity) and initial cell concentration parameters. The simulations were run for straight and bended channels to mimic the pattern of a single cell moving through a porous scaffold. For the validation, protein-coated and uncoated tygon tubing (1.02 mm diameter) was seeded at 0.0003 ml/min with hMSC previously labelled with superparamagnetic particles (CD105 Microbeads, Miltenyi Biotec Ltd, UK) and placed in a "U" holder. Samples were CT imaged at low voltage and high current using a Nikon Custom 320 kV bay. Reconstructed images were cropped into straight sections and 90 degrees section for the validation.

RESULTS: Mathematical modelling of 90 degrees sections revealed that when particles of different sizes are present in the perfusion system, large particles push the small particles to the edges; meanwhile, cells in straight sections always are concentrated in the centre of the channel. Validation data showed that cells seeded onto uncoated tygon tubing did not attach regardless of seeding time. Protein-coated tubing confirmed cell adhesion to the internal walls in the lower region of the conduit.

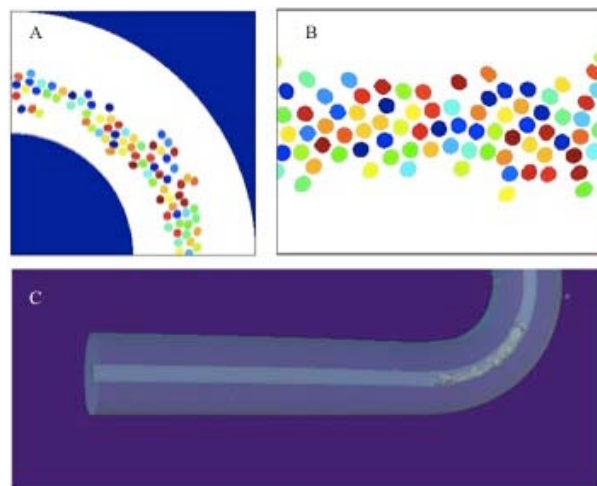


Fig. 1: Math model of cells through (A) a 90 degree section and (B) a straight section compared to (C) a microCT reconstruction of the tubing bended at 90 degrees containing hMSCs (flow direction is from left to right in all the cases)

DISCUSSION & CONCLUSIONS: The cell attachment simulations produced by the lattice-Boltzmann code provided useful information on cell behaviour and attachment for our perfusion model. CT data of labelled cells showed specific adhesion patterns. Cells accumulated near the bend as suggested in the model, however the main deposition occurred in the bottom section. We hypothesise this was caused by gravity. Our model did not include that component, which would explain why the data did not match the simulation. Current work incorporates gravity to our lattice-Boltzmann model to confirm the influence of this element.

REFERENCES: ¹ I. Halliday, T.J. Spencer, and C.M. Care (2009) *Phys. Rev.* **E79**: 016706 ² T.J. Spencer, I. Halliday, C.M. Care, et al (2011) *2011arXiv1101.2103S* ³ R. Whittaker, R. Booth, R. Dyson, et al (2009) *J Theor Biol* **256**(4):533-46.

ACKNOWLEDGEMENTS: This project has been supported by the BBRSC research grants BB/F013892/1 and BB/F013744/1.

Biomechanical Properties of Thin Collagen-Elastin Constructs for Lung Tissue Engineering

S. Dunphy¹, N. Forsyth² & A. El Haj²

¹*Doctoral Training Centre for Regenerative Medicine, Loughborough University, UK*

²*Institute for Science and Technology in Medicine, Keele University, UK*

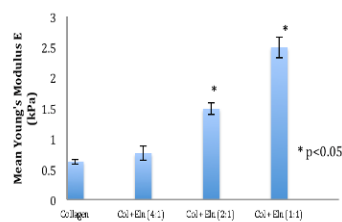
INTRODUCTION: There is a paucity of research in the area of lung tissue engineering. Few biomaterials have been investigated for this purpose. The aim of this study was to start with the smallest functional unit of the lung, the single alveoli, and produce a material capable of mimicking its mechanical and structural characteristics. It has been shown by Yuan et al that the macroscopic elastic and dissipative properties of alveolar tissue are dominated by both collagen and elastin^{1,2}. The average Young's modulus of a single alveolar wall has been calculated by Cavalcante et al to be ~5kPa³. In this study collagen-elastin hydrogel constructs were manufactured and tested. The effect of elastin concentration and cell seeding density on Young's modulus was examined.

METHODS: Type I rat-tail collagen (BD Bioscience), soluble bovine elastin (Sigma Aldrich), and human lung fibroblasts were used to make thin hydrogel constructs using a previously described protocol⁴. Collagen only hydrogels and hybrid constructs with varying collagen to elastin ratios (4:1, 2:1, and 1:1) were manufactured. A constant collagen concentration of 3.5 mg/ml was used for all gels. Cells were seeded throughout the hydrogels and concentrations of 5×10^3 , 2.5×10^5 , and 5×10^5 cells per hydrogel construct were prepared. Hydrogels were cultured at 37°C 5% CO₂ over a period of 8 days.

Biomechanical testing was carried out on the constructs using a non-destructive spherical indentation technique previously described by Ahearne et al.⁵ The thickness of each construct was measured using an optical coherence tomography (OCT) system⁶.

RESULTS: The Young's modulus was found to increase linearly with increasing elastin concentration (Fig.1).

Fig. 1: Mean Young's modulus \pm standard error at different elastin concentrations. (n=4)



When cells were added an elastic modulus comparable to that found in the literature was achieved (Fig. 2).

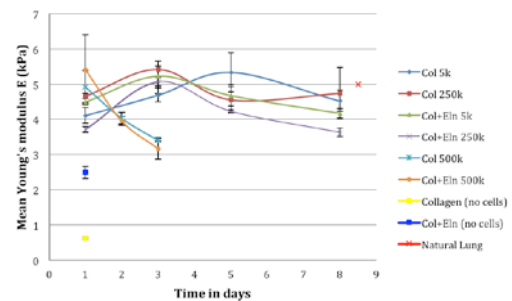


Fig. 2: Young's modulus \pm standard error versus time in days for various hydrogels with and without cells. The literature value for Young's modulus of a single alveolar wall is shown. (n=3)

DISCUSSION & CONCLUSIONS: The feasibility of manufacturing a scaffold using extracellular matrix components capable of mimicking the mechanical characteristics of native alveolar tissue has been demonstrated. Increasing the elastin concentration resulted in a corresponding rise in Young's modulus. When cells were added to the constructs the relationship between collagen and elastin broke down and the modulus became dependent on cell concentration. Hydrogels with a higher initial cell seeding concentration increased in elastic modulus faster than those with a lower cell seeding concentration.

REFERENCES: ¹ H. Yuan et al. (1997) *J Appl Physiol.* 83:1420-1431. ² H. Yuan et al. *J Appl Physiol.* 89:3-14. ³ F.S.A. Cavalcante et al. (2005) *J Appl Physiol.* (Bethesda, Md. : 1985). 98:672-9. ⁴ M. Ahearne et al. (2008) *The Brit J Ophthalmol.* 92:268-71. ⁵ M. Ahearne et al. (2005) *J R Soc Interface.* 2:455-63. 34:L91-L94. ⁶ Y. Yang et al. (2006) *Phys Med Biol.* 51:1649-59.

ACKNOWLEDGEMENTS: This work was funded by the EPSRC Doctoral Training Centre for Regenerative Medicine. I would like to thank everyone in the Institute for Science and Technology in Medicine, Keele University, in particular Khondoker Akrim, Samantha Wilson, and Ian Wimpenny.

Tissue Non-Specific Alkaline Phosphatase Expression by Human Dental Pulp Cells: A Selectable Marker for Mineralisation

Matthew J Tomlinson¹, Cairtriona Dennis¹, Xuebin B Yang^{1,2} and Jennifer Kirkham^{1,2}

¹Department of Oral Biology, Leeds Dental Institute, University of Leeds, Leeds, UK and ²NIHR Leeds Musculoskeletal Biomedical Research Unit, Chapel Allerton Hospital, Leeds, UK

INTRODUCTION: Expression of alkaline phosphatase is associated with mineralisation potential in cell culture [1]. Recently, tissue non-specific alkaline phosphatase (TNAP), also known as mesenchymal stem cell antigen 1 (MSCA-1), was utilised to identify a sub-population of bone marrow mesenchymal stem cells (BM-MSCs) [2]. We aimed to study TNAP expression by human dental pulp cells (HDPCs) under a range of conditions and with a variety of other HDPC markers. Ultimately we aimed to use cell sorting to determine further the mineralisation potential of TNAP+ HDPCs.

METHODS: HDPCs were enzymatically liberated from human third molar dental pulps and either culture expanded or analysed by flow cytometry for TNAP expression. Subsequent markers used for co-expression analysis of cultured HDPCs included: CD29, CD44, CD73 and CD90. HDPCs and BM-MSCs were cultured over a range of densities and time periods before flow cytometric analysis for TNAP expression. FACS sorted TNAP+, TNAP- and unsorted HDPCs were cultured in pro-osteogenic media before alizarin red and von Kossa staining, SEM imaging and energy dispersive X-ray (EDX) analysis.

RESULTS: It was found that both primary and culture expanded HDPCs expressed TNAP (Fig.1). Co-expression studies of expanded HDPCs revealed that TNAP is expressed in conjunction with other HDPC markers.

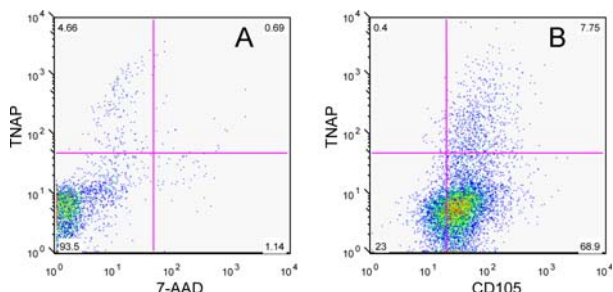


Fig.1: Flow cytometric analysis of TNAP expression on (A) primary HDPCs and (B) culture expanded p0 HDPCs.

Furthermore it was found that increased cell density and prolonged culture (3 weeks) enhanced TNAP expression in HDPCs whereas in BM-MSCs TNAP expression was shown to be consistently high. FACS sorted TNAP+ HDPCs were osteogenically differentiated and histology, SEM and EDX showed greater mineral deposits than with unsorted cells (Fig.2).



Fig.2: Alizarin red and von Kossa staining (with van Gieson's counterstain) of day 28 osteogenic cultures of TNAP+ and unsorted HDPCs.

DISCUSSION & CONCLUSIONS: These data confirm that TNAP is co-expressed by HDPCs alongside other established markers. Cell density appears to affect the level of TNAP expression, potentially through cell-cell signalling mechanisms. Sorting for TNAP+ cells gives a subpopulation of HDPCs which are pro-mineralising compared to TNAP- and unsorted HDPCs. We conclude that TNAP is a potentially useful marker for HDPC selection in osteoinductive regenerative therapies.

REFERENCES: ¹ E.E. Golub and K. Boesze-Battaglia (2007) *Curr Opin Orthop* **18**: 444-8. ² V.L. Battula, S. Treml, P.M. Bareiss, et al (2009) *Haemtaologica* **94**: 173-184.

ACKNOWLEDGEMENTS: This work was funded through WELMEC, a Centre of Excellence in Medical Engineering funded by the Wellcome Trust and EPSRC, under grant number WT 088908/Z/09/Z. XY and JK are supported by the NIHR Leeds Musculoskeletal Biomedical Research Unit.

Cryopreservation of Limbal Epithelial Stem Cells for Transplantation to Treat Limbal Stem Cell Deficiency

Elsie Fok¹, Sheraz M Daya², Nigel R Jordan¹, Susan Sandeman³ and Justin R Sharpe⁴

¹Queen Victoria Hospital, East Grinstead, ²Centre for Sight, East Grinstead, ³University of Brighton, Brighton, ⁴Blond McIndoe Research Foundation, East Grinstead

INTRODUCTION: Studies have shown that limbal stem cell deficiency can be treated using limbal epithelial stem cells derived from cadaveric donor tissue. An increase in demand for such treatment coupled with a shortage in cadaveric donor tissues requires that alternative culture, storage and delivery methods are developed to increase the availability of limbal epithelial stem cells (LESC). The purpose of this study was to optimize the usage of cadaveric donor tissue as well as to investigate further expansion and cryopreservation as a method for storing LESCs for the treatment of limbal stem cell deficiency. The cryopreservation of LESCs would allow a larger number of patients to benefit from cells derived from a single donated limbal ring. Additionally, cryopreserved cells could be transported to other centres.

METHODS: LESCs were harvested from cadaveric limbal tissues stored in Optisol and organ culture media and expanded in tissue culture. Sub-confluent expanded cells were further expanded and cryopreserved in liquid nitrogen for a minimum of 30 days prior to thawing and characterisation. Cell morphology and the expression of genes and proteins typical of a LESCs phenotype were assessed before and after expansion and cryopreservation using light microscopy, quantitative RT-PCR and immunocytochemistry.

RESULTS: Tissues stored in Optisol yielded a greater percentage of cultures attaining 80% confluence. All primary cultures demonstrated an epithelial cobblestone like cell morphology. Secondary and cryopreserved cultures however were loosely packed when compared with primary cultures. Further expanded and cryopreserved LESCs maintained all limbal stem cell phenotype characteristics as shown by immunocytochemistry for putative limbal cell markers K3, K19, p63, ABCG2 and Pax6 (Fig.1). Analysis of the same genes by RT-PCR showed no statistically significant difference following expansion and cryopreservation. Cryopreserved cells maintained 72% cell viability following thawing.

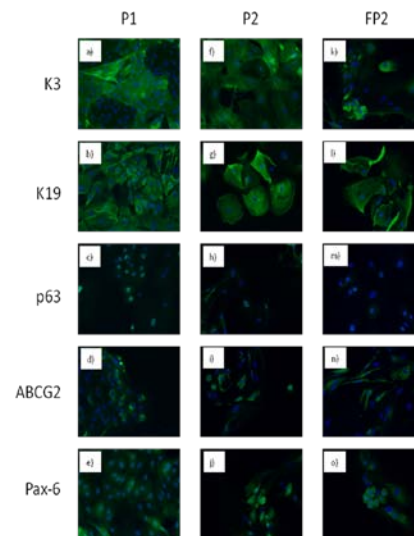


Fig. 1: Immunocytochemistry for putative limbal cell markers K3, K19, p63, ABCG2 and Pax6

DISCUSSION & CONCLUSIONS: Tissue stored in Optisol was found to provide maximal primary cell culture yield. Positive staining of putative stem cell markers indicated that a LESCs phenotype was maintained following expansion and cryopreservation. Our findings suggest that both expanded and cryopreserved cell cultures maintain the necessary characteristics required to establish a limbal epithelial stem cell bank. However, loosely packed cells observed in secondary and cryopreserved cultures may require a different delivery method to the recipient than that currently employed at QVH. The development of bio-degradable membranes or nano-fibres matrices may provide suitable solutions.

ACKNOWLEDGEMENTS: The authors would like to thank staff at Queen Victoria Hospital, Mr. Tony Ryan at East Grinstead Eye Bank, staff at MEH Lions Eye Bank, Moorfields Eye Hospital, London for their assistance in co-ordinating limbal tissue usage, and staff at the Blond McIndoe Research Foundation for all of their support.

Fluid-solid interaction model of the mitral valve

Nicholas R. Roberts*, Eileen Ingham*, Zhongmin Jin*, Sotiris Korossis*

*Institute of Bio Medical Engineering, University of Leeds, Leeds LS2 9JT, UK, efy2nrr@leeds.ac.uk

INTRODUCTION: The way the macroscale (organ level) haemodynamic environment is translated to mesoscale (tissue level) and, subsequently, microscale stresses and strains that regulate valvular cell function is of paramount importance to the tissue engineering of heart valves. The aim of this study was to develop 3D fluid solid interaction (FSI) computational models of stress and strain distributions in natural mitral valve components during normal valve function, with a view to optimizing the *in vitro* conditioning of recellularised pericardial and patellar tendon acellular scaffolds, suitable for mitral leaflet and chordae reconstruction.

METHODS: Mitral valve leaflets and chordae tendineae were dissected from porcine hearts within 2 hours of slaughter. Histological sections were stained with Sirius red and Millers elastin stains to determine gross collagen and elastin fibre alignment. Uniaxial tensile testing of chordae and leaflets in both circumferential and radial directions was undertaken using an Instron tensile testing machine. The histological results indicated that the collagen fibres in the anterior leaflet samples were predominantly orientated along the circumferential direction, figure 1. Collagen fibres emerged from the annulus into the posterior leaflet in a radial direction but lost any clear directionality in the body of the leaflet. Commissural chordae featured more densely packed collagen fibres compared to a looser arrangement in the strut chordae. Significant differences ($p > 0.05$; ANOVA) were found in the biomechanical parameters between the circumferential and radial, and the posterior and anterior, leaflet groups. There was no significant difference in the biomechanics between the radial and circumferential posterior leaflet groups. The commissural chordal group displayed a significantly increased modulus compared to the strut group.

Using histological and mechanical data, a biaxial pseudo-fibre Fungian constitutive relationship for the stress and strain in the leaflets was arrived at and implemented in LS-DYNA. Chordal groups were modeled using discrete cable elements which allowed the use of uniaxial stress/strain look up tables to be inputted directly into the model.

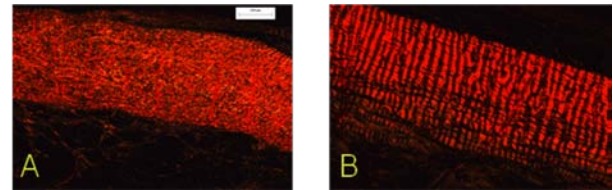


Fig. 1: A) Radial slice through the anterior leaflet
B) Circumferential slice through the anterior leaflet, both pictures under polarized light

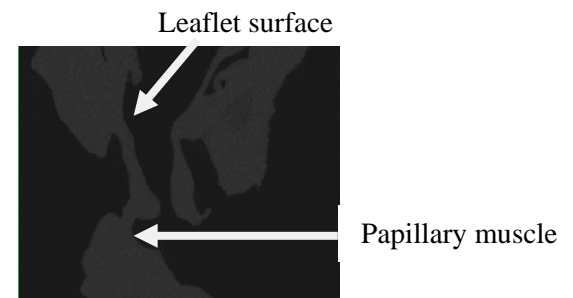


Fig. 2: Typical CT slice image

DISCUSSION & CONCLUSIONS:

The 3D FSI models developed in this study predicted significant differences in the stress and strain distributions between anatomical sites on the mitral valve leaflets and between chordae. The results from this study indicated the need for regional differentiation of mitral valve treatments in terms of mitral valve component replacement with suitable natural or synthetic biomaterials that are tailored to the biomechanics of the replaced component. The stress-strain distributions of specific mitral valve sites will be used as boundary conditions for modeling microscale stress and strain distributions, and fluid flow-induced species transport in and out of the mitral leaflet throughout the cardiac cycle.

Bioprinting as a Tool for Osteochondral Tissue Engineering

M.J.Sawkins^{1,2}, B.N. Brown², L.J. Bonassar², F.R.A.J. Rose¹ & K.M. Shakesheff¹

¹ School of Pharmacy, University of Nottingham, Nottingham, UK.

² Department of Biomedical Engineering, Cornell University, Ithaca, NY, USA.

INTRODUCTION: The Fab@Home solid freeform fabrication platform¹ has the potential to be a very useful tool for bioprinting scaffolds for cell and tissue engineering. Here, scaffolds are produced from a thermoresponsive, microparticulate polymer² suitable for applications in bone repair. Production via printing offers the opportunity to incorporate growth factor-releasing components with a precise, non-uniform spatial distribution. This in turn brings the possibility of engineering matrices with structures which are much closer to those seen in native tissues.

METHODS: Thermoresponsive microparticles were produced by melt blending PLGA 85:15 (53 kDa) with PEG 400, milling and sieving to obtain the 50 – 100 µm size fraction. Microspheres, with or without HSA/BMP-2 (1% (w/w) total protein, ratio 0.99:1), were produced via a W/O/W double emulsion technique using 90% PLGA and 10% PLGA-PEG-PLGA triblock copolymer (TB, 4.6 kDa). Release of BMP-2 into PBS from scaffolds composed of 3:2 mixes of microparticles and microspheres was measured at 37°C over 14 days. Fab@Home was used to print MC3T3 cells in crosslinked alginate, and post-printing viability was assessed. Dual material scaffolds were also produced, comprising a PLGA-PEG/PLGA-TB phase and an alginate phase. These scaffolds were then sintered for 24 hours at 37°C (22 hours submerged in aqueous solution).

RESULTS:

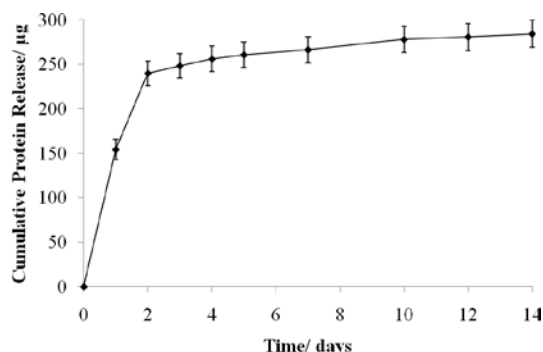


Figure 1 – Cumulative release of protein from PLGA-TB microspheres into PBS at 37°C.

Viability of printed MC3T3 cells is $84 \pm 8\%$ of pre-print viability, indicating that bioprinting can

be used successfully as a tool for producing scaffolds (or scaffold portions) containing cells.

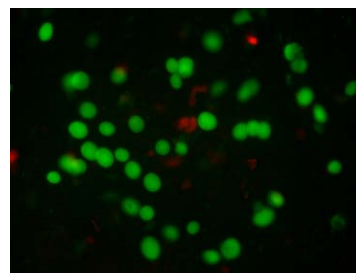


Figure 2 – Representative image of live/dead stained (calcein AM/ethidium homodimer) MC3T3 cells post-printing.

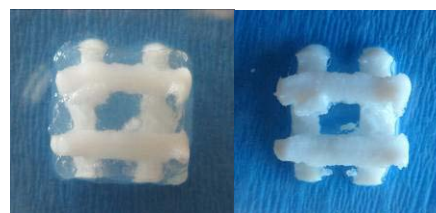


Figure 3 – Representative images of dual material scaffold produced using Fab@Home bioprinter, both before (left) and after (right) sintering.

DISCUSSION & CONCLUSIONS: Following a burst release in the first two days of incubation, PLGA-PEG/PLGA-TB scaffolds then release protein at a steady rate for at least twelve days. This system can thus deliver BMP-2 over timescales required for osteogenic differentiation of many cell types. The polymer phase of printed scaffolds can be sintered to form solid structures, with retention of the alginate phase if desired. These scaffolds have significant potential for application in osteochondral tissue engineering, the polymer phase providing mechanical strength and delivering growth factors in a spatially-defined manner, and the alginate phase acting as a medium for cell delivery.

REFERENCES: ¹ E. Malone & H. Lipson (2007) *Rapid Prototyping Journal* 13:245-255

ACKNOWLEDGEMENTS: Helen Cox, Lisa White & Giles Kirby for training and general assistance. EPSRC, BBSRC, EMDA and ERC for funding.

A novel caged carbonyl for biomaterial modification and cell patterning

L. O' Donovan & P.A. De Bank

Department of Pharmacy and Pharmacology & [Centre for Regenerative Medicine](#), University of Bath, BA2 7AY, UK.

INTRODUCTION: Natural tissues require a specific 3D configuration of multiple cell types in order to ensure their correct function. Many strategies have been described to recreate this complex patterning.^{1,2} A fundamental flaw in most approaches is that once a pattern has been created and cells seeded, subsequent patterning and seeding of additional cell types is not compatible with cell culture. Photolabile protecting groups (PPGs) have gained interest due to their rapid removal by UV light. The use of PPGs to “cage” carboxylic acids and amines has been reported,^{3,4} and enables patterning by coupling of biomolecules to uncaged functional groups following UV exposure. However, cells are rich in these functionalities and so these approaches are unsuitable for sequential patterning strategies. We have synthesized a novel, bifunctional linker with a caged carbonyl, a functional group not naturally found in biology. This ensures that, following uncaging with UV light, only areas with free carbonyls are chemoselectively modified with cell-adhesive species (e.g. hydrazides). We propose that following seeding and growth of one cell type on the patterned area, a second area can be uncaged and the process repeated.

METHODS: A novel bi-functional linker, which possesses a “caged” carbonyl at one end and a free amine for facile attachment to a variety of natural and synthetic cell scaffolds was synthesized. This molecule was subsequently attached to biomaterials including collagen, alginate and PLGA using carbodiimide coupling chemistry. Its attachment and subsequent loss of PPG following exposure to UVA light was monitored by UV/Vis spectroscopy and HPLC. Simple photo-resistant masks were also employed to shield areas of modified surfaces in an attempt to produce patterned surfaces. Cell adhesion and viability on modified surfaces was assessed *via* the MTS assay and Hoechst staining.

RESULTS: Attachment of the caged carbonyl to various biomaterials and loss of PPG following UV exposure proceeded smoothly as demonstrated by the UV absorbance of the material (Fig. 1). Full uncaging occurred within 10 minutes of exposure. The resultant free carbonyl groups were successfully utilized to further modify surfaces with the fluorescent molecule fluorescein-5-thiosemicarbazide (FTS). UVA exposure using

photo-resistant masks and subsequent ligation of FTS enabled the formation of basic patterns.

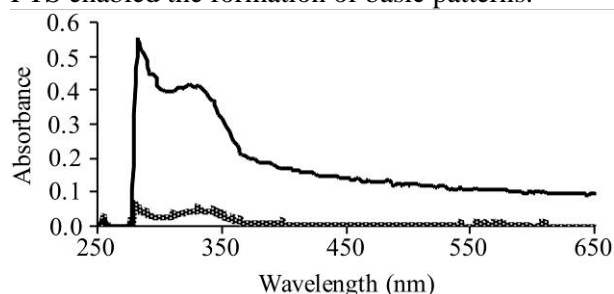


Fig. 1: Absorbance of modified alginate films before (*solid*) and after (*dotted*) exposure to UVA light.

The adhesion and viability of C2C12 cells on collagen films following modification with the caged carbonyl was investigated. Cells did not attach or grow on modified collagen (Fig. 2).

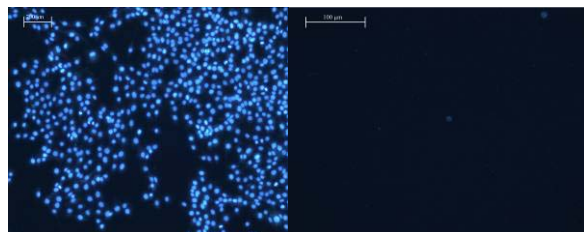


Fig. 2: Untreated collagen film (left) and collagen film modified with caged carbonyl (right), seeded with C2C12 cells and stained with Hoechst.

DISCUSSION & CONCLUSIONS: A novel, versatile caged carbonyl has been synthesized and its compatibility with several cell scaffold materials has been demonstrated. This ability to modify scaffolds and precisely uncage carbonyl groups will allow subsequent chemoselective ligation of cell-adhesive hydrazides or thiosemicarbazide, thus enabling patterning with multiple biomolecules and cell types.

REFERENCES: ¹ J. Nakanishi et al (2008) *Anal Sci* **24**:67-72. ² D. Falconnet et al (2006) *Biomaterials* **27**:3044-63. ³ K. Lee et al (2004) *Langmuir* **20**:1812-18. ⁴ J. Nakanishi et al (2011) *Phys. Chem. Chem Phys.* **13**:4051-4059.

ACKNOWLEDGEMENTS: We would like to thank the EPSRC for funding (EP/G049572/1).

PROMOTION OF NEURITE OUTGROWTH VIA INCORPORATION OF POLY-L-LYSINE INTO ALIGNED PLGA NANOFIBRE SCAFFOLDS

M. Krämer^{1,3}, J.B. Chaudhuri^{1,3}, M.J. Ellis^{1,3} & P.A. De Bank^{2,3}

¹ Department of Chemical Engineering, ² Department of Pharmacy and Pharmacology & ³ Centre for Regenerative Medicine, University of Bath, Bath, BA2 7AY, UK.

INTRODUCTION: Nerve injury, particularly to the central nervous system, can have traumatic consequences such as permanent disability due to loss of motor function. Many scaffold designs have been utilized in order to promote the growth of neurons across areas of nerve injury, bridging the gap created by trauma and offering a permissive environment for neuronal extension. Poly(lactic-co-glycolic acid) (PLGA) has been widely used as a scaffold material for tissue engineering applications, as it is biodegradable, biocompatible and FDA approved¹. However, cell adhesion and growth can be hampered due to the lack of natural adhesion sites on the polymer. For this reason, many strategies have been explored in order to modify PLGA scaffolds to improve cell adhesivity, including hydrolysis², aminolysis², blending and covalent attachment of adhesive peptides. Here we demonstrate that aligned PLGA nanofibres are a suitable scaffold for nerve tissue engineering applications and their biological properties can be improved by incorporating poly-L-lysine (PLL) in the polymer matrix.

METHODS: Pure PLGA nanofibre scaffolds were prepared by electrospinning³ a 10% w/w solution of 75:25 PLGA in chloroform/methanol (3:1) with a flow rate of 3ml/h, applied voltage of 15kV and needle to collector distance of 11cm. To generate aligned nanofibres, the collector consisted of two parallel aluminium electrodes separated by a gap of 1cm. For incorporation of PLL, 0.1mg/ml PLL in dH₂O was added dropwise to a vigorously stirred solution of PLGA to give a final organic/aqueous ratio of 18:1. The resulting emulsion was immediately electrospun as above. To verify incorporation of PLL in the nanofibres, the PLL solution was doped with FITC-PLL and green fluorescence determined using fluorescence microscopy. PC12 cells were then used as a model neuronal cell in order to assess the ability of the scaffolds to support neurite outgrowth following incubation of the cells with nerve growth factor (NGF). Cell adhesion, neurite alignment and mean neurite length were determined for each type of scaffold and SEM was used to examine both fibre and cell morphology.

RESULTS: Aligned PLGA nanofibres were fabricated in the absence and presence of PLL, with PLL incorporation apparent from FITC-PLL fluorescence. No significant differences were observed in the physical parameters of each scaffold type. PC12 adhesion to PLGA and PLGA-PLL nanofibre scaffolds was comparable, with 51±10% and 65±11% seeding efficiency, respectively. Following incubation of cells with NGF for 7 days, neurites from cells on both scaffolds were predominantly aligned in the direction of the nanofibres. When neurite length on both scaffolds was compared, the mean length on PLGA nanofibres was 132±85µm compared with 251±30µm on PLGA-PLL scaffolds. There was clearly a greater proportion of long neurites on PLL-containing scaffolds (Fig. 1).

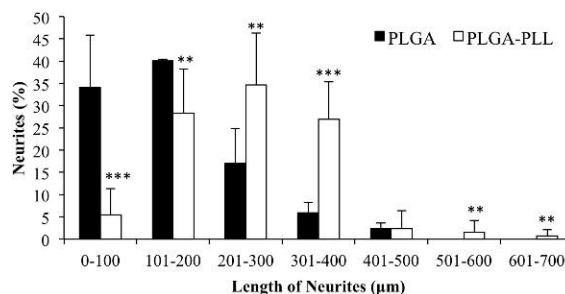


Fig. 1: Effect of scaffold material on neurite extension from NGF-treated PC12 cells on aligned nanofibres. ** $P < 0.01$; *** $P < 0.001$.

DISCUSSION & CONCLUSIONS: The incorporation of PLL into aligned PLGA nanofibres increases neurite extension from a model neuronal cell line in comparison to pure PLGA nanofibres. This approach of electrospinning an emulsion of an aqueous bioadhesive or bioactive species with an organic-soluble polymer offers great potential for modifying scaffold characteristics for a number of tissue engineering applications.

REFERENCES: ¹ L. Lu, S.J. Peter, et al (2000) *Biomaterials* **21**:1837-45. ² T.I. Croll et al. (2004) *Biomacromolecules* **5**:463-473. ³ M. Bognitzki et al. (2001) *Adv Mater* **13**: 70-72.

ACKNOWLEDGEMENTS: We would like to thank the University of Bath for funding.

***In vitro* 3D tissue modelling: insights into ameloblastoma pathogenesis**

C. Raison, S. R. Porter, S. Fedele, M. P. Lewis¹, V. Salih

Division of Biomaterials & Tissue Engineering, UCL Eastman Dental Institute and ¹University of Bedfordshire, 256 Gray's Inn Road, London, WC1X 8LD, UK

INTRODUCTION: Ameloblastoma is a rare, benign oral tumour. Tumours develop within the jaw bone and are highly destructive and invasive, with cells migrating into the jaw and surrounding soft tissue. This is a little-understood disease which if left untreated causes dramatic bone destruction and maxillofacial disfigurement. Current treatment is radical surgery, often resulting in extensive loss of function and tissue. An ameloblastoma-derived cell line, AM-1, has been established [1]. Cells were isolated from a human tumour and immortalised by the addition of HPV-16 DNA. This study aims to (i) make a 3D *in vitro* ameloblastoma disease model, using plastic-compressed collagen gel [2] seeded with AM-1 cells, and (ii) use this bone construct to characterise tissue remodelling, cell growth and invasiveness.

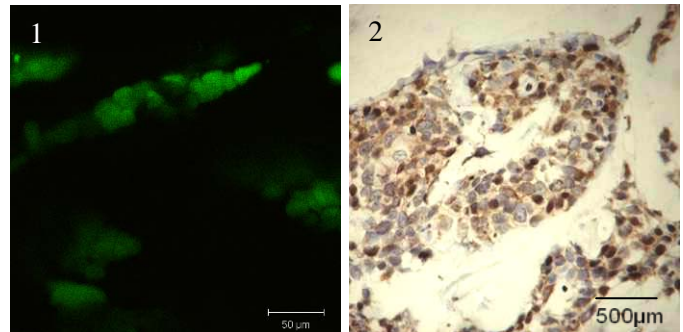
METHODS: Collagen type I, isolated from rat tails (First Link UK), was used to make hydrated gels suitable for seeding cells. Ameloblastoma AM-1 cells [1] cells were added to the gel. Plastic compression was then used to expel the water content, rapidly increasing the gel's mechanical strength without compromising cell viability [2]. Compressed gels were rolled into spirals to provide easy handling and provide a biomimetic 3D environment to observe cell viability and behaviour. Gels were incubated at 37°C with 5% CO₂, in keratinocyte-serum-free medium (Gibco) supplemented with fibroblast growth factor (Peprotech UK).

Constructs were cultured for up to 4 weeks to observe the extent of collagen remodelling and differences in cell viability at different time points. Immunohistochemistry was performed to visualise the expression of bone- and cancer-associated proteins (Abcam, Vector Labs). The alamarBlue cell growth assay (AbD Serotec) and live/dead fluorescence assay (Invitrogen) were carried out to assess AM-1 cell growth and viability in bone construct culture. IHC was carried out at the Royal London Hospital Pathology laboratory.

RESULTS: AM-1 cells are viable in this bone construct, demonstrated by the alamarBlue growth curve and live/dead fluorescence assay (see Fig. 1).

Expression of epithelial marker vimentin, early bone marker alkaline phosphatase and matrix metalloproteinase-2 (MMP-2) was detected in AM-1 seeded bone constructs (see Fig. 2).

Fig. 1: Live/dead fluorescence assay; green = live,



red = dead. AM-1 cells are viable in the construct.

Fig. 2: IHC shows vimentin expression (brown) in AM-1 seeded bone construct.

DISCUSSION & CONCLUSIONS: Compressed collagen gel is an appropriate tissue model for research into ameloblastoma, as it is a native material which provides good mimicry of bone tissue; its construction is ultrarapid and reproducible; and it allows cell growth and migration. AM-1 cells proliferate in the bone construct, as shown by the viability assays. Expression of vimentin, alkaline phosphatase and MMP-2 show that this disease model retains *in vivo* behaviours of ameloblastoma, therefore we have made progress towards a representative disease model.

REFERENCES: ¹ H. Harada, T. Mitsuyasu, N. Nakamura, Y. Higuchi, K. Toyoshima, A. Taniguchi (1998) *J. Oral Pathol. Med.* **27**: 207-212. ² R.A. Brown, M. Wiseman, C. Chuo, U. Cheema, S.N. Nazhat (2005) *Adv. Funct. Mater.* **15**: 1762-1770.

ACKNOWLEDGEMENTS: This work was funded by an anonymous donor and the UCL Development Fund. Laboratory instruction was provided by Pauline Levey and Dr Nicky Mordan. The AM-1 human ameloblastoma cell line was a kind gift from Professor Harada, Iwate Medical University, Japan.

Nanomagnetic gene transfection: Efficient gene delivery using nanoparticles and oscillating magnet arrays

A Fouriki¹, MA Clements^{1,2,3}, N Farrow^{1,2}, J Dobson^{1,2,4}

¹Institute for Science & Technology in Medicine, Guy Hilton Research Centre, University of Keele, Thornburrow Drive, Hartshill, Stoke-on-Trent ST4 7QB United Kingdom ²nanoTherics Limited, Guy Hilton Research Centre, Thornburrow Drive, Hartshill, Stoke-on-Trent ST4 7QB UK, ³Waggoner Center for Alcohol and Addiction Research, University of Texas, Austin, Texas, USA, ⁴Departments of Biomedical Engineering and Materials Science & Engineering, University of Florida, Gainesville, Florida, USA

INTRODUCTION: Nanomagnetic gene transfection has been effectively used with both viral and non-viral vector systems¹. In these systems plasmid DNA or siRNA is attached to magnetic nanoparticles and incubated with cells while a magnet below the surface of the cell culture pulls the particles into contact with the cell membrane. The use of oscillating magnets further stimulates endocytosis of the particle-gene complex².

In our studies the human osteoblastic/osteosarcoma cell line, MG63, has been used to demonstrate the efficiency of the nanomagnetic gene transfection using oscillating magnet arrays, based on this cell line's extensive use for *in vitro* research on bone cancers, tissue engineering and regenerative medicine³⁻⁴.

METHODS: MG63 cells were transfected with nTMag and PolyMag nanoparticles coated with pEGFP green fluorescent protein reporter construct using oscillating magnet arrays (magnefect-nanoTM system) for 30 min. The cationic lipid transfection agent Lipofectamine 2000TM was used for comparison.

RESULTS: At 48hr post-transfection, fluorescent microscopy and Fluorescence Activated Cell Sorting (FACS) analysis showed that the magnefect-nano oscillating system enhances overall *in vitro* transfection levels in MG63 cells in comparison with the Lipofectamine 2000TM ($p < 0.001$) (Figures 1 & 2). Transfection efficiency averaged 49% and cell viability was largely unaffected.

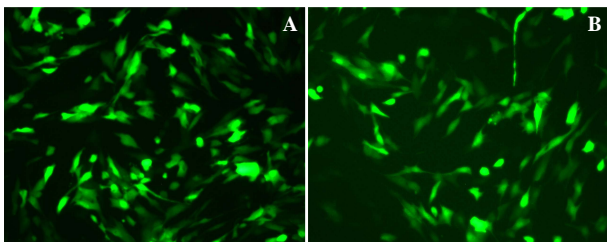


Figure 1: EGFP expression in MG63s transfected with 100nm (A) nanoTherics nTMag and (B) OzBioSciences PolyMag magnetic nanoparticles coated with pEGFPN1 DNA using the magnefect-nanoTM oscillating array (200 μ m amplitude, 2 Hz, for 30 min). During transfection cells were incubated at 37°C, 5% CO₂.

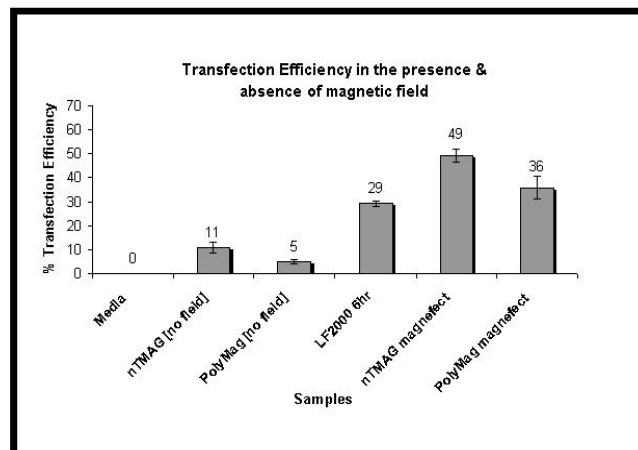


Figure 2: FACS results showing transfection efficiency of the tested groups in MG63 cells. $N = 3$ per group.

CONCLUSIONS: The oscillating magnetic field of the magnefect-nano system outperforms the best currently available cationic lipid-based agent. Furthermore, it retains the advantages of magnetic transfection such as short transfection times, lower reagent concentrations and little or no cytotoxicity.

In addition, similar positive results have been obtained using primary human mesenchymal stem cells where transfection levels of 40% were achieved causing no adverse effect on cell viability and proliferation.

Magnetic nanoparticle-based gene transfection shows promising results for non-viral gene delivery for both *in vitro* and *in vivo* applications.

ACKNOWLEDGEMENTS: A Fouriki thanks Keele University, nanoTherics Ltd. and EPSRC for funding support.

REFERENCES: ¹Mah et al (2002) *Molec Ther* **1**: S239 ²McBain et al. (2008) *Nanotech* **3**: 139-143 ³Alonso et al (2008) *J Cell Physiol* **217**:717-72. ⁴Hsu et al (2008) *J Bone Miner Res* **23**:949-960.

Dorsal root ganglion neurons maintained in a 3D culture model exhibit similar electrophysiological properties to fresh explants.

E. East, K. P. S. J. Murphy & J. B. Phillips

Department of Life Sciences, The Open University, Milton Keynes, UK

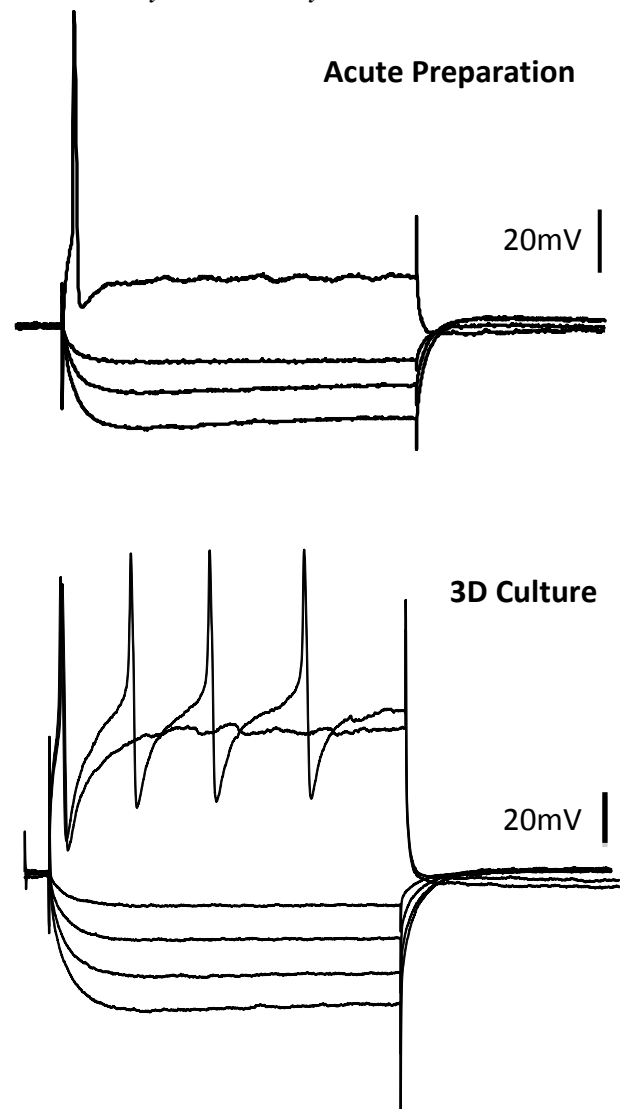
INTRODUCTION: Tissue engineered culture models provide a powerful tool for neuroscience research¹. They overcome limitations associated with monolayer cultures of neurons and glia by maintaining cells in a more realistic 3D spatial arrangement, and permit continuous monitoring and control of variables that cannot be achieved in animal models. Here we report the development of a system for recording electrophysiological behaviour in neurons in 3D culture.

METHODS: Dorsal root ganglia (DRGs) were harvested from adult rats, dissociated using collagenase, then seeded within 2 mg/ml Type I collagen gels and maintained in culture for 20 hours. Preparations were transferred to an interface recording chamber at 29 °C, perfused with culture medium at 150 μ l/min and exposed to warmed and humidified oxygen (95 %) and carbon dioxide (5 %). Recordings were made using glass micropipettes filled with 3M KCl (electrode series resistance 60-80 MOhms) attached to an Axoclamp 2B amplifier and stored on a Macintosh computer. Neurons in 3D culture were compared to those in acutely hemi-sectioned DRG explants.

RESULTS: Resting membrane potential and input resistance were recorded from neurons in both 3D cultures and acutely hemi-sectioned control tissue. Characteristic membrane voltage responses to hyperpolarising current were obtained and injection of depolarising current elicited action potentials (Fig 1).

Fig 1: Upper Panel: traces recorded from a cell in an acutely hemi-sectioned DRG. The neuron had a membrane potential of -81 mV and input resistance of 110 MOhms. Traces show the membrane voltage responses to injections of hyperpolarising current (-0.1, -0.2 and -0.3 nA; 150 ms duration) and a depolarising current sufficient to elicit an action potential.

Lower panel: traces recorded from a DRG neuron in 3D culture. The neuron had a membrane potential of -87 mV and input resistance of 68 MOhms. Traces show the membrane voltage responses to injections of hyperpolarising current (-0.2, -0.4, -0.6 and -0.8 nA; 150 ms duration) and injections of depolarising current that elicited



either a single action potential or a train of action potentials.

DISCUSSION & CONCLUSIONS: Adult rat DRG neurons maintained in 3D culture exhibit electrophysiological responses comparable to their counterparts in fresh tissue explants. This system provides a functional model in which neuronal responses can be monitored. The reproducibility and control make this approach suitable for further development as a model for toxicity testing.

REFERENCES: ¹ E. East & J.B. Phillips (2008) Tissue engineered cell culture models for nervous system research in *Tissue Engineering Research Trends* (ed G. N. Greco) Nova Science Publishers.

Peptide β -sheet self-assembly for the modification of acellular vascular grafts

R S Guillatt^{1&2}, R P W Davies¹, S-P Wilshaw², A Aggeli¹ & E Ingham²

¹ Centre for Molecular Nanoscience, School of Chemistry, University of Leeds. ² Institute of Medical and Biological Engineering, University of Leeds.

INTRODUCTION: There is clinical need for small diameter blood vessel replacements and decellularised natural vessels have potential. There are several well established and emerging products on the market¹. Current products, however, suffer from poor patency. Self-assembling peptides offer an opportunity for modifying acellular natural scaffolds to increase biocompatibility. The long term aims of this project are to test the hypothesis that self-assembling rationally designed peptides within decellularised scaffolds will overcome the problems of thrombosis and intimal hyperplasia associated with decellularised scaffolds in small diameter grafts.

METHODS: Self assembling peptides were initially tested for their effects on blood clotting using the Chandler loop model. Citrated sheep blood was added to a loop of PVC tubing with Tris buffered saline (1X) and calcium chloride (250 mM). Peptide was added to the blood to make a final peptide concentration of 0.2 mM. Distilled water and human α -thrombin served as negative and positive controls. The loops were rotated for 90 minutes at 30 rpm (shear rate 428 s⁻¹). The clots that formed were weighed. P₁₁-4 (Q-Q-R-F-E-W-E-F-E-Q-Q), a peptide rationally designed to self-assemble under physiological conditions was tested for self assembly into acellular porcine femoral arteries. Monomer solutions of P₁₁-4 or P₁₁-4 plus fluorescein conjugated P₁₁-4 [ratio 1:30] were prepared using distilled water [pH 8.0]. The decellularised vessel was added to the solution. The pH was lowered to pH 5 (Conc HCl) to trigger self-assembly. The vessel was left in the self-assembled solution over night and then removed. Vessels were imaged using a MPLSM or cryoembedded and sectioned then imaged using fluorescence microscopy. Peptide loaded vessels were also imaged by FEGSEM (LEO 1530). Samples were dried over night in vacuum and sputter coated in a 7nm layer of 50:50 Pt/Pd.

RESULTS: The mean clot size formed with different peptides in the Chandler loop model is shown in Figure 1. The RADA peptide showed an increase and P₁₁-12 a decrease in clot formation compared to the negative control. The other peptides had no effect. As shown in Figure 2, P₁₁-4 was present on the surface of the acellular vessel on the collagen fibre bundles. The coating shown

in Figure 1B was likely the result of dried excess peptide. The cross section in Figure 1D showed the peptide had fully penetrated the vessel. The peptide coating of fibres (Figure 1F) may be explained by the preferential self-assembly of peptide at the surface interface compared to in solution².

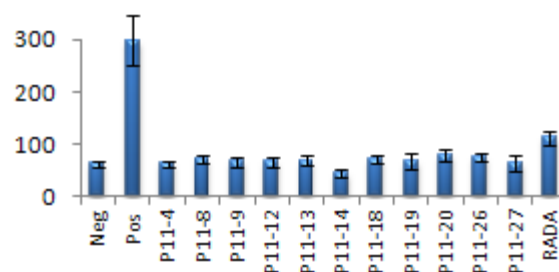


Fig 1: Chandler loop, average mean blood clot size (mg). n=6 with 95% confidence error bars

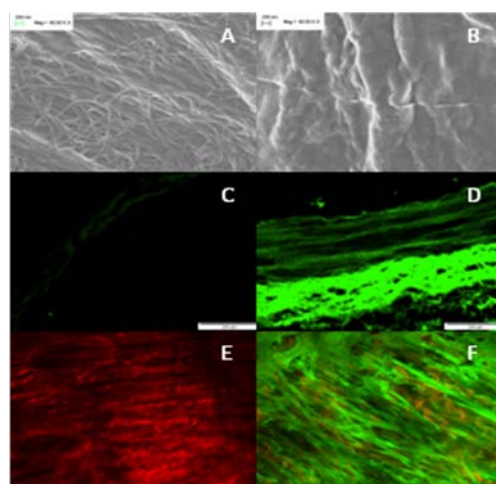


Fig 2: A&B FEGSEM images C&D Fluorescent images E&F MPLSM images. A, C&E control images of vessel. B, D&F images of vessel with 18.8 mM P₁₁-4 Red = collagen Green = peptide

DISCUSSION & CONCLUSIONS: The majority of peptides had no effect on blood clotting. Studies of peptide self-assembly showed peptide would self-assemble throughout the acellular vessel, thus demonstrating the feasibility of this approach. Future studies will focus on bio-functionalisation of the peptides to overcome the problems of thrombosis and intimal hyperplasia.

REFERENCES: ¹ Wilshaw et al Tissue Eng 12; 1-13 (2006) ² Taylor et al Accounts Chem Res 23(10) 338-344 (1990)

ACKNOWLEDGEMENTS: MPLSM images taken by Gareth Howell

In Situ Cell Monitoring in Organ Culture

K M Elson¹, J L Tipper¹, J Kirkham², R M Hall¹ & E Ingham¹

¹*Institute of Medical and Biological Engineering, University of Leeds, Leeds, UK* ²*Division of Oral Biology, Leeds Dental Institute, University of Leeds, Leeds, UK*

INTRODUCTION: Mechanical simulations of medical devices coupled with biological investigations have delivered significant health benefits to patients. One of our long term aims is to integrate simulator and bioreactor technology to provide physiologically relevant whole-joint models for the assessment of tissue-engineered biomaterials. Several key challenges need to be addressed. A whole organ culture must maintain cell viability, stable matrix composition and retain structural integrity. Currently the standard practice for assessing tissue viability in organ cultures is by tissue destructive methods. Our initial aim is therefore to develop *in situ* methodologies for assessing cell and tissue viability by measuring a group of molecular markers that accumulate in the conditioned medium of organ cultures.

METHODS: Femoral condyle bone plugs (9 mm diameter x approximately 5-6 mm) were retrieved from porcine knees. Cartilage was removed and bone marrow washed out using PBS. The cancellous bone was then cultured in DMEM supplemented with 10% (v/v) FCS, 1 mM sodium pyruvate, 25 mM HEPES, 2 mM L-glutamine, 50 U/mL penicillin/streptomycin, and either 4.5 g/L (normal) glucose/pH 7.3, or 45 g/L (ultra-high) glucose/pH 8.5. Ultra-high glucose medium was used to induce cell death to compare levels of markers to those in normal glucose cultures. Medium was changed every 7 days to 28 days and replicate [n=4] cultures were sacrificed at days 14, 21 & 28 for analysis. Conditioned medium samples collected on days 0, 7, 14, 21 & 28 were assessed for levels of glucose (indication of metabolism), lactate dehydrogenase (LDH; marker of cell death), alkaline phosphatase (AP; marker of bone cell activity), nitric oxide (NO) and accumulation of glycosaminoglycan (GAG; markers of ECM degradation) using colourimetric assays. Tissue samples were assessed on days 0, 14, 21 and 28 by XTT assay and fluorescent live/dead stain.

RESULTS: Live/dead staining showed a clear difference in viability between cultures from day 14 onwards with more live cells in normal glucose than ultra-high glucose cultures. Results from the XTT assays supported this finding with higher XTT readings from day 14 in normal glucose compared to ultra-high glucose cultures (Figure 1).

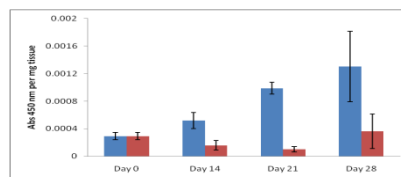


Fig. 1: XTT viability assay over 28 days in culture with normal glucose/pH 7.3 (blue) and ultra-high glucose/pH 8.5 (red). Error bars are SEM (n=4).

Ultra-high glucose cultures used less glucose and produced less AP compared to normal glucose cultures. However, normal glucose cultures had higher levels of GAG and NO from day 21, and LDH production was higher at days 14 & 21.

Table 1. Marker levels in cultures.

Day	7	14	21	28
Glucose use	↑	↑	↑	↑
AP	↔	↑	↑	↔
GAG	↔	↑	↑	↑
NO	--	--	↑	↑
LDH	↔	↑	↑	↔

↑ = higher in normal glucose culture. ↔ = not significantly different. -- = not tested.

DISCUSSION & CONCLUSIONS: The approach taken generated viable and non-viable cultures for comparison of molecular marker levels. Viable cultures used more glucose for metabolism and produced more bone cell activity marker AP than non-viable cultures. Glucose and AP may therefore be good markers of bone tissue viability in organ culture. GAG and NO levels indicated more ECM degradation from day 21 onwards in the viable cultures. This could have been due to the cultures not being mechanically loaded, causing ECM degradation, whilst the cells remained viable. LDH levels were higher in the viable cultures at day 14 and 21. This was most likely due to the fact that by day 14 all of the cells in the non-viable cultures were dead and incapable of metabolism. Overall, these studies indicated that it will be necessary to mechanically load the viable organ cultures in order to prevent ECM breakdown.

ACKNOWLEDGEMENTS: This work was funded through WELMEC, a Centre of Excellence in Medical Engineering funded by the Wellcome Trust and EPSRC, under grant number WT 088908/Z/09/Z.

Self-assembled peptide-based hydrogels as scaffolds for *in vitro* cartilage repair

[A Mujeeb](#), [JE Gough](#) & [A Saiani](#)

Materials Science Centre, University of Manchester, Grosvenor Street, Manchester, M13 9PL, UK

INTRODUCTION: *De novo* designed peptides are attracting considerable interest due to their structural simplicity, diverse functionality and their ability to self-assemble into a variety of structures and form hydrogels.¹⁻² We have recently investigated the self-assembling and gelation properties of a series of ion-complementary peptides based on the alternation of non-polar hydrophobic and polar hydrophilic residues.³ In this work we focus on two specific octapeptides: FEFKFEFK and FEFKFEFK (F: phenylalanine, E: glutamic acid, K: lysine). These two peptides were shown to self-assemble in solution and form β -sheet rich nanofibres which, above a critical gelation concentration (CGC), entangle to form self-supporting hydrogels.

METHODS: The octapeptides were synthesised using a solid phase peptide synthesiser (a ChemTech ACT 90 peptide synthesiser). The fibre morphology of the hydrogels was analysed using TEM and Cryo-SEM. The mechanical properties of the hydrogels were determined using oscillatory rheology. Bovine chondrocytes were used to assess the biocompatibility of the scaffolds under 2D and 3D cell culture conditions, particularly looking into cell morphology, proliferation and extra cellular matrix (ECM) formation using light microscopy, live-dead, ESEM, immunochemical staining, LDH (lactate dehydrogenase), Alamarblue and collagen assays.

RESULTS: The purity of the peptide was found to be >85%. These hydrogels consist of a dense fibrillar network of nanometer size fibres which present similarities with the ECM (Figure 1A). The gelation dynamics and mechanical properties of these gels could be controlled through concentration and processing. Protocols for the preparation of scaffolds for 2D and 3D (homogeneous incorporation of cells) culture have been developed using the cell culture medium properties (pH and ionic strength) to trigger the gelation. These mechanically stable gels were subsequently used to culture bovine chondrocytes over 21 days in 2D and 3D conditions *in vitro*. The light microscopy and ESEM images revealed the cells in 3D demonstrated a classic rounded morphology (Figure 1B). The live-dead staining

and the collagen antibody-staining results show the presence of living chondrocytes in the scaffold (Figure 1C). The cell proliferation results demonstrated the scaffolds to be cytocompatible with the cells showing varying metabolic activity.

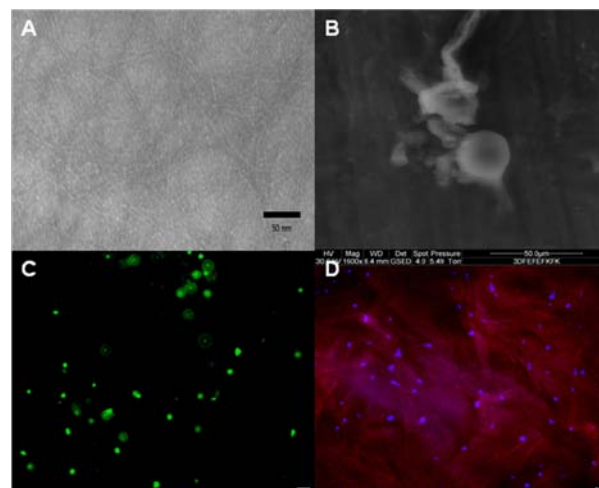


Figure: 1. (A) TEM micrograph of FEFKFEFK hydrogel showing a fibrillar network (scale bar = 50 μ m); (B) ESEM micrograph showing cells in 3D (scale bar = 50 μ m); (C) Live-dead staining of chondrocytes in 3D (scale bar = 50 μ m); (D) Collagen II antibody staining of cell-encapsulated gel (scale bar = 50 μ m).

DISCUSSION & CONCLUSIONS: We have created scaffolds exploiting the self-assembly properties of short ionic-peptides. These scaffolds were shown to be biocompatible and sustain the culture of chondrocytes over 21 days in 2D and 3D. The research is now focusing on the potential of these peptide-based gels as ‘injectable’ biomaterials for *in vitro* cartilage repair.

REFERENCES:

1. S.G. Zhang *Nature Biotechnology* 21, 1171 (2003)
2. L. Haines-Butterick et al. *PNAS* 104, 7791 (2007)
3. A. Saiani et al. *Soft Matter*, 5, 193 (2009)

Complementary self-assembling peptides: effect of molecular design on biological properties

S Kyle^{1,2,3}, MJ McPherson¹, A Aggeli² & E Ingham^{1,3}

¹ Institute of Molecular & Cellular Biology, University of Leeds, UK. ² Centre for Molecular Nanoscience, University of Leeds, UK. ³ Institute of Medical & Biological Engineering, University of Leeds, UK.

INTRODUCTION: Self-assembling peptides have great potential as tissue engineering scaffolds. The aims of this project were to investigate novel self-assembling peptides for the development of molecular scaffolds for tissue engineering. A binary complementary peptide system P₁₁-13 (CH₃CO-EQEFWEFEQE-NH₂) and P₁₁-14 (CH₃CO-QQOFOWOFOQQ-NH₂) was compared to a previously reported, single component self-assembling peptide P₁₁-4 (CH₃CO-QQRFWEFEQQ-NH₂) [1-2] for capacity to support cell proliferation.

METHODS: Peptides P₁₁-13, P₁₁-14 and P₁₁-4 were purchased from NeoMPS Groupe SNPE (Strasbourg, France) at >98% purity by HPLC. P₁₁-13 and P₁₁-14 were prepared at a concentration of 10 mg.ml⁻¹ and P₁₁-4 at 37.5 mg.ml⁻¹ in DMEM plus supplements. Primary human dermal fibroblasts (PHDF) were added to the peptide gels at a concentration of 5,000 cells.well⁻¹. Aliquots (100 µl) were added to wells of a flat bottomed 96 well plate. Collagen gels containing cells were used as controls. The gels were allowed to form for 3 hours at 37°C in 5% CO₂ (v/v) in air. Cell culture medium (150 µl) was then added. Replicates (n=3) were cultured for 7, 14, 21 and 28 days. ATP levels (as an indicator of viable cell number) were determined at these time points. For histological analysis, PHDFs were seeded into peptides as described above at a density of 5 x 10⁴ cells.ml⁻¹ and cultured for 14 days. P₁₁-13/P₁₁-14 and P₁₁-4 hydrogels containing no cells were used as a control. Hydrogels were fixed, dehydrated and wax embedded. Serial sections were mounted and stained with H&E.

RESULTS: Hydrogels of P₁₁-13/P₁₁-14 and of P₁₁-4 were cytocompatible with PHDFs. In P₁₁-13/P₁₁-14 hydrogels, the numbers of PHDFs declined over the 28 day culture period. By contrast, P₁₁-4 was able to support cell proliferation over 28 days. Histologically, P₁₁-13/P₁₁-14 hydrogel showed a brick-like network of large fibres and cell remnants were observed, whereas P₁₁-4 hydrogel was much less dense and the cells elaborated neomatrix and ECM components at 14 days.

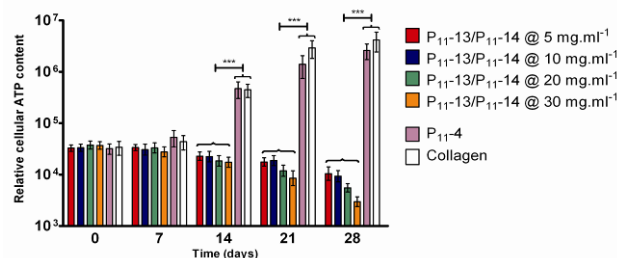


Fig. 1 Proliferation of PHDFs within P₁₁-13/P₁₁-14 and P₁₁-4 hydrogels over 28 days.

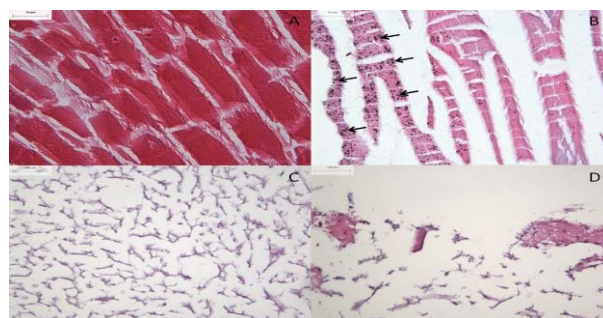


Fig. 2 Histological images of P₁₁-13/P₁₁-14 hydrogels (A) without and (B) with cells, and P₁₁-4 hydrogels (C) without and (D) with cells stained with H&E. Black arrows indicate possible cell remnants

DISCUSSION & CONCLUSIONS: It is clear that molecular design criteria can influence the properties of self assembling peptide materials. Here, the complementary peptides produced rigid hydrogels that did not support cell proliferation. There is a need for further research into the relationship between peptide matrix rigidity/compliance and cell behavior, and to further understand how we can predict molecular level dynamics in order to achieve a functional tissue engineering substrate with the required properties.

REFERENCES: ¹ A. Aggeli, M. Bell, L.M. Carrick, et al (2003) *J Am Chem Soc* **125**:9619-28. **33**:1471-77. ² L. Carrick, M. Tassieri, T.A. Waigh et al (2005) *Langmuir* **21**:3733-7.

ACKNOWLEDGEMENTS: Stuart Kyle was supported by a Wellcome Trust studentship.

Biocompatibility and immunoreactivity of acellular xenogeneic and allogeneic arteries

*S-P. Wilshaw, H. Berry, P. Rooney, J. N. Kearney, S. Homer-Vanniasinkam, J. Fisher, & E. Ingham.
Institute of Medical and Biological Engineering, The University of Leeds, Leeds, LS2 9JT, UK.*

INTRODUCTION: Coronary artery and peripheral vascular disease remain the largest cause of morbidity and mortality western societies, and is becoming a growing health and socio economic burden in developing countries. Vascular grafting is carried out to replace damaged or diseased vessels restoring normal blood flow. When available, autologous saphenous vein is currently the gold standard used for bypass procedures. In patients where the saphenous vein is absent or diseased a synthetic graft composed of Dacron or ePTFE may be used. Synthetic grafts suffer from compliance mismatch, early graft occlusion and have a propensity for infection. A protocol has been developed to remove all cellular material from porcine carotid, external iliac and human common femoral arteries; these have the potential to be used as vascular bypass grafts. The aim of the work was to determine the biocompatibility and immunoreactivity of the acellular arteries.

METHODS: Human common femoral (CFA), porcine carotid (ICA) and iliac arteries (EIA) were decellularised using a method based on Wilshaw *et al.* (2006).

In vitro biocompatibility assays: Samples of acellular arteries or their soluble extracts were incubated with monolayers of murine 3T3 and Baby Hamster kidney cells. The cells were assessed for changes in morphology or viability.

α -Gal determination: Immunoperoxidase labeling using an antibody against α -gal was used to assess the presence of the epitope in fresh and acellular tissue sections. An antibody absorption assay followed by ELISA was developed to quantify any residual α -gal in the acellular arteries. Fresh, human and no tissue were used as controls.

Complement activation: Following ethical review and written informed consent serum was isolated from healthy volunteers (n = 6). The serum was incubated with the luminal surface of samples of fresh and acellular arteries for one hour with and without EGTA (which inhibits the antibody-dependent pathway of complement activation). Following this, levels of C3a and C5a were determined using commercially available ELISA's. Zymosan (10 mg.ml⁻¹), BSA- α -Gal and tissue culture plastic were included as controls. Three commercially available surgical materials were also tested for comparative purposes: Surgisis, Permacol and CollaMend.

RESULTS: Acellular arteries were biocompatible, cells grew in contact with the tissue and there was no decrease in cell viability following incubation with soluble tissue extracts for 48 hours.

Immunoperoxidase labeling of the α -Gal epitope showed an absence of staining acellular porcine and human arteries. Following absorption of anti- α -Gal antibodies by tissues, ELISA to detect levels of unabsorbed antibodies showed that the level of α -Gal present in acellular porcine arteries was not significantly different to levels in human arteries (Figure 1).

Fresh porcine arteries and Surgisis and CollaMend activated complement in normal human serum. Production of C3a and C5a in normal human serum in the presence of fresh porcine tissues and Surgisis was blunted in the presence of EGTA. Acellular arteries and samples of Permacol failed to activate complement in normal human serum.

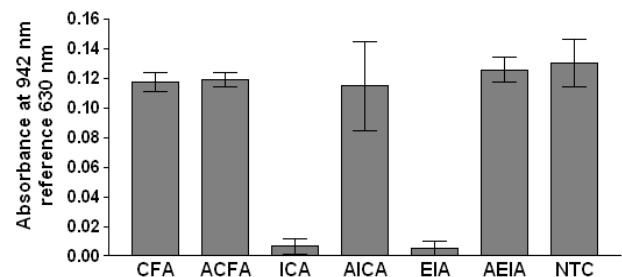


Figure 1: Semi quantitative inhibition ELSIA to determine the presence of α -Gal. (n=6) +/- 95% confidence limits.

DISCUSSION & CONCLUSIONS: The decellularisation protocol resulted in biocompatible acellular porcine and human arterial grafts. Porcine acellular conduits were shown to be free of the major xenoantigen α -Gal using qualitative and quantitative assays. A functional assay for complement activation in human serum indicated a lack of humoral immunoreactivity with the acellular biological scaffolds.

REFERENCES: S. Wilshaw, *et al.* (2006) *Tissue Engineering*.

ACKNOWLEDGEMENTS: This work was part funded through WELMEC, a Centre of Excellence in Medical Engineering funded by the Wellcome Trust and EPSRC, under grant number WT 088908/Z/09/Z.

Cell Life Support System for Transportation

T.W.A. Gould¹, R.J. Thomas², F.R.A.J. Rose¹, K.M. Shakesheff¹

¹ *Tissue Engineering Group, Division of Drug Delivery and Tissue Engineering, School of Pharmacy, University of Nottingham, NG7 2RD,* ² *Healthcare Engineering Group, Centre for Biological Engineering, Loughborough University, LE11 3TU*

INTRODUCTION: As cellular therapies and hybrid scaffold/cellular tissue engineering products begin to reach the market, there will be a requirement for a solution to the transport of the viable cellular products. Current methodology involves cryopreservation of cells and shipping and distributing cold-chain¹. There is also the requirement of post transport manipulation to resuscitate the cells and remove toxic cryoprotectant. These factors could render a potentially valuable product cost prohibitive.

The basis for this proposed technology is to use controlled release and capture technology to maintain acceptable levels of nutrients and waste products in an enclosed, low volume culture vessel at room temperature.

Ammonia is a well known toxic metabolite. It is formed during the catabolism of amino acids, in particular glutamine. Increased levels of ammonia have the effect of increasing necrotic and apoptotic cell death, reducing proliferation and interfering and inhibiting cell processes². Ammonia is present as ammonium ions in solution at physiological pH.

An ion exchange material has been used to selectively adsorb ammonium ions from solution. Coupled to this the tailored release of key media components in enclosed static cultures of human mesenchymal stem cells (hMSCs) over a period of days the metabolic products, viability and functionality of these cells are examined.

METHODS: Human mesenchymal stem cells are cultured at room temperature and pressure in proprietary sealed units. These units provide the media surrounding the cells contact with the metabolite exchange and nutrient release materials. Viability is examined using a FITC conjugated Annexin V antibody and Propidium Iodide flow cytometry technique including an absolute count of cells enabling the assessment of proliferation further to viability and onset of early stage apoptosis. Media aliquots are examined using a BioProfile Flex Bioanalyser (Nova Biomedical) for key nutrient components and metabolites to assess media quality and metabolic activity.

RESULTS: Early results show that the use of selected ion exchange materials is compatible with the culture of mesenchymal stem cells and is able to reduce ammonium concentrations to within acceptable limits. Results also show that these cells retain a 20% viable population after 7 days at 25°C (fig. 1).

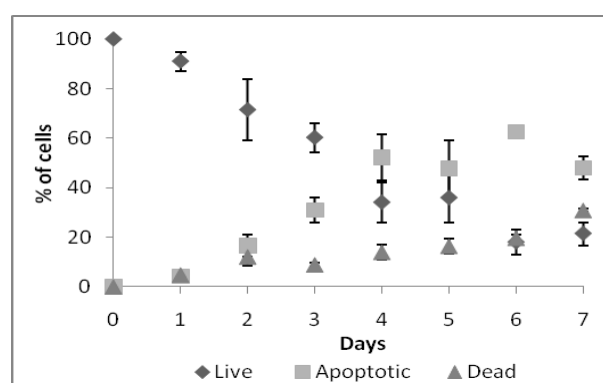


Fig. 1: Effect of culturing hMSCs at room conditions with no change of media on onset of apoptosis and viability

The number of cells over the seven days is shown to stay static when assessed with the flow cytometric counting method.

DISCUSSION & CONCLUSIONS: The ion exchange material is shown to be effective at removing the ammonium ions at the concentrations produced by cells in culture. The controlled release of the key nutrients used by the cells over the culture period is still to be tailored to overcome the lack of metabolic substrate being the limiting factor. It is apparent that there is a window of opportunity where there are viable cells could be taken from a population cultured at room conditions and extending this period is paramount.

REFERENCES: ¹ E.J. Woods, B.C. Perry (2009), *Cryobiology.*, **59** 150-157, ² M. Schneider et al (1996), *J. Bio Tech* **46**:161 -185.

ACKNOWLEDGEMENTS: The EPSRC and University of Nottingham for funding.

The Immunology of Adult Mesenchymal Stromal Cells

A. Aldridge¹, E. Jones², E. Ingham¹

¹*Institute of Medical and Biological Engineering, Faculty of Biological Sciences, University of Leeds,* ²*Academic Unit of Musculoskeletal Disease, Leeds Institute of Molecular Medicine, UK.*

INTRODUCTION: Adult mesenchymal stromal cells (MSCs) have enormous potential in tissue engineering and regenerative medicine applications due to their multilineage capacity. MSC have been reported to have immunomodulatory properties and to be immune-privileged¹. Previous studies investigating the immune-privileged nature of MSC have utilised *in vitro* assays of direct antigen presentation. We hypothesize that MSCs will not directly stimulate allogeneic lymphocytes in classical lymphocyte proliferation assays due to lack of expression of immune-regulatory molecules (CD40, CD80, CD86, MHC Class-II) but will be capable of stimulation of allogeneic lymphocytes via the indirect pathway of antigen presentation. In order to test this hypothesis we optimised the *in vitro* assay conditions and extended the duration of assays beyond the normal 7 day culture period.

METHODS: MSCs were isolated from 4 donor bone marrows (BM) by mixing aspirate in a 1:1 ratio with culture medium, and culturing for 48 hours at 37°C 5% (v/v) CO₂. After 48 hours the adherent cells were washed with PBS, and medium replaced. Adherent cells were grown to confluency changing medium twice weekly. MSC phenotype was analysed by flow cytometry using antibodies to: CD34, CD45, CD14, CD19, HLA-DR, CD73, CD90, and CD105. MSCs were assayed for their ability to differentiate into bone, fat and cartilage via staining with alizarin red, Oil red-O, and alcian blue respectively. Peripheral blood mononuclear cells (PBMCs) were isolated from 6 volunteer whole bloods by Lymphoprep® density gradient centrifugation. Lymphocyte proliferation assays were performed using 2.5 x10⁴ PBMCs and 2.5 x10⁴ mitomycin C treated MSCs [1:1 ratio]. The assays were performed in uncoated U-bottom 96 well plates in replicates of 6, with PBMC plus PHA a positive control, PBMCs without MSC and MSC alone as negative controls [all 2.5 x10⁴ cells] The culture medium was changed on day 12. On days 3, 5, 7, 12, 16, and 21 the incorporation of low activity ³H thymidine into DNA was determined over an 18h period. The stimulation indices: mean (n=6) cpm PBMC plus MSC/ mean (n=6) PBMC alone were calculated at each time

point.

RESULTS: Flow cytometry demonstrated that MSC from the 4 donors expressed MSC markers: CD73⁺, CD90⁺, CD105⁺, CD34⁺, CD45⁻, CD14⁻, CD19⁻ and , HLA-DR⁻. MSC phenotype was confirmed through trilineage differentiation into bone, fat, and cartilage. In the lymphocyte transformation assays for 3 of the MSC donors, 2 or less of the six donor PBMC responded with a positive stimulation within the normal seven day culture period. Extension of the culture duration showed that the between days 12 and 16, on average four/five of the six PBMC donors responded to the 4 MSC donors with an SI greater than 3 although stimulation between replicate culture wells was variable. Data is shown in Figure 1.

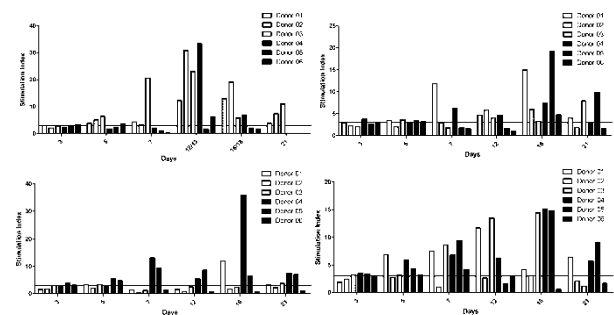


Figure 1: Stimulation index (SI) of PBMC from 6 donors cultured with MSC from 4 donors over 21 days. A SI of above 3 is considered significant.

DISCUSSION & CONCLUSIONS: By extending the culture time of lymphocyte proliferation assays beyond 7 days we were able to show that MSC were able to stimulate allogeneic lymphocytes *in-vitro*. We believe that the extended culture time allowed for indirect antigen presentation, however this requires further confirmation. These studies indicate that, hMSC are not be immunoprivileged and that this may limit the potential for the use of allogeneic MSC in tissue engineering applications.

ACKNOWLEDGEMENTS: This work was funded by the BBSRC and also WELMEC, a Centre of Excellence in Medical Engineering funded by the Wellcome Trust and EPSRC, under grant number WT 088908/Z/09/Z.

The self-assembly of optimised tape-forming *de novo* peptide gels and their evaluation as matrices for cell growth

D.E.Miles^{1,2}, S.Maude¹, S.H.Felton^{1,2}, R.K.Wilcox², E.Ingham² and A.Aggeli¹

¹ Centre for Molecular Nanoscience (CMNS), School of Chemistry, University of Leeds

² Institute of Medical and Biological Engineering (iMBE), University of Leeds

INTRODUCTION: The β -sheet peptide motif has been optimised to form self-supporting gels above a certain concentration and these gel materials are advantageous as they can be designed to be responsive, remodelable and injectable, all of which are useful for biological applications. This research into peptide self-assembly in physiological-like conditions has focussed on the study of positively charged peptide variants.

METHODS: During this study the self-assembly behaviour of positively charged peptides as a function of concentration & time has been investigated using nuclear magnetic resonance, NMR, circular dichroism ultra-violet spectroscopy, CD UV, Fourier transform infra-red spectroscopy, FTIR & transmission electron microscopy, TEM. Peptide cytotoxicity was tested using L929 murine fibroblast cell lines and the propensity for cell growth on the peptide gels was assessed using ATPlite assays.

RESULTS & DISCUSSION: The newly designed positively charged peptides in physiological conditions behave as expected according to the theoretical model that describes the hierarchical self-assembly of β -sheet tapes in pure water. They have a critical concentration above which aggregates are formed and a critical concentration above which gelation occurs (Figure 1).

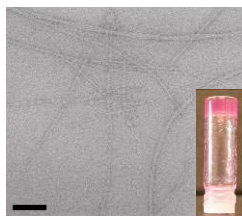


Figure 1: TEM image of serine based peptide variant aggregates (scale bar = 100 nm) and inset photograph of 10 mg/ml self-supporting peptide gel.

It has been found that in physiological like conditions the presence of an overall charge on the peptides leads to slower self-assembly kinetics with a higher critical aggregation concentration than neutrally charged peptides.

It has also been confirmed that glutamine based peptides have lower C^* values than serine based

peptides due to the polar zipper effect, as demonstrated in Figure 2.

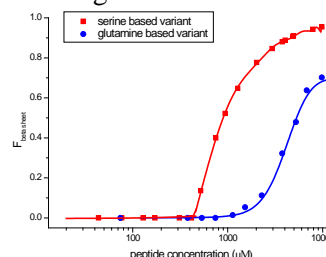


Figure 2: Fraction of peptide as β -sheet as a function of peptide concentration.

The higher C^* value for a peptide therefore means that there is a higher fraction of monomers present at peptide concentrations above C^* . Therefore it will have faster dissolution times due to the need for the system to establish an equilibrium, which results in weaker gels that are less suited for cell growth.

The cytotoxic tests indicated that the peptides studied were non-cytotoxic. (Figure 3)

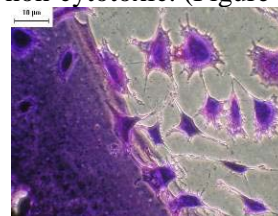


Figure 3: L929 murine fibroblasts growing in contact with and onto a glutamine based variant peptide gel matrix. (magnification of 400 \times)

CONCLUSIONS: Knowledge of the self-assembly behaviour and C^* values allow us to predict the stability and dissolution characteristics of the gels in physiological conditions, as well as the types of aggregates present, which can lead to different nanotoxicity profiles.

It is essential to study simple model peptides so that the basic scientific principles can be used to develop new and useful materials.

REFERENCES: S.Maude *et al.* (2011) *Soft Matter* 2011, in press.

ACKNOWLEDGEMENTS: Funding for this work was provided by the School of Chemistry, University of Leeds, the Medical Research Council and EPSRC grant EP/F010575/1.

alvetex®: Technology that Enables Routine 3D Cell Culture for Use in ResearchE.G. Knight^{1,2} & S.A. Przyborski^{1,2}¹ School of Biological Science, Durham University, South Road DH1 3LE UK² Reinnervate Ltd, NETPark Incubator, Thomas Wright Way, Co. Durham, TS21 3FD UK

INTRODUCTION: When a cell is grown in a monolayer the majority of its surface area is either exposed to the plastic or the culture medium with minimal opportunity for interactions. This has an impact on a cell's performance and consequently influences the representation of any biological assays. A more realistic environment for *in vitro* cell growth is required to better mimic the cell-cell three-dimensional (3D) interactions that promote growth and differentiation *in vivo*. This realistic 3D environment requires optimisation of the culture conditions including the interaction of the scaffold with nutrients from the cell culture media. Many commercially available media formulations are not able to support the large number of cells achieved during 3D cell culture leading to regular disturbance of the cells and large peaks and troughs in media quality.

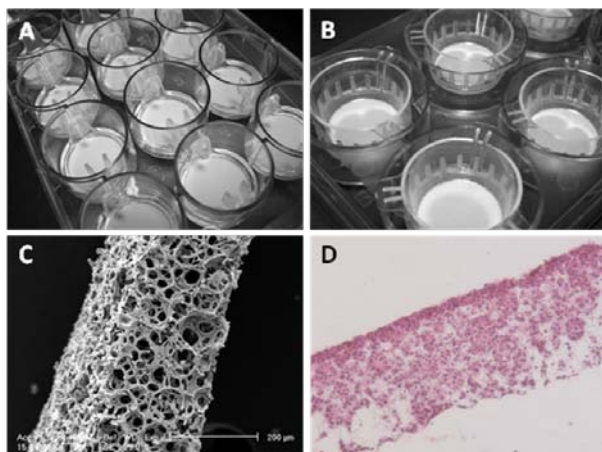


Fig. 1: Alvetex in different formats – 12 well (A), 6 well insert (B), SEM showing porous structure (C) and H&E staining of pluripotent stem cells in alvetex after 7 days growth(D).

METHODS: We have developed an inert, non-degradable scaffold termed Alvetex® (Fig. 1A-B) which allows for convenient routine culture of cells in 3D. The scaffold displays a highly porous 3D structure where each void is connected to the neighbouring voids via interconnects (Fig.C). This allows cells into the interior of the scaffold and addresses the issues of mass transfer concerning exchange of gases and nutrients [1-2]. We have observed the growth of the human pluripotent stem cell line TERA2.cl.SP12, within the 3D scaffold.

We investigated the metabolic demands of these cells during 3D culture by monitoring glucose consumption and lactic acid production.

Cells grown in Alvetex® can be processed for many biological assays, for histology and immunostaining in a similar way to tissue samples (Fig.1D). Pluripotent stem cells grown in the scaffold are induced to differentiate in response to retinoids allowing cells to form complex 3D structures similar to tissues found in teratomas derived from these cells *in vivo*, including neurons.

RESULTS: Alvetex® enables routine 3D cell culture. The range of scaffold formats (including Fig. 1A-B) allows for both short- and long-term culture. We have demonstrated how the issues concerning cell metabolism and movement through the scaffold can be addressed by providing cells with a larger reservoir of media and large surface area for penetration and exchange.

We have begun to investigate the benefit of the 3D environment afforded by our scaffold in terms of the developmental potential of stem cell populations. To date we have observed the growth of human pluripotent stem cells in the 3D scaffold. Undifferentiated cells proliferate and fill the 3D space indicating a role for the scaffold in cell expansion (Figure 1D). Cells induced to differentiate in response to retinoids form complex 3D structures. Immunostaining of RA-treated cells shows evidence of neural differentiation throughout the scaffolds.

DISCUSSION & CONCLUSIONS:

Optimisation of a system for routine 3D cell growth and being able to form complex structures *in vitro* could potentially lead to a more accurate model for investigative research into the developmental potential of pluripotent stem cells, and the generation of human tissue for screening applications.

REFERENCES: ¹Carnachan,R.J. et al (2006)*2 Soft Matter*, ²Maltman,D.J. (2010) **38**(4) *Biochem Soc Trans*,

ACKNOWLEDGEMENTS: This research is funded by an MRC CASE studentship in collaboration with Reinnervate Ltd.

Polyelectrolyte multilayers for cell and tissue engineering

Laura Pastorino, Neda Habibi, Federico Caneva Soumetz, Massimo Giulianelli and Carmelina Ruggiero

Department of Communication, Computer and System Sciences – DIST, Nanobiotechnology and Medical Informatics Laboratory, University of Genoa, Italy

INTRODUCTION: The fabrication of functional hybrid materials composed of nanoscale building blocks represents one way in which nanotechnology can contribute to biology and medicine. To this regard, the layer-by-layer technique (LbL), due to its versatility, provides a simple and inexpensive method for the fabrication of complex nanostructured capsules. The method is based on the sequential absorption of oppositely charged polyelectrolytes onto supports on any shape and dimension. Most of the advantages of such method lies on the possibility to fabricate biocompatible multifunctional ultra-thin films/nanocarriers whose properties can be tuned at the nanoscale [1]. Such nano-structures can be formed by either synthetic and natural polyions, such as proteins, and nanoparticles. Polyelectrolyte nanofilms have a variety of applications ranging from optical and electrochemical materials to biomedical devices. Currently we are using the LbL technique for the development of biocompatible and bioactive surfaces for tissue repair and stem cell differentiation [2], for the development of nanobiosensors [3], and of nanoengineered capsules for drug targeting and release [4]. In this paper, the main concepts involved in the fabrication and functionalization of polyelectrolyte multilayers are described.

METHODS: as synthetic polyelectrolytes, we use PSS (Sodium poly styrene sulfonate, 2 mg/ml) and PAH (Poly allylamine hydrochloride, 2 mg/ml). Biopolymers such as collagen, sodium alginate, poly-lysine, type G immunoglobulins, adhesion proteins and growth factors are used to impart a specific bioactivity to the multilayers. Magnetic nanoparticles and bacterial S-layers are employed to impart a targeting activity to nanocarriers obtained by LbL. The assembly process is carried out on metal and polymeric scaffolds, and on carbonate microparticles. The assembly process is monitored and optimized by quartz crystal microbalance. Optical, atomic force, scanning electron and fluorescent microscopy are used to visualize the nanosystems. Functionality is assayed by immunological test.

RESULTS: the structure and the thickness of the multilayers are controlled at the nanometre scale level in a predetermined fashion. Bioactivity can be imparted and modulated as well as targeting activity. Successful encapsulation and release of pharmacological molecules have been also demonstrated. The possibility to combine the LbL technique with bacterial self assembled proteins to introduce Functional groups on the top of the polyelectrolyte layers has been also demonstrated.

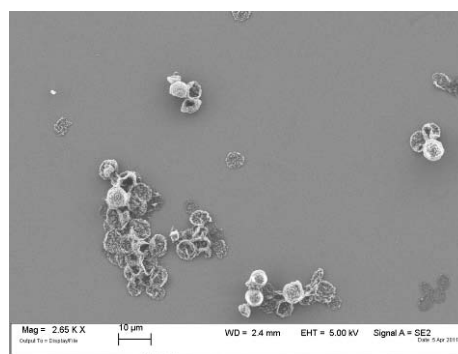


Fig. 1: Scanning electron microscopy image of collagen/sodium alginate capsules and covered templates.

DISCUSSION & CONCLUSIONS: The results show that the LbL technique due to its versatility and ease represents a powerful tool for the assembly of biocompatible and bioactive two and three-dimensional layered architectures. The future perspectives of this technique lie on the creation of free standing multilayers to be utilized as scaffold in tissue engineering, in the coating of individual cells and in the development of minimal artificial cells.

REFERENCES: ¹ P. R. Gil, L. del Mercato, P. del_Pino, A. Muñoz_Javier and W.J. Parak, (2008) *Nanotoday*, 3:12-21. ² F. Caneva Soumetz, L. Pastorino, C. Ruggiero, (2008) *Journal of Biomedical Materials Research: Part B - Applied Biomaterials*, 84: 249-255. ³ L. Pastorino, F. Caneva Soumetz, M. Giacomini, C. Ruggiero, (2006) *Journal of Immunological Methods*, 313: 119-198. ⁴ Laura Pastorino, Svetlana Erokhina, Federico Caneva Soumetz, et al., (2011), *Journal of Colloid and Interface Science*, 357: 56-62.

The Biology of the Ovine Functional Spinal Unit

CS Gough¹, VN Wajayathunga², JL Tipper¹, RK Wilcox², RM Hall² & E Ingham¹

Institute of Medical and Biological Engineering, ¹Faculty of Biological Sciences and ²School of Mechanical Engineering, University of Leeds, UK.

INTRODUCTION: The functional spinal unit (FSU) is an intact section of the spine comprising two adjacent vertebrae with undisturbed cartilage end plates, the intervertebral disc and the two articulating facet joints. Facet joint osteoarthritis can lead to chronic back pain. Early intervention with cartilage substitution therapies to prevent disease progression is an attractive solution. The overall aim of this project is to characterise the biology of the ovine facet joint and end plate cartilage. This work is a key element in the development of a degenerative ovine model of the FSU to be used in *in vitro* simulations.

The aim of this initial study was to determine the phenotype of the ovine FSU cells and changes to the phenotype over time. This was achieved by isolating and characterising FSU cells over 8 passages in monolayer culture.

METHODS: Cells were isolated from ovine facet joint cartilage, end plate cartilage, annulus fibrosus and nucleus pulposus using a collagenase and hyaluronidase enzyme digestion solution. The cells were grown in monolayer culture in Dulbecco's modified Eagle's medium (DMEM) supplemented with 10% FBS (v/v), 100 U.ml⁻¹ penicillin, 100 U.ml⁻¹ streptomycin and 2mM L-glutamine in PBS and plated onto multi-spot slides at passage 4, 6 and 8. After 24 hours, the slides were fixed in 1:1 acetone:methanol for 2 minutes.

The cells were then characterised using a panel of primary antibodies by in-direct immunofluorescence using FITC-conjugated secondary antibodies. Antibodies were to aggrecan, chondroitin-6-sulphate, CD44, collagen I and II, and SOX-9. The primary and secondary antibody dilutions were initially optimized by chess-board titration. Cells were counterstained with Hoechst dye to identify nuclei. Images were captured using fluorescence microscopy and Olympus Cell B software.

RESULTS: Cells from each tissue were successfully isolated and they were positive for collagen II, chondroitin-6-sulphate, SOX-9 and CD44 at passage 4 as in Figure 1 but negative for aggrecan and collagen I. At passage 6, collagen II was no longer expressed in any of the cell lines and chondroitin-6-sulphate expression was reduced. At

passage 8, the facet cartilage cells no longer expressed SOX-9 and CD44, all the cell lines showed increased expression of chondroitin-6-sulphate and maintained expression of the other proteins expressed at passage 6.

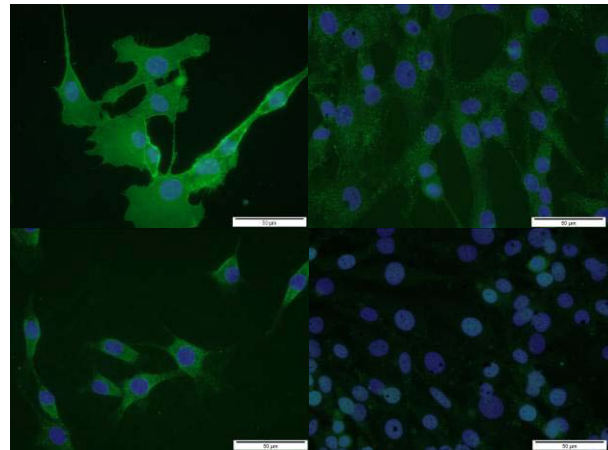


Figure 1: Facet cartilage cells (passage 4) stained by in-direct immunofluorescence using antibodies to CD44 (top left), chondroitin-6-sulphate (top right), collagen II (bottom left) and SOX-9 (bottom right).

DISCUSSION & CONCLUSIONS: The cells isolated from the ovine facet cartilage, cartilage end plate, annulus fibrosus and nucleus pulposus all had similar morphology in culture and phenotype up to passage 6 which was indicative of chondrocytes. This may indicate that the cells isolated from the annulus were nucleus pulposus cells. The lack of aggrecan expression may indicate that this was down-regulated very early during culture. The cell phenotype changed with extended passage as has been reported for chondrocytes in monolayer¹.

Future work will involve characterisation of the cells in-situ by immunohistochemistry and biological and biomechanical characterisation of the FSU.

REFERENCES: ¹ K von der Mark, V Gaus, H von der Mark and P Muller (1977) *Nature* **267**: 531-532.

ACKNOWLEDGEMENTS: Iraklis Papageorgiou and Elizabeth Mitchell for assistance during the work and the Engineering and Physical Sciences Research Council (EPSRC) for funding.

Natural Demineralised Bone as a Scaffold for Bone Regeneration

M. Eagle, P. Rooney & J. N. Kearney

NHS Blood and Transplant, Tissue Services, Estuary Banks, Liverpool, UK

INTRODUCTION: New bone formation involves the presence of existing bone (osteoconduction), bioactive factors (osteinduction) and osteogenic cells. Bone repair could be enhanced if osteogenic cells could be added to a bone scaffold prior to tissue grafting or if a graft could be produced which stimulated osteogenesis *in vivo*. Demineralised bone matrix (DBM) is known to stimulate rapid bone formation leading to improved tissue regeneration, however, DBM is generally a powder from cortical bone mixed with a carrier to produce a paste/putty, it does not resemble the structure of natural bone and provides little osteoconductive properties. We describe here a process which removes blood, bone marrow, soluble protein and DNA from cancellous bone, making a decellularised natural bone scaffold. We also report on a method to demineralise the bone resulting in a spongy, deformable scaffold with natural bone size, shape, porosity etc. This scaffold could be used for assessing bone differentiation from precursor cells *in vitro* or could be inserted into a bony defect *in vivo*, acting as a scaffold to direct new bone formation.

METHODS: Human knee joints were obtained with full ethical approval and consent. Soft connective tissue and articular cartilage was dissected away and then 1 cm slices of cancellous bone were cut radially from the tibia and femur. The slices were then cut into 1 cm³ cubes and processed using a combination of warm water washes, chemical washes and centrifugation. The cubes were then demineralised in 0.5N hydrochloric acid under vacuum, inside a specially designed container to ensure immersion in solution at all times. Rate of demineralisation was monitored continuously by measuring pH values and demineralisation was stopped when pH rise ceased. Demineralisation was confirmed by measuring levels of residual calcium in the bone and by histology. Biocompatibility was assessed by contact cytotoxicity assays using a human osteoblastic cell line (MG63) and NIH-3T3 cells.

RESULTS: The washing protocol removed a mean of 99.9% of soluble protein, DNA and haemoglobin from bone cubes – a 3 Log₁₀ removal (Table 1) with no evidence of cells or cellular

fragments. This mineralised bone was found to be non-cytotoxic. Demineralisation of up to 25 x 1 cm³ cubes was completed within 2 hours, resulting in a natural scaffold which could be easily compressed (Figure 1). Histological examination demonstrated little or no calcium in the scaffold and maximum residual calcium levels of 3% of dry weight were recorded. This demineralised bone also demonstrated no cytotoxicity.

Component	% Removed	Log ₁₀ Removal
Soluble protein	99.83	2.73
DNA	99.92	3.10
Haemoglobin	99.95	3.30
Mean	99.90	3.00

Table 1. Mean bone marrow component removal from washed bone cubes.

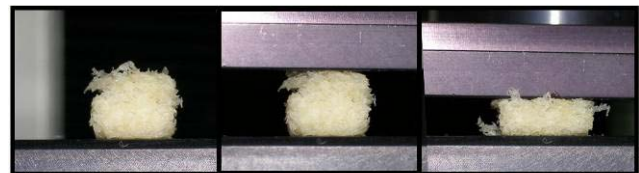


Figure 1. Demineralised bone cube before and after compression. The cube returned to size after compression was removed.

DISCUSSION & CONCLUSIONS: We have developed a protocol for removing cellular and bone marrow components from human bone; this washed bone can be demineralised resulting in a spongy, natural, biocompatible scaffold. We suggest that this scaffold could be used to aid bone repair/regeneration by implantation into a wound site with or without pre-addition of osteogenic cells. The scaffold could also be a useful tool for investigating osteogenic differentiation *in vitro*.

Design and Characterisation of Novel complementary Peptide Gel in Physiological conditions

R.P.W.Davies¹, E.Ingham² & A Aggeli¹

¹ Centre for Molecular Nanoscience, School of Chemistry, University of Leeds, U.K. ²Institute of Medical and Biological Engineering, University of Leeds

INTRODUCTION: Peptides hold therapeutic and commercial promise due to their enormous structural diversity¹. Our focus is on exploiting the self-assembly properties of a class of beta sheet tape forming peptides for use in regenerative medicine. This includes the design and production of new, optimized self-assembling peptides following an iterative approach guided by biological and functionality experiments and rigorously characterising their self-assembling and material properties.

METHODS: Novel peptides were synthesised using manual F-moc solid phase synthesis², the target molecule was identified using mass spectroscopy and was purified using high performance liquid chromatography. The net peptide purity was determined by U.V. spectroscopy, elemental analysis and amino acid analysis.

Spectroscopic techniques such as U.V. spectroscopy, FTIR spectroscopy and Circular Dichroism, are used to quantify and analyse the self-assembling properties of the peptide. The microscopic characteristics are probed using TEM and fluorescence microscopy. Finally the mechanical and structural properties are investigated using rheological techniques.

RESULTS: The complementary peptides P₁₁₋₁₃ and P₁₁₋₁₄ have been found to form monomeric fluids in physiological conditions. When mixed the immediate formation of stable self supporting gels can be observed. The gels have been found to form anti parallel β -sheets and well defined morphologies

Table 1. Peptide primary structure of the complementary peptides P₁₁₋₁₃ P₁₁₋₁₄

	Peptide Primary Structure
P ₁₁₋₁₃	CH ₃ CO-E-Q-E-F-E-W-E-F-E-Q-E-HN ₂
P ₁₁₋₁₄	CH ₃ CO-Q-Q-O-F-O-W-O-F-O-Q-Q-NH ₂

Specific design criteria have been developed to optimise the self-assembly in order to form stable gels in physiological conditions and produce a larger library of complementary peptides with varying mechanical properties.

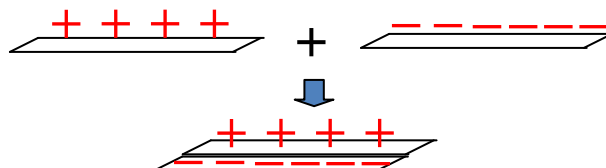


Fig. 1: A schematic representation of the self-assembly of negatively and positively charged complementary peptides.

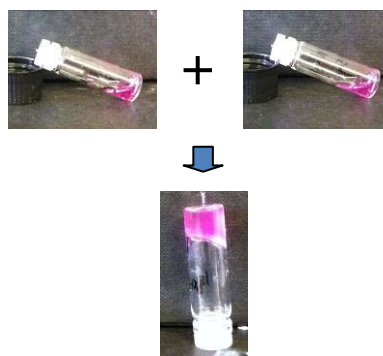


Fig 2: Complementary peptides existing in the fluid state prior to mixing (top) The resulting stable gel, resulting from their addition (bottom)

DISCUSSION & CONCLUSIONS: Evaluation and development of this novel class of biological materials in physiological conditions is intended for applications in tissue engineering. The subsequent self-assembling properties can be tailored by subtly changing the peptide primary structure. Indeed the ability to manipulate peptide self-assembly without changing environmental factors such as pH or salt levels³ allows for an environment that can be designed for specific cells and tissues.

REFERENCES: ¹Maude S; Miles D; Felton S et al (2011) Soft Matter ² Aggeli A; Bell, M; Carrick, L,M; Fishwick, C,W,G, et al (2002) Journal Of The American Chemical Society ³ Carrick, LM; Aggeli, A; Boden, N, et al. (2007) Tetrahedron **63** 7457-7467

ACKNOWLEDGEMENTS: This work funded through WELMEC, a Centre of Excellence in Medical Engineering funded by the Wellcome Trust and EPSRC, under grant number WT 088908/Z/09/Z.

A Novel Method for Characterising Mechanical Properties of Hydrogels

Grahame A Busby¹, Phil Riches¹, Simon MacKay², M. Helen Grant¹

¹Bioengineering Unit, University of Strathclyde G4 0NW. ²Strathclyde Institute of Pharmacy and Biomedical Sciences, University of Strathclyde G4 0QU.

INTRODUCTION: Collagen, the most abundant structural protein in the human body, has become the most widely used matrix for tissue engineering [1]. However, collagen that has been implanted in the body undergoes a constant process of remodelling, and the gradual degradation of the collagen within the matrix must be kept in balance with collagen synthesis if the scaffold is to maintain its strength and integrity. To better understand and assess this process, it is necessary to be able to characterise the mechanical properties of collagen hydrogels.

We have developed a non-destructive technique that facilitates the mechanical characterisation of hydrogels. Biphase theory [2] has often been used to characterise cartilaginous tissues [e.g. 3, 4], yet to our knowledge it has not been applied to collagen-based scaffolds. The initial validation of the theory for this biomaterial, and the testing of the technique, is reported below.

METHODS: Collagen (type 1) was prepared in-house from rat tail tendon and hydrogels were set in standard 24 well tissue culture plates. Hydrogels were detached from the sides of the culture dish prior to testing and compressed with a porous indenter attached to a BOSE ElectroForce® 3200 test instrument via a 10 N load cell. To validate the theory and technique, eight collagen gel samples (16 mm diameter, approx. 5 mm thick) were made in each of three collagen concentrations (0.2%, 0.3% and 0.4%). Samples were compressed by 250 μm (~5% strain) at 0.025 mm/s and held for 300 seconds.

Biphase theory [3] was fitted to the ramp and hold phases using a Nelder-Mead scheme and the obtained tissue parameters, namely aggregate modulus (stiffness in confined compression) and initial hydraulic permeability, and experimental stress values were compared using ANOVA with respect to collagen content.

RESULTS: The collagen based scaffolds exhibited typical biphasic behaviour in confined compression allowing the biphasic theory to be applied. Aggregate modulus, initial hydraulic permeability, peak stress and equilibrium stress all varied significantly with collagen content.

Aggregate modulus (stiffness) was approximately 1 kPa for 0.3% collagen gels and increased relative to collagen concentration ($p < 0.01$), while Fig. 1 shows that as collagen content increases hydraulic permeability decreases ($p = 0.015$).

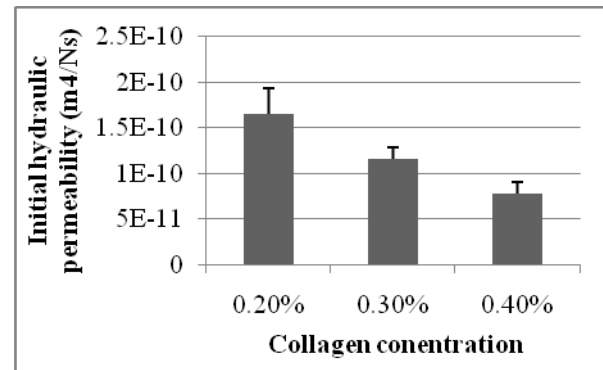


Fig. 1: Relationship between initial hydraulic permeability and collagen concentration in hydrogels ($n=8$). Error bars indicate + SEM.

DISCUSSION: These initial results suggest that confined compression, together with biphasic theory, is a suitable technique for assessing the mechanical properties of collagen based scaffolds. Both material properties and test-dependent experimental stress values exhibited sensitivity to collagen content. Therefore the technique is clearly able to discriminate between hydrogels of different collagen concentrations, and potentially may be sensitive to factors that affect matrix remodelling.

CONCLUSIONS: Biphasic theory has been successfully applied to collagen based scaffolds in confined compression. We hypothesise that the technique may also be suitable for the characterisation of other inherently weak hydrated tissues. Work continues to assess the effects of matrix remodelling on the mechanical properties of the matrix.

REFERENCES: ¹ K. Y. Lee and D. J. Mooney (2001) *Chem. Rev.* **101**(7): 1869-1880. ² V. C. Mow, S. C. Kuei, W. M. Lai, and C. G. Armstrong (1980) *J. Biomech. Eng.* **102**(1): 73-75. ³ G. A. Ateshian, W. H. Warden, J. J. Kim et al (1997) *J. Biomech.* **30**: 1157-1164. ⁴ D. Périé, D. Korda and J. C. Iatridis (2005) *J. Biomech.* **38**: 2164-2171.

Development of a Tissue Engineered 3D Immunocompetent Model of the Human Upper Respiratory Tract

PA Cato^{1,2}, A Ghaemmaghani¹, FRAJ Rose²

¹Allergy Research Group, School of Molecular Medical Sciences, University of Nottingham, UK. ²Division of Drug Delivery and Tissue Engineering, Centre for Biomolecular Sciences, University of Nottingham, UK.

INTRODUCTION: Development of *in vitro* models of disease are required as alternatives to animal models, which lack biological relevance¹. Advances in tissue engineering are leading toward more complex *in vitro* and *ex vivo* models that better mimic native functional tissue². We aim to develop an immunocompetent 3D human upper respiratory model: a tri-culture of human epithelial, fibroblast and dendritic cells each supported on multi-layered scaffold sheets that mimic the extracellular matrix (ECM).

METHODS: PLA dissolved in dichloromethane (15-20% w/w) and electrospun under steady flow rate and set voltage and collected on an aluminium collection plate. Scaffold morphology assessed using SEM. Upper left lobe lung tissue decellularised through treatment with trypsin/EDTA, triton-X, SDS, and deionised H₂O. CALU-3 and MRC-5 seeded (2×10^5 cells/scaffold) onto sterilised PLA scaffolds and maintained at 37°C, 5% CO₂. Samples for light microscopy imaging stained with May-Grunwald and Giemsa.

RESULTS: Fibrous electrospun PLA scaffolds have been constructed which mimic the structure of human ECM (Fig. 1.)

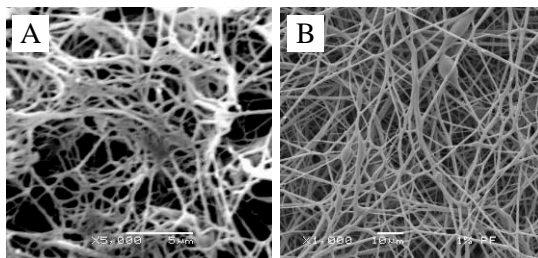


Fig. 1: SEM images comparing the structure of decellularised human lung tissue (A) ($\times 5000$ magnification) & nanometer scale PLA Electrospun Scaffold (B) ($\times 1000$ magnification).

CALU-3 epithelial cells and MRC-5 fibroblasts were assessed for attachment and proliferation over 7 day culture on PLA scaffolds. CALU-3 attachment to a nanometer scale scaffold (mean fibre diameter 800nm) was achieved, where cells attach and proliferate on the surface of the scaffold (Fig. 2). MRC-5 fibroblast attachment and proliferation was achieved to a micrometer scale scaffold (mean fibre diameter 5 μ m) (Fig. 3).

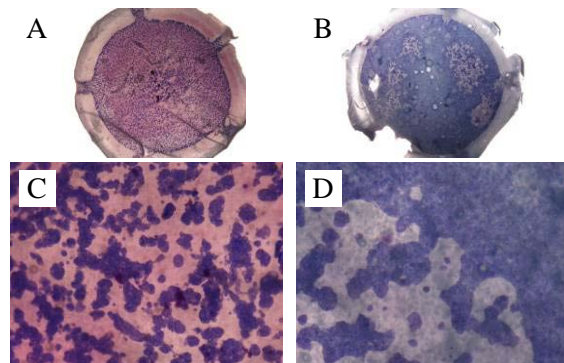


Fig. 2: Light microscopy images of CALU-3 epithelial cells cultured for 7 days on nanometer PLA scaffold: Day 1 (A & C), Day 7 (B & D). Top row $\times 1$, bottom row $\times 11$ magnification.

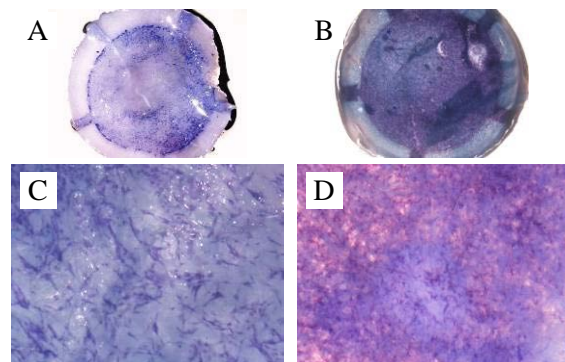


Fig. 3: Light microscopy images of MRC-5 fibroblasts cultured for 7 days on micrometer PLA scaffold: Day 1 (A & C), Day 7 (B & D). Top row $\times 1$, bottom row $\times 11$ magnification.

CONCLUSION: Fibrous 3D PLA electrospun scaffolds, which mimic in structure the ECM *in vivo*, have been constructed to support *in vitro* culture of CALU-3 epithelial cells and MRC-5 fibroblasts.

REFERENCES: ¹Y.S. Shin et al., (2009) Understanding asthma using animal models *Allergy Asthma Immunol Res* 1:10-18.
²A. Holmes, et al., (2009). Engineering tissue alternatives to animals: applying tissue engineering to basic research and safety testing. *Regen Med* 4:579-592.

ACKNOWLEDGEMENTS: We would like to thank the MRC for funding.

FLUID AND MASS TRANSPORT MODELLING TO DRIVE THE DESIGN OF CELL-PACKED HOLLOW FIBRE BIOREACTORS

RJ Shipley^{1,2}, SL Waters¹ & MJ Ellis²

¹Mathematical Institute, University of Oxford and ²Department of Chemical Engineering, University of Bath

INTRODUCTION: A significant challenge in the development of tissue engineering bioreactors is cell-type specificity – the design and operation of the bioreactor should be motivated by the demands of the cell type under consideration. This requires the provision of operating equations that enable an end-user to design the bioreactor geometry and set its operating conditions (*e.g.* pressures, flow rates, concentrations) to obtain the desired cell culture environment. The objective of this study is to define these operating equations based on mathematical models of fluid flow, nutrient delivery and waste product removal from a cell population seeded in a hollow fibre membrane bioreactor (HFB). We parameterize the models using experimental data for two specific cell types (cardiomyocytes and chondrocytes), and present operating data for each of these examples.

METHODS: A schematic of the setup is shown in Fig. 1. HFBs use a controlled fluid flow coupled with diffusion to augment mass transport throughout the bioreactor. We investigate the option of opening the ECS port to promote radial flow through the module (as well as axial flow through the lumen) and thus enhance nutrient supply (and waste product removal) to (and from) the cell population. Fluid flow in the lumen is described by the Navier-Stokes' equations for an incompressible fluid with constant viscosity. Fluid flow in the membrane and ECS are both described using Darcy's law for an isotropic porous medium (this mimics a cell population seeded in gel throughout the ECS). Mass transport of nutrients or waste products is described using advection-diffusion-reaction equations, where the reaction term captures uptake of nutrients (or production of waste products) throughout the cell population.

RESULTS: Based on typical parameter values, the Reynolds number based on the lumen length is $Re \approx 10^4$ and the aspect ratio of the lumen is $\varepsilon \approx 10^{-3}$. Therefore, the reduced Reynolds number is $\varepsilon^2 Re \ll 1$ and lubrication theory may be used to exploit the geometry of the system and simplify the underlying equations. Similarly the reduced Péclet number for transport (which represents the relative importance of advection versus diffusion in a small aspect ratio

geometry) is order 1 so that radial diffusion balances both radial and axial advection. Analytical solutions of the transport equations (in steady state) enable operating equations to be derived that describe the dependence of the (a) minimum oxygen and (b) maximum lactate concentrations on the geometric (lumen length and diameter, membrane and ECS depths) and operating (inlet flow rate, retentate pressure, seeded cell density, inlet oxygen concentration) parameters for the bioreactor. By parameterizing the model with cell-type specific oxygen/lactate diffusivities and uptake/production, we present a comparison of the optimal geometric and operating conditions for cardiomyocytes and chondrocytes, when the ECS port is either closed or shut.

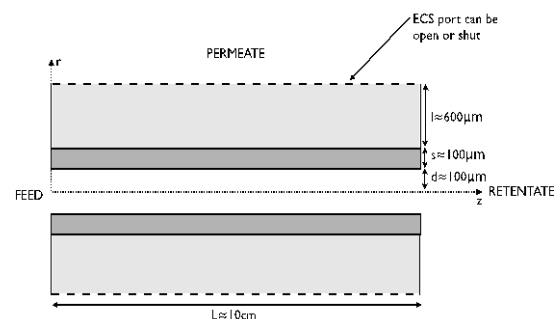


Fig. 1: Schematic of an axial cross-section through a single module of a HFB comprised of a central lumen (white), surrounding porous membrane (dark grey) and ECS seeded with cells (light grey)

DISCUSSION & CONCLUSIONS: Our approach uses analytical modelling techniques to inform bioreactor design and operation. This includes (a) relationships to estimate the desired membrane pore size and seeded cell density that promote radial flow in the bioreactor, (b) operating equations that enable the design parameters to be determined to satisfy cell culture conditions on the oxygen and lactate concentrations. For example, opening the ECS port to enable radial flow allowed a 333% increase in the ECS depth for cardiomyocytes cultured throughout the ECS.

ACKNOWLEDGEMENTS: This work was funded by the John Fell Oxford University Press Research Fund, together with a Royal Society Research Grant.

Net peptide charge influences the formation of self-assembling β -sheet peptide hydrogels in model physiological conditions

S Maude¹ & A Aggeli¹

¹ Centre for Molecular Nanoscience, School of Chemistry, University of Leeds, LS2 9JT, UK

INTRODUCTION: Self-assembling peptides are promising new tissue engineering materials¹. The rationally designed, β -sheet peptide P₁₁-2 is known to produce fibrous aggregates that can form hydrogels². To improve this design for cell growth, an important question is what modifications can we make while still retaining self-assembly? Here the effect of net charge is considered: how much charge on each peptide monomer can the favourable intermolecular interactions tolerate before self-assembly is no longer possible?

METHODS: Peptides (Table 1) were prepared in 130 mM NaCl/D₂O at pD 7.4. ¹H NMR spectroscopy monitors peptide aggregation by measuring the peptide aromatic peak integral, relative to an internal standard (TMSP). Below the c* (critical aggregation concentration), peptide concentration relates directly to this integral. Above c*, any additional peptide self-assembles. As aggregates have an NMR linewidth too broad to contribute to the measurable integral, the fraction of (non-)assembled peptide can be determined. Amide I' FTIR spectra were analysed to confirm peptide secondary structure.

Table 1. Peptide net charge at pH 7.4. O is ornithine; peptides are acetylated and amidated.

Peptide	Sequence	Charge
P ₁₁ -14	QQOFWOFQOQ	+4
P ₁₁ -5	QQOFWOFQOQ	+3
P ₁₁ -8	QQRFWOFEQQ	+2
P ₁₁ -3	QQRFWQFQOQ	+1
P ₁₁ -2	QQRFWQFEQOQ	0
P ₁₁ -3'	QQQFWQFEQOQ	-1
P ₁₁ -4	QQRFEWFEQOQ	-2
P ₁₁ -13	EQFEWFEQOQ	-6

RESULTS: P₁₁ peptides were found to exhibit one of two behaviours. Either no aggregation, and no gelation, occurs over the concentrations studied (NMR signal proportional to concentration), or they show nucleated self-assembling behaviour (signals stop increasing above c*). Increasing the net charge on the peptide increases its critical aggregation concentration (c*) and reduces the amount of beta sheet content at high concentration (Fig. 1a). IR measurements confirmed these findings: (Fig. 1b).

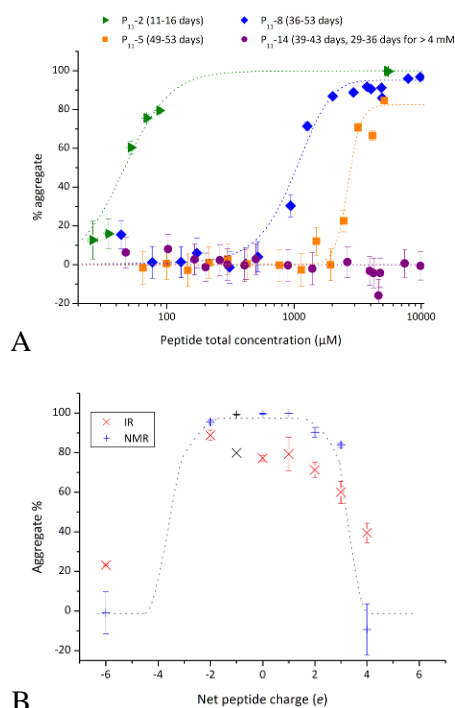


Fig. 1A: Self-assembly curves for positive peptides (log scale); B: IR and NMR data at 10 mg ml⁻¹.

DISCUSSION & CONCLUSIONS: Self-assembly exhibits a strong dependence on net charge. Large charges disfavour self-assembly. P₁₁ with the smallest charges (0 and ± 1) have lower c* and a greater proportion of aggregate at moderate concentration. However, these peptides with very small charge tend to have poorer solubility, producing flocculates or precipitates. Peptides with a moderate, non-zero (± 2) charge, which have moderate c* (of the order of 0.5-1 mM), are a good starting point for designing cell compatible peptide gel matrices; a lower c* may mitigate the possibility of unwanted peptide-cell membrane interactions³.

REFERENCES: ¹ Collier et al (2010) *Chem. Soc. Rev.* **39**:3413-24 ² Aggeli et al (2001) *PNAS* **98**:11857-62 ³ Protopoulos et al (2009) *Langmuir* **25**:3289-96.

ACKNOWLEDGEMENTS: The work was partly supported by the Leeds Centre of Excellence in Medical Engineering funded by the Wellcome Trust and EPSRC, WT088908/z/09/z.

Metabolomic Investigation of MSC Responses to Titania Nanopillars

Laura E. McNamara^{1*}, Terje Sjöström³, Karl V. Burgess², Joseph Kim⁴, Er Liu⁴, Simon Gordonov⁴, Prabhas Moghe⁴, Richard O.C. Oreffo⁵, Bo Su³ and Matthew J. Dalby¹

¹Centre for Cell Engineering, and ²SHWFGF, University of Glasgow, UK, ³Department of Oral and Dental Science, University of Bristol, UK. ⁴Department of Biomedical Engineering, Rutgers University, USA. ⁵Bone and Joint Research Group, University of Southampton, UK.

*laura.mcnamara@glasgow.ac.uk

INTRODUCTION: Functionalisation of bioinert implant materials (including titania; Ti) with defined osteogenic nanopatterns would have great potential to facilitate biological implant fixation. In this study, the osteogenic capacity of Ti nanopillar-like features was examined in relation to mesenchymal stem cells (MSCs). Metabolomics was used to study the metabolic response of the cells, in conjunction with staining of early-stage transcription factors (TFs) (such as the osteogenic marker phospho-Runx 2), focal adhesion (FA) quantification and Haralick analysis.

METHODS:

Nanofabrication: Pillar-like titania nanofeatures (of 15 nm, 55 nm and 90 nm high) were fabricated as in [1]. **Cell Culture:** Primary human MSCs were cultured for 2d (TF), 3d (FA and computational analysis) or 7d (metabolomics) on the surfaces. **FA Quantification, TF and Computational Analysis:** MSCs were labelled using BrdU to identify S-phase cells and allow FA quantification in a single phase of the cell cycle. Immunostaining was performed to assess induction of early-stage TFs. Morphometric descriptors [2] were derived from cytoskeletal data and subject to Haralick analysis to assess morphological relatedness of the MSCs between surfaces. **Metabolomics:** Mass spectrometry was used to identify differentially abundant metabolites and metabolites were categorised by function using Ingenuity Pathways Analysis.

RESULTS: MSCs cultured on 15 nm pillars showed enrichment of interesting metabolites with relevance to osteogenesis, including signalling lipids and several amino acids. In addition, the FA profile was also distinctive on the 15 nm substrate; these cells had the highest proportion of large-sized adhesions (an osteogenic characteristic), and showed increases in amount and clustering of the osteogenic TF phospho-Runx 2 (Fig. 1). Haralick analysis, used to assess phenotypic relatedness based on cytoskeletal features, confirmed that the cell response to the 15 nm surface was distinct from the other nanosurfaces (Fig. 1).

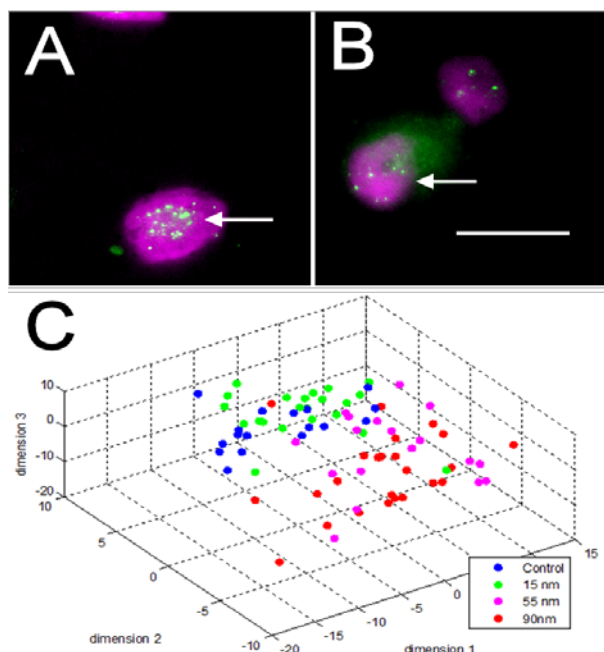


Fig. 1: The osteogenic TF phospho-Runx 2 (green) showed greater clustering and abundance in nuclei on 15 nm (A) versus 90 nm (B) pillar-like features (DNA is purple); (C) Haralick computational analysis could distinguish between the surfaces based on cytoskeletal features.

DISCUSSION & CONCLUSIONS: MSCs cultured on 15 nm pillars showed most osteogenic character, with increased levels and clustering of an osteogenic TF, as well as interesting metabolic and morphological distinctions from cells on the other surfaces. The observed differences in FAs would likely contribute to altered mechanosignalling, resulting in the phenotypic changes. Metabolomics shows promise as a tool for the molecular characterisation of cell responses to biomaterials.

REFERENCES: ¹Sjöström, T., Dalby M.J., Hart, A. *et al.* (2009) *Acta Biomaterialia* **5**:1433-41
²Treiser, M.D., Yang, E.H., Gordonov, S. *et al.* (2010) *PNAS* **107**:610-54

ACKNOWLEDGEMENTS: The authors thank the EPSRC (Grant: EP/G048703/1) for financial support. We thank Ms. K. Murawski for stem cell isolation.

Polymeric Scaffolds by Interface Engineering

P. Viswanathan¹, S. Chirasatitsin², A. Engler² and G. Battaglia¹

¹ Department of Biomedical Sciences, Western Bank, University of Sheffield, Sheffield S10 2TN

² Department of Bioengineering, University of California San Diego, La Jolla, CA 92093

INTRODUCTION: Novel materials design for the tissue engineering and regenerative applications often require both chemical and physical cues both on the nano and micro scales.^{1,2} Here, we report the synthesis of emulsion templated porous polystyrene scaffolds chemically modified by amphiphilic block copolymers; polystyrene-*b*-poly(ethylene oxide) (PS-PEO) and polystyrene-*b*-poly acrylic acid) (PS-PAA). By varying the molar ratio of these polymers, distinct cell adhesive (PAA) and cell inert binding sites mimicking *in vivo* extracellular matrix. Such binding sites providing a novel way to control mesenchymal stem cell morphology and differentiation.

METHODS: Porous polystyrene foams were prepared using water-in-oil emulsion templating using previously established methods.³ However, the amphiphilic diblock copolymers PS-PEO and PS-PAA were used as surfactants for this process. Scaffolds with various mixtures (by molar ratio) of the copolymers were prepared to induce phase separation at the oil-water interface also seen in bilayer block copolymer systems.⁴ Scaffolds were polymerized at 60 C and then Soxhlet extracted for 24 hours. Scanning electron microscopy (SEM) was carried out to assess the morphology of the scaffolds. Surface chemistry was determined by X-ray photoelectron spectroscopy (XPS) and contact angle measurements. Finally block copolymer phase separation was imaged using chemical force spectroscopy mapping (CFSM).

RESULTS: Low magnification SEM images revealed macroscopic porosity in the order of 100 μm while high magnification SEM images show topography on the nano scale on the surface of these foams introducing a hierarchy of physical cues. However, our aim here was to chemically pattern the surface with distinct domains of the hydrophilic blocks (PAA and PEO) of the block copolymer. While XPS and contact angle measurements gives us critical information about surface chemistry and wettability, respectively, as a result of the block copolymers, CFSM data on corresponding 2D films, showed the formation PAA and PEO domains. Here, a standard Au AFM tip was functionalized with the cationic polymer

poly(L-lysine) (PLL) and the Coulombic forces between PLL and PAA were mapped, showing the phase separation of PS-PEO and PS-PAA at the oil water interface.

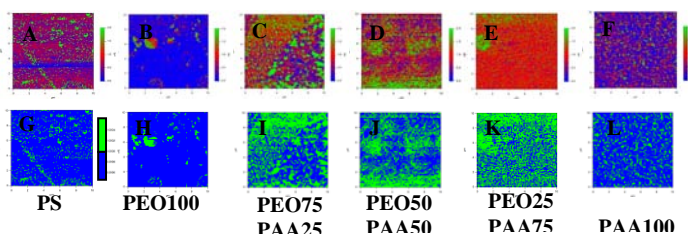


Fig 1. Chemical force spectroscopy mapping of 2D films containing the block copolymers PS-PAA and PS-PEO.

DISCUSSION & CONCLUSIONS: We have shown that the surface chemistry of scaffolds can be achieved in 3D in a one step synthesis using block copolymers. These scaffolds provide a novel route to controlling stem cell morphologies and eventual differentiation in a 3D environment.

REFERENCES: ¹ A. Engler et. al. (2006) *Cell*, **126**:677-689, ² M. Dalby et. al. (2007) *Nat. Mater.*, **6**:997-1003, ³ M. Bokhari et. al. (2007) *J. Mater. Chem.* **17**:4088-4094. ⁴ M. Massignani et. al. (2009) *Small*, **5**:2424-2432

ACKNOWLEDGEMENTS: We would like to thank Dr. Adrian Boatwright, University of Nottingham for this help and the use of XPS services.

Sheer Thinning Self-assembling Hydrogels

E. F. Banwell¹, D.N. Woolfson² & J. G. Heddle¹

1. [RIKEN](#), Institute of Advanced Science, Wako-shi, Japan
2. [University of Bristol](#), School of Chemistry, Cantocks Close, Bristol, UK.

INTRODUCTION: The layer-by-layer build up of three-dimensional (3D) tissues from two-dimensional (2D) cell sheets is an exciting alternative to traditional methods of tissue and organ engineering. Traditionally, scaffolds are seeded with cells that infiltrate and replace the artificial structure with their own extracellular matrix (ECM), but layering of 2D sheets has many advantages over this method; cell layers can be interleaved with pre-formed vasculature, they are more easily micropatterned and do not contain scaffold materials which can release toxic or immunogenic substances.

Previously, we have designed a novel hydrogelating self-assembling fibre (hSAF) system¹. The gel comprises two peptides, unfolded separately, that fold and assemble on mixing into fibres and networks. We have shown that the characteristics of the gel can be controlled and they have been shown to support cell growth.

Here we describe the iterative redesign of one particular promising hSAF; the glutamine-containing hSAFs (hSAF_{QQQS}). The hSAF_{QQQS} gel via a hydrogen bonding network that can be easily shear disrupted, making them ideal as a quick-release substrate for cell sheets. The two-component nature of SAFs makes them ideal for coating applications, while their flexible amino-acid sequence makes the design of a variety of degradation mechanisms feasible.

METHODS: Peptides were synthesized on a Liberty Peptide Synthesis System (CEM Microwave Technology) using standard Fmoc/*t*Bu solid-phase protocols and HBTU/ DIPEA as coupling reagents. All standard Fmoc coupled amino acids were purchased from Novabiochem. Peptides were purified by RP-HPLC and confirmed by mass spectrometry (ESI and MALDI-TOF).

RESULTS: Iterative redesign of short peptides is a powerful method for the development of novel materials. The first generation hSAF_{QQQ} peptides have a melting temperature of 20 °C, making them unsuitable for mammalian cell culture

applications. Initially, we sought to stabilize the peptide overlap through the extension of the asparagine-containing half of the peptide to 3 heptads. Assemblies were alpha-helical in nature (Fig. 1) and demonstrated a biphasic melt, however, the two peptides are both neutral in charge and there was significant self-aggregation. The peptide mixtures, although viscous, did not form gels. In order to solve this problem a new design with one entirely basic and one entirely acidic peptide was produced. These peptides are likely to assemble into an undesirable dimer with a four-heptad overlap that is unable to undergo further assembly into fibres. Glycine residues are very poorly tolerated in alpha-helices and consequently a Gly residue was introduced at the centre of each peptide sequence on order to destabilize the read-through dimer and push assembly towards the desired higher-order product.

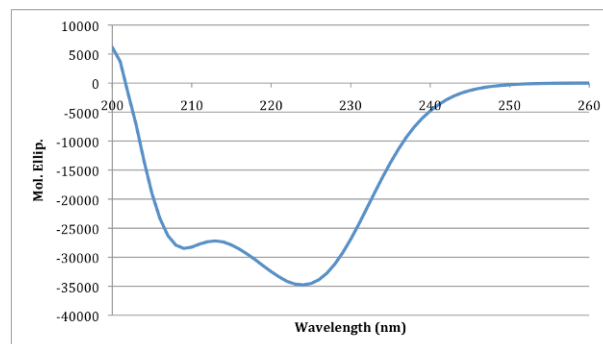


Figure 1. Circular Dichroic spectrum of an hSAF_{QQQ}-ext mixture.

DISCUSSION & CONCLUSIONS: hSAF peptides are promising 2D cell culture substrates. Their ability to sustain cell growth, together with their sheer thinning behaviour and amenability to iterative design make them ideal candidates for continued development.

REFERENCES:

1. Banwell, E *et al.* *Nature materials*. **2009**, *8*, 596–600.

ACKNOWLEDGEMENTS: This work is funded by RIKEN.

Poly(butyl methacrylate) for enhanced cell adhesion

K. Cox-Nowak & S. Rimmer

¹ *Polymer Centre, Department of Chemistry, University of Sheffield, Sheffield*

INTRODUCTION: Cell adhesive coatings and gels are currently a growing area of research within both academia and industry. The aim of this project is to explore the biocompatibility of poly(butyl methacrylate) in various forms.

These includes the effect of molecular weight; the difference between branched and linear polymers; acid and amine functionality and finally, the effect of casting polymers as films and also entrapping them within semi-interpenetrating polymer networks (semi-IPNs).

Human primary osteoblasts are being used for the majority of biocompatibility studies, with human renal epithelial cells being used as a secondary cell line.

METHODS: Butyl methacrylate is co-polymerised with butadiene to form a linear copolymer that can be cleaved into shorter oligomers using ozonolysis. Further modifications allow the introduction of acid and amine functionality to these polymers.

Hyperbranched polymers are synthesised using Reversible Addition-Fragmentation chain Transfer (RAFT), utilising two separate chain transfer agents with the monomers t-butyl acrylate and n-butyl methacrylate. Post-polymerisation modifications upon these polymers allow end-group control.

RESULTS: Cell growth upon linear poly(BMA) with a molecular weight of 30,000 has been observed. *Figure 1.*

A library of hyperbranched, acid-ended polymers has been formed and chemically characterised, ready for insertion into semi-IPNs.

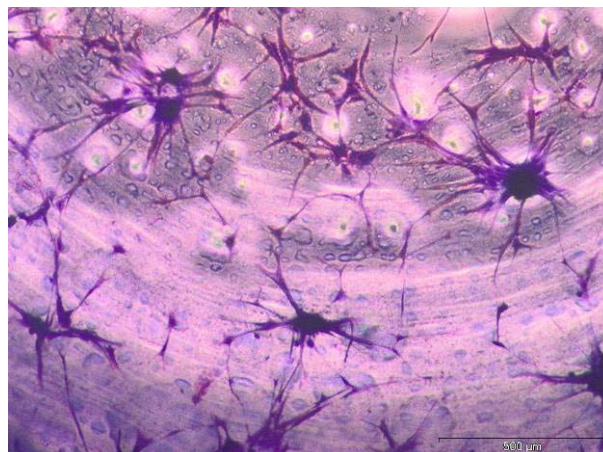


Fig. 1: Giemsa stained primary human osteoblasts upon poly(butyl methacrylate) film. 48hrs incubation.

REFERENCES:

- S Rimmer, C Johnson, B Zhao, J Collier, L Gilmore, S Sabnis, P Wyman, C Sammon, N Fullwood and S MacNeil (2007) *Biomaterials* **28**: 5319-5331
- Moad, G., E. Rizzardo, and S.H. Thang (2006) *Australian Journal of Chemistry* **59**(10): 669-692
- Kostanski, L. K., R. Huang, C. D. M Filipe and R. Ghosh. (2009) *Journal of Biomaterials Science, Polymer Edition* **20**(3): 271-297.

ACKNOWLEDGEMENTS: J. Louth, S. Canning.

LOW-AFFINITY NERVE GROWTH FACTOR RECEPTOR (NGFR) IS A MARKER OF BASAL UROTHELIAL CELLS – IMPLICATIONS FOR UROTHELIAL REGENERATION AND RENEWAL

[Felix Wezel](#) & Jennifer Southgate

Jack Birch Unit of Molecular Carcinogenesis, Department of Biology, University of York, UK

INTRODUCTION:

The urinary bladder is an epithelial organ that is susceptible to a large range of age-related benign, dysfunctional and malignant conditions where novel regenerative medicine and tissue engineering therapies are required.

The bladder is lined by urothelium - a mitotically-quiescent epithelium in situ characterised by an extremely low turnover rate and long-lived cells. However, in response to injury, infection or other stimuli, the urothelium develops a highly regenerative response. As a self-renewing tissue, there is assumed to be a resident progenitor population. However, no specific population has yet been identified that acts as a stem cell in human urothelium.

NGFR has been implicated in regulation of cell survival and cell death [1] and was identified recently as a marker of human airway epithelial stem cells [2] and tumor-initiating melanoma cells [3]. The aim of this study was to investigate expression of NGFR in human and porcine urothelium and relate it to proliferative, clonogenic and differentiation characteristics in vitro.

METHODS: Immunolabelling on paraffin wax – embedded tissue was performed using two independent monoclonal antibodies against NGFR. A MoFlo™ cell sorter (Beckman Coulter) was used to isolate NGFR+ /CD45- cells from fresh porcine bladder urothelium. alamarBlue® (Serotec) and colony-forming efficiency (CFE) assays were used to quantitatively assess proliferation characteristics and clonogenicity of porcine urothelial cells in vitro. Terminal urothelial differentiation after induction in vitro was monitored by the ability of cell cultures to establish of a functional epithelial barrier by measuring transepithelial electrical resistance (TER) and by immunolabelling for urothelial differentiation-associated markers.

RESULTS: NGFR was found to be a basal cell marker in normal human and porcine urothelium. After isolation, porcine NGFR+/CD45- cells showed a highly proliferative and clonogenic phenotype compared to NGFR-/CD45- cells, but

both populations displayed similar long-term growth characteristics and differentiation potential and both were able to regenerate a hierarchically-organised and fully-differentiated tissue structure similar to native urothelium in vitro.

DISCUSSION & CONCLUSIONS:

This study provides novel observations on the existence of urothelial subpopulations and establishes NGFR as a basal urothelial cell marker. The results indicate that basal cells are ‘primed’ for proliferation but that all cells are able to switch into a proliferative phenotype. Our findings tend to argue against the existence of a distinct stem cell population in favour of a model where urothelial cell phenotype is plastic and determined by factors in the local environment.

These results have important implications for understanding urothelial regeneration and in the development of regenerative medicine/ tissue-engineering strategies for bladder reconstruction.

REFERENCES: [1] Mukai J, Hachiya T, Shoji-Hoshino S, et al. NADE, a p75NTR-associated cell death executor, is involved in signal transduction mediated by the common neurotrophin receptor p75NTR. *J Biol Chem* 2000;275:17566-70. [2] Rock JR, Onaitis MW, Rawlins EL, et al. Basal cells as stem cells of the mouse trachea and human airway epithelium. *Proc Natl Acad Sci U S A* 2009;106:12771-5. [3] Boiko AD, Razorenova OV, van de Rijn M, et al. Human melanoma-initiating cells express neural crest nerve growth factor receptor CD271. *Nature*;466:133-7.

ACKNOWLEDGEMENTS: This work was supported by The European Urological Scholarship Program (EUSP), York against Cancer (YAC) and The Yorkshire Kidney Research Fund (YKRF).

Engineering of Natural Cartilage Substitution Biomaterials

H Fermor¹, S Russell², S Williams², J Fisher² & E Ingham¹

¹ *Institute of Medical and Biological Engineering, Faculty of Biological Sciences, University of Leeds, UK.* ² *IMBE, School of Mechanical Engineering, University of Leeds, UK.*

INTRODUCTION: Osteoarthritis is a painful, debilitating degenerative disease. Initial damage to cartilage results in increased friction and wear, leading to further damage and the development of end-stage osteoarthritis. Repair of these initial defects could provide an early intervention treatment which would prevent or delay osteoarthritis progression. This project aims to develop an acellular cartilage biomaterial from animal tissue, with biological, biochemical and biomechanical properties similar to those of natural cartilage. Initial studies focussed upon determination of the optimal starting material for the development of a decellularisation protocol.

METHODS: Osteochondral pins, 9 mm in diameter, were extracted from various regions of the porcine (6 month), bovine (18 month) and ovine (1 year & >4 year) hip and knee. Cartilage was analysed by histology using H&E and alcian blue staining to determine glycosaminoglycan (GAG) distribution. From the resultant images, cellularity and cartilage thickness was determined. Quantitative analysis of GAGs was performed following papain digestion using the dimethylmethylene blue assay.

RESULTS: Bovine and older ovine cartilage had a more defined cellular organisation (Figure 1); in line with the maturity of these tissues compared to porcine. Bovine and porcine cartilage was thickest (Figure 2), had the highest GAG content (Figure 3), and was more similar than ovine to human cartilage.

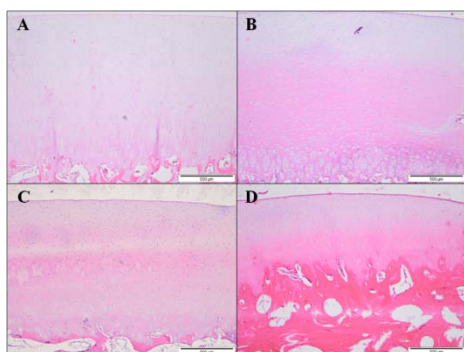


Fig. 1: H&E staining of cartilage from the medial condyle of A - Cow, B - Pig, C - 1 year old sheep and D - > 4 year old sheep. Size bars are 500 μ m.

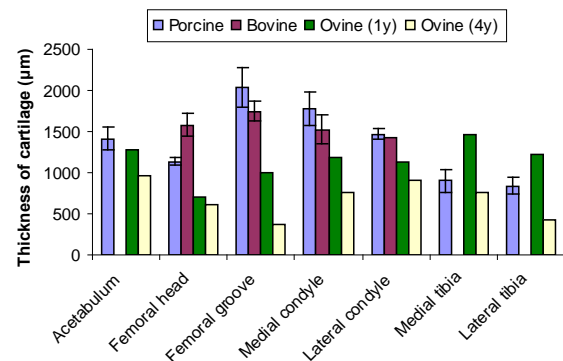


Fig. 2 Thickness of cartilage from various joint regions of pig, cow and sheep. Data expressed as mean (porcine n=5, bovine n=4, ovine n=1) \pm SE.

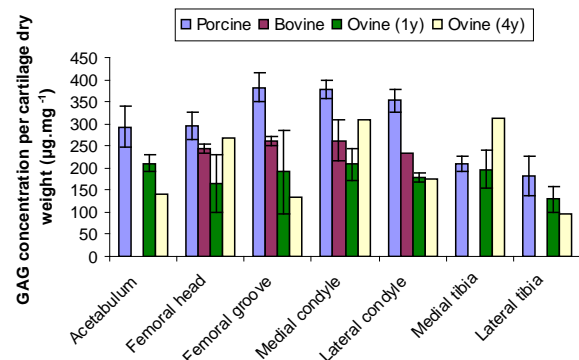


Fig. 3 GAG content of cartilage from various joint regions of the pig, cow and sheep. Data expressed as the mean (porcine and bovine n=5, ovine (1 yr) n=3 and ovine (>4 yr) n=1) \pm SE.

DISCUSSION & CONCLUSIONS: Porcine and bovine tissues are most appropriate starting materials for use as acellular cartilage grafts. Osteochondral pins from the porcine medial condyle and bovine femoral groove and medial condyle will be taken forward for decellularisation. The decellularisation process, based upon the work of Stapleton et al. [1] will now be optimised in future studies.

REFERENCES: ¹ TW Stapleton, J Ingram, J Katta et al (2008) *Tissue Engineering Part A*. **14(4)**: 505-518.

ACKNOWLEDGEMENTS: This work was partially funded through WELMEC, a Centre of Excellence in Medical Engineering funded by the Wellcome Trust and EPSRC, under grant number WT 088908/Z/09/Z.

Mechanical Stimulation Of Adult Human Mesenchymal Stem Cells Influences CCNL2 and WDR61 Gene Expression Levels

S Rathbone¹, J Glossop², J Gough¹ & S Cartmell¹

¹ *Materials Science Centre, University of Manchester*

² *Institute for Science and Technology in Medicine, Keele University*

INTRODUCTION: Mesenchymal stem cells (MSCs) are multipotent, unspecialized cells which have the capacity to differentiate into specific cell types of various cell lineages [1], making them an attractive cell source for tissue engineering applications. They have the potential to produce cartilage, bone, muscle, tendon, ligament or fat [2] in response to specific stimuli [3]. The literature indicates that tensile strain can alter gene expression and affect cell behaviour, subsequently regulating proliferation, apoptosis, cell alignment, and differentiation. Evidence exists to confirm that human MSCs can be encouraged to differentiate in response to tensile loading forces [4]. We investigated the effects of tensile straining forces on gene expression for human MSCs in 2D cell culture and aim to compare this to future work with 3 dimensional peptide gel constructs.

METHODS: MSCs (Lonza) at passage 6 were cultured in monolayer on pronectin-coated 6-well plates (Flexcell). They were seeded at 5×10^4 cells/well in DMEM supplemented with 10% FBS, 1% L-glutamine and 1% antibiotics. Uniaxial strain, equivalent to 3% elongation, with a cycle speed of 1Hz, was applied to cells for 1 or 24 hours using a FX-4000T system (Flexcell International), while controls remained static. Samples were collected at 2hours or 24hours post strain. A full human genome microarray (Affymetrix human genome U133 Plus 2.0 array) was performed to highlight consistent differential expression of genes. Two genes of interest were then selected and real-time RT-PCR was performed (n=6) to assess reproducibility.

RESULTS: Microarray data highlighted 229 and 269 genes, and 405 and 179 genes that were differentially expressed following 1hour and 24hours strain durations respectively (2 and 24hours post strain for each duration). Two genes selected of interest that consistently showed differential expression were CCNL2 (cyclin L2) and WDR61 (WD repeat domain 61). Real time RT-PCR indicated that CCNL2 was significantly downregulated after 1hour strain and 2hours latency (post strain). Although WDR61 also

showed downregulation after 1hour strain (2hours latency), this was not significant.

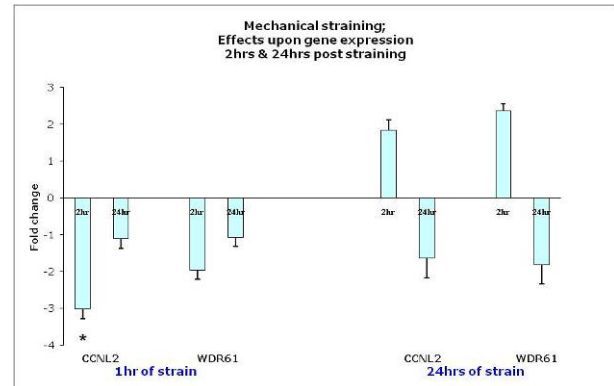


Figure 1: Gene expression analysis in strained samples compared to controls (n=6).

DISCUSSION & CONCLUSIONS: CCNL2 is thought to be involved in the cell cycle where it regulates the pre-mRNA splicing process. WDR61 is part of the SKI complex which is thought to be associated with mRNA degradation.

The latency period appeared to be the main factor which affected the level of gene expression in the strained samples compared to controls. We are currently investigating the role of these genes in long-term cell activity such as differentiation. We are also investigating this gene expression role in MSCs strained in a 3D hydrogel environment.

REFERENCES: ¹ J. Centeno, D. Busse, J. Kisiday, et al (2008) *Medical Hypotheses* **71**: 900-908. ² A. Papathanasopoulos and P. Gaiannoudis (2008) *Injury: International Journal of the Care of the Injured* **39S2**: S21-S32. ³ R. Lanza, R. Langer and J. Vacanti (2007) *Principles of Bone Tissue Engineering - Tendons & Ligaments*. Third edition, Elsevier Inc. ⁴ G. Altman, R. Horan, I. Martin et al (2001) *FASEB Journal*: DOI 10.1096-fj.01-0656fje.

ACKNOWLEDGEMENTS: We acknowledge funding from BBSRC BB/D000548/1 and EPSRC IMPACT Pathfinder grants.

Establishment of a 3D engineered skeletal muscle-motoneuron co-culture using fibrin-cast gels

S.L. Passey¹, A.S.T Smith^{1,2}, V. Mudera³, L. Greensmith², K. Baar⁴ and M.P. Lewis^{1,5}.

¹ Muscle Cellular and Molecular Physiology Research Group, Institute of Sport and Physical Activity Research (ISPAR), Bedford. ² The Sobell Department of Motor Neuroscience and Movement Disorders, UCL Institute of Neurology. ³ UCL Institute of Orthopaedics and Musculoskeletal Science, Stanmore. ⁴ Functional Molecular Biology Lab, UC Davis, California, USA. ⁵ UCL School of Life and Medical Sciences, London, UK. School of Sport, Exercise and Health Sciences, Loughborough University and Cranfield Health, Cranfield University, UK.

INTRODUCTION: The successful *in vitro* engineering of complex tissues such as skeletal muscle would be of great benefit in the fields of tissue engineering and regenerative medicine, muscle physiology and neuromuscular research. A number of *in vitro* engineered models of skeletal muscle have been described that demonstrate many structural, biochemical and physiological similarities to *in vivo* muscle. As yet, however, there is no truly biomimetic *in vitro* model of skeletal muscle. An important aspect of *in vivo* muscle development and maintenance is the presence of a neuronal input via neuromuscular junctions (NMJs). Here we have increased the complexity of existing muscle models by introducing primary motoneurons with the aim of engineering a functional neuronal input in an established *in vitro* skeletal muscle model.

METHODS: The fibrin gel model of skeletal muscle culture has been described elsewhere (1) and fibrin gels were supplemented with 8µl/ml aprotinin. Rat MDCs were isolated from the hind limbs of P1 Sprague-Dawley rat pups by collagenase digestion, and cultured in fibrin gels until confluent (approximately 4-5 days) before the addition of MNs. MNs were isolated from the ventral horn of spinal cords from Sprague-Dawley rat E14 embryos and plated at 50,000 cells per gel. Co-cultures were maintained for up to 7 days prior to processing for immunocytochemistry or Q-PCR.

RESULTS: Microscopic analysis of skeletal muscle fibrin constructs revealed the formation of tight bundles of myotubes aligned along the long axis of the construct and often displaying the striated pattern characteristic of skeletal muscle. Expression of genes involved in muscle cell differentiation (myogenin) and contraction (Myosin heavy chain, MYH3) was higher in 3D fibrin constructs compared to conventional 2D culture, illustrating the improved maturation of the

muscle constructs in 3D fibrin cast gels. MNs survive within the co-culture system neurites could be seen extending through the construct in association with myotubes (Figure 1). Preliminary data indicates that co-culture of MDCs with primary MNs results in increased expression of the NMJ genes acetylcholine receptor (AChR) and Choline acetyltransferase (ChAT).

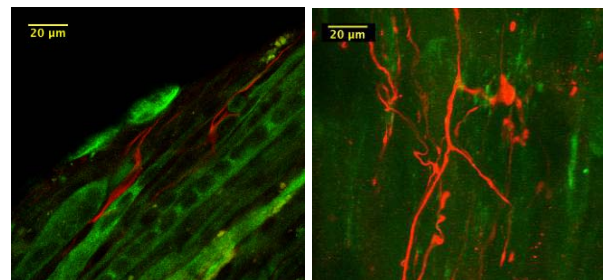


Figure 1. (A) MN neurites (red) can be seen extending in association with the myotubes (green) within fibrin-cast skeletal muscle constructs. (B) Maximum intensity projection from a confocal z-stack showing a network of neurites extending in 3 dimensions within the muscle construct. Scale bar = 20µm.

DISCUSSION & CONCLUSIONS: Using an established model of skeletal muscle, we have added extra complexity through the addition of a neuronal input. Fibrin cast skeletal muscles can be rapidly engineered together with MN, producing contractile neuromuscular constructs. The presence of MNs in the co-culture system induces the expression of NMJ genes within the muscle cells indicating physiological interactions between the two cell types which represent the first step towards the formation of organized NMJs. Establishment of a 3D muscle-MN culture system will be of great benefit to the study of NMJ formation, maturation, and function and will reduce reliance on animal models for such studies.

REFERENCES: ¹ Rapid Formation of functional muscle *in vitro* using fibrin gels. Yen-Chih Huang, et al. J Appl. Physiol. 98:706-713, 2005.

MEDICAL GRADE STERILISATION OF ELECTROSPUN POLY(ϵ -CAPROLACTONE) FIBROUS SCAFFOLDS

A Gibb, LA Bosworth, SA Mobasseri & S Downes

Biomaterials Group, Material Science Centre, Faculty of Engineering and Physical Sciences, The University of Manchester, UK

INTRODUCTION: There is widespread use of fabricated scaffolds made from materials with appropriate physico-chemical properties to support and sustain the cells of tissues they are intended to replace¹. Laboratory characterisation and development of these scaffolds commonly employs sterilisation techniques, such as, ultraviolet (UV) radiation or ethanol soaking. Whilst these sterilisation methods are satisfactory for non-clinical laboratory assessment, they are not recognised by Regulatory bodies, such as the MHRA and FDA. Research projects can often neglect the importance of sterilisation and the effects sterilisation may have on the material properties², which could lead to many years of research never reaching their translational potential due to sterility complications. Hence, the importance of incorporating approved sterilisation techniques at an earlier research stage in order to facilitate translation from the bench to the clinic. The objective of this study is to ascertain whether medical grade gamma irradiation affects properties of electrospun nanofibres, including molecular weight, mechanical strength, surface structure and cellular response.

METHODS:

Poly(ϵ -caprolactone) (PCL) Scaffolds

PCL (M_n 80,000) is dissolved in Hexafluoroisopropanol (HFIP) (10% w/v) and electrospun using pre-determined parameters: voltage-20kV, flow rate-1ml/hr, distance to collector-20cm. Aligned fibres are collected on a fine edged mandrel (\varnothing 120mm, width 3mm) rotating at 600RPM (Fig. 1).

Sterilisation Procedures

Fibrous strips cut into 3cm lengths and placed within appropriate packaging (Steribag; Fisher) will undergo gamma irradiation at seven incremental doses (15-45kGy) (Isotron).

Characterisation

Physico-chemical properties of the fibres will be assessed compared to non-sterilised fibres, using Gel Permeation Chromatography, Differential Scanning Calorimetry, Fourier Transform Infra-red, and mechanical testing. Response of tendon fibroblasts to gamma irradiated fibres will be compared to ethanol sterilised fibres, in terms of cell number and proliferation and imaging including, Scanning Electron Microscopy and immunocytochemistry.

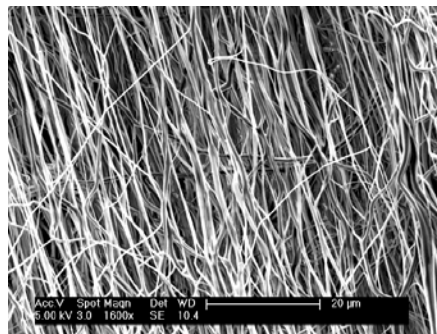


Figure 1 – SEM image of electrospun PCL nanofibres collected on a rotating mandrel

DISCUSSION & CONCLUSIONS: This study focuses on the effect of medical grade sterilisation on electrospun fibrous scaffolds which have potential clinical applications. Currently electrospun PCL scaffolds are under investigation for potential regeneration of several tissues including, tendon, bone and peripheral nerves. The results of this study will shape the translational development of such projects towards their clinical use.

REFERENCES: ¹Pham QP, Sharma U, Mikos AG (2006) Electrospinning of Polymeric Nanofibers for Tissue Engineering Applications: A Review. *Tissue Engineering* 12(5):1197-1211. ²Selim M, Bullock AJ, Blackwood KA, Chapple CR, MacNeil S (2010) Developing Biodegradable Scaffolds for Tissue Engineering of the Urethra. *BJUI* 107(2):296-302